universität wien

MASTERARBEIT / MASTER'S THESIS

Titel der Masterarbeit / Title of the Master Thesis

„Estrogenic Activity of Isoflavone Metabolites“

verfasst von / submitted by

Dimitra Bella-Velidou, BSc

angestrebter akademischer Grad / in partial fulfilment of the requirements for the degree of

Master of Science (MSc)

Wien, 2023 / Vienna, 2023

Studienkennzahl lt. Studienblatt / degree programme code as it appears on the student record sheet:	A 066 659
Studienrichtung lt. Studienblatt / degree programme as it appears on the student record sheet:	Masterstudium Lebensmittelchemie
Betreut von / Supervisor:	Univ.-Prof. Dr. Doris Marko
Mitbetreut von / Co-Supervisor:	DI Dr. Elisabeth Varga

Acknowledgements

First and foremost, I would like to thank Univ.-Prof. Dr. Doris Marko for allowing me to conduct my master thesis in her working group at the Department of Food Chemistry and Toxicology at the University of Vienna. It was most interesting to partake in such an interesting subject and I am thankful for this opportunity.

I would specially like to thank both of my supervisors, DI Dr. Elisabeth Varga and (soon to be Dr.) Dino Grgic. Both of you were extremely patient and kind with me during this past year. You were both available at any time for any questions I might have had and none of this work would have been possible without your guidance. Delving into the various subjects I researched was made more fun with both of you and I can happily say I learned a lot during my time in the institute.

Moreover, I'd like to thank all of my colleagues that I may or may not have pestered with questions when needed. Lab work was strenuous on occasion but was made enjoyable when other students and co-workers were around. I am happy the working environment was either cheerful or mutually to complain about and I'd love to visit once in a while.

Also, I would like to thank the Austrian Research Promotion Agency (FFG) and DSM-BIOMIN Holding GmbH for funding the "ISOMYCOTOX" project. Without them, it would not have been possible for me to investigate such an interesting subject. Furthermore, I want to thank Prof. Dr. Sabine E. Kulling and her group for providing the isoflavone metabolites.

Last but not least, I want to warmly thank my parents for fully supporting me through the entirety of my studies. Their trust in me has been, and will always be a driving force. The same goes for my dear friends who I also consider my family. Without their mental encouragement and continuous strength, few things would have been possible. Thank you for making life perfectly splendid.

Declaration of originality

I, Dimitra Bella-Velidou, confirm to have compiled this work in my own words and am the sole author of it. Furthermore, I declare that used sources in the text have been acknowledged and correctly listed. This work has not yet been published.

Vienna, Signature

Dimitra Bella-Velidou

Table of contents

Abbreviations

4-NPP ..... *4-nitrophenyl phosphate*

5-OH-EQ *5-hydroxy-equol*

6-OH-ODMA ..... *6'-hydroxy-O-demethyl-angolensin*

ACN ..... *acetonitrile*
AF ..... *activation factor*
ALP ..... *alkaline phosphatase*

BMD ..... *bone mineral density*

CD-FBS ..... *charcoal stripped fetal bovine serum*
CID ..... *collision induced dissociation*
CTB ..... *CellTiter-Blue*
CYP ..... *cytochrome P450*

D4',7dG ..... *DAI-4',7-diglucuronide*
D4',7dS ..... *DAI-4',7-disulfate*
D4'G ..... *DAI-4'-glucuronide*
D4'G7S ..... *DAI-4'-glucuronide-7-sulfate*
D4'S ..... *DAI-4'-sulfate*
D7G *DAI-7-glucuronide*
D7G4'S ..... *DAI-7-glucuronide-4'-sulfate*
DAI ..... *daidzein*
DBD ..... *DNA-binding domain*
DHD ..... *dihydro-daidzein*
DHG ..... *dihydro-genistein*
DMEM ..... *Dulbecco's modified eagle medium*
DMSO ..... *dimethyl sulfoxide*
DS ..... *daidzein-sulfate*
DW ..... *dry weight*

E2 ..... *17β-estradiol*
E4'S ..... *EQ-4'-sulfate*
E7G *EQ-7-glucuronide*
EFSA ..... *European Food Safety Authority*
EQ ..... *equol*
ERE ..... *estrogen response element*
ERα ..... *estrogen receptor alpha*
ERβ ..... *estrogen receptor beta*
ES ..... *equol-sulfate*
ESI ..... *electrospray ionisation*

FBS ..... *fetal bovine serum*
FSH ..... *follicle-stimulating hormone*

G4',7dG ..... *GEN-4',7-diglucuronide*

G4',7dS ..... *GEN-4',7-disulfate*
G4'G ..... *GEN-4'-glucuronide*
G4'G7S ..... *GEN-4'-glucuronide-7-sulfate*
G7G *GEN-7-glucuronide*
G7G4'S ..... *GEN-7-glucuronide-4'-sulfate*
G7S *GEN-7-sulfate*
GEN ..... *genistein*
GIT ..... *gastrointestinal tract*
GLY ..... *glycitein*
GS ..... *genistein-sulfate*

HDAC ..... *histone deacetylase*
HPG ..... *hypothalamic-pituitary-gonadal*
HPLC ..... *high performance liquid chromatography*
Hsp70 ..... *heat shock protein 70*
Hsp90 ..... *heat shock protein 90*

IF ..... *isoflavone*

k_{cat} ..... *catalytic rate constant*
K_m ..... *Michaelis constant*

LBD ..... *ligand-binding domain*
LH ..... *luteinizing hormone*
LOD ..... *limit of detection*
LOQ ..... *limit of quantification*

m/z ..... *mass-to-charge ratio*
MAPK ..... *mitogen-activated protein kinases*
MEM ..... *minimal essential medium*
MRM ..... *multiple reaction monitoring*
MS ..... *mass spectrometry*

NHR ..... *nuclear hormone receptor*
NLS ..... *nuclear localisation signal*
NTD ..... *N-terminal domain*

ODMA ..... *O-demethyl-angolensin*

P/S ..... *penicillin-streptomycin*
PBS ..... *phosphate buffered saline*

Q ..... *quadrupole*

RAP ..... *receptor associated protein*
RF ..... *radio frequency*
RP ..... *reversed-phase*

SERM ..... *selective estrogen receptor modulator*

SHBG ..... *sex hormone-binding globulin*
SRB ..... *sulforhodamine B*
SRC ..... *steroid receptor co-activators*
SRM ..... *selected reaction monitoring*
SULT ..... *sulfotransferase*

TAF ..... *tightly associated factor*
TBP ..... *TATA box binding protein*
TCA ..... *trichloroacetic acid*
TF ..... *transcription factors*
THD ..... *tetrahydro-daidzein*
THG ..... *tetrahydro-genistein*
Tris ..... *tris (hydroxymethyl-) aminomethane*

UGT ..... *uridine-5'-diphosphate glucuronyltransferase*
UHPLC ..... *ultra-high performance liquid chromatography*

1. Introduction

Plants of the *Fabaceae* family, including sprouts and by-products have been increasingly demanded due to their nutritional value and health-promoting effects. These characteristics are often attributed to the polyphenolic content, which includes isoflavones (IFs). IFs are non-steroidal, secondary plant metabolites and known phytoestrogens, due to their structural similarity to the female sexual hormone 17β-estradiol. Examples of potential dietary sources for these substances include soybeans (*Glycine max L.*) and red clover (*Trifolium pratense L.*) (Bucar, 2013), with the latter currently investigated as a functional food (Galanty, et al., 2022). Extracts from these sources were marketed in the past as food supplements and other commodities due to the positive effects they may have on bone mineral density, antioxidant activity, cardiovascular health and prostate function (Hüser, et al., 2018). However, the European Food Safety Authority (EFSA) over the course of the past two decades has concluded, that the scientific evidence provided was not sufficient to establish any substantial cause and effect between IF consumption and the aforementioned claims (EFSA, 2009; EFSA, 2011; EFSA, 2012), thus prohibiting an advertisement of said health effects in relation to IFs in food supplements and other products.

Regardless, the research for both positive and negative effects of IFs moves forwards not only in the East, where soy products are widely beloved and consumed even at the early stages of life, but also in the West with the rise of vegetarian and vegan diets (Inbaraj & Chen, 2013) as well as with regard to animals, since soybeans are a preferred protein source in farm feed (Penagos-Tabares, et al., 2021). So far, the risk assessment of EFSA stated that soy IF dosages up to 100 mg per day for the duration of ten months were acceptable for healthy post-menopausal women with no significant adverse effects on the target organs of interest, namely breasts, uterus and thyroid (EFSA, 2015). Be that as it may, the proposed values were only applicable to post-menopausal women with no current cancer diagnosis and with focus on IF supplements. Not only does this exclude certain individuals that may be more sensitive to the estrogenicity caused by the substances, it simplifies their intake, since mechanical and thermal processing of soy products yields different IF contents (Kao, et al., 2004; Privatti, et al., 2022) and does not represent combinatory effects nor take into consideration the role metabolism plays between individuals.

Indeed, the majority of studies focuses on the aglycones themselves and disregard IF metabolites. Although phase I and II metabolic pathways are generally considered detoxifying, recent studies have found that not only sulfates may contribute to the biological

activity of IFs but may even enhance it, in the case of daidzein (Pugazhendhi, et al., 2008). Even glucuronides, which are much larger, hydrophilic molecules, have been found to exert weak estrogenicity (Beekmann, et al., 2015). Generally, not much is known for the rest of phase II metabolites of IFs, namely diglucuronides, disulfates and the glucuronide-sulfate combination. This could be particularly concerning since recent data on human plasma samples identified the latter as a major metabolite (Soukup, et al., 2016). Therefore, this thesis should provide a more detailed insight on the role phase II metabolism plays with regards to the biological activity of IFs. The focus here will be on the IFs genistein (GEN), daidzein (DAI), S-equol (EQ) and specifically 16 of their metabolites consisting of sulfates, glucuronides, disulfates, diglucuronides and the sulfate-glucuronide modification differing in positions of the functional groups. The estrogenicity and cytotoxicity of individual compounds will be investigated via cell assays in addition to a liquid chromatography tandem mass spectrometry analysis on the profile of aforementioned substances to better elucidate whether our results are a direct effect or caused by deconjugation or even further metabolization.

2. Theoretical background

Organs and tissues must communicate with each other in order for the human body to function properly and maintain a constant internal environment (i.e. homeostasis). The endocrine and nervous systems play an important role by producing and secreting hormones in response to stimuli through endocrine glands as well as mediating the distribution of said hormones to their target cells via the bloodstream. The cells contain receptors which function as docking molecules for the hormones and after a bond is formed between the two, a cascade of biochemical reactions is generated. This results in modulation of activity or function of the target cells (Rogers, 2012).

However, exogenous compounds may interfere with the hormonal system of humans and animals. By being structurally similar to a hormone, a substance may bind to its corresponding receptor and either activate or block it, thus functioning as agonists or antagonists (Rogers, 2012). Isoflavones (IFs) are such an example of endocrine disruptive compounds. Commonly found in legumes like soybeans they mimic the action of estrogens and are thus categorized as phytoestrogens. Although there are numerous studies on the beneficial effects IFs have on humans and animals, there is controversy surrounding their potential use to alleviate menopausal symptoms or against osteoporosis because of adverse effects relating to breast cancer. In order to better understand their role in health, the biotransformation and metabolism of IFs is crucial (Soukup, et al., 2016).

2.1. Estrogenicity

Steroid sexual hormones are synthetized in the gonads and are therefore part of the hormones belonging to the hypothalamic-pituitary-gonadal (HPG) axis of the endocrine system (Rogers, 2012). Estrogens, like all other hormones, are derived from cholesterol (Ceccarelli, et al., 2022). They are produced primarily in females by ovarian follicle cells but may also be produced by conversion of other steroid hormones. Such examples are the aromatization of androgens after diffusion in the granulosa cells, where follicle-stimulating hormone (FSH) stimulates aromatase activity (Ceccarelli, et al., 2022) or the aromatization of testosterone in Leydig and Sertoli cells in males under the stimulation of luteinizing hormone (LH) (Cooke, et al., 2017). Estrogens also play an important role in males and are associated not only with their reproductive organs, but also the brain, bones, adipose, cardiovascular and immune tissues (Cooke, et al., 2017).

The natural estrogens depicted in Figure 1 include estrone (E1), 17β-estradiol (E2) and estriol (E3). E2 is the most dominant estrogen in humans and the main sexual hormone in

premenopausal females. E1 is the main representative of endogenous estrogens post-menopause (de Padua Mansur, et al., 2012) and E3 is related to pregnancy. Both E1 and E3 are found in much lower levels compared to E2 (Ceccarelli, et al., 2022).

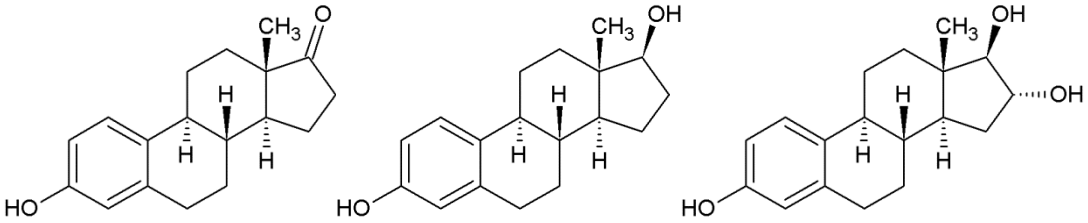

Figure 1: Molecular structures of estrone (E1), estradiol (E2) and estriol (E3) (from left to right).

After the estrogens are released from their steroidogenic cells, only 5% of them circulate freely in the bloodstream. The rest (95%) is transported by binding to glycoproteins, either serum albumin or sex hormone-binding globulin (SHBG), both of which are produced mainly in the liver. Plasma concentrations of albumin are much higher however its binding affinity to hormones is low. On the other hand, the high specificity and affinity of SHBG gives them a dynamic role not only in blood circulation of estrogens but possibly in their entrance in target cells. To date it is believed that only free steroid hormones passively diffuse through the membrane of cells to exert their activities (Hammond, 2016).

2.1.1. Estrogen signaling pathways

Understanding the effects of estrogens is directly related to the mechanism of estrogenic activity. The second half of the 1960s has been pivotal with regard to the research performed to elaborate on the action of estrogens (Noteboom & Gorski, 1965; O'Malley & McGuire, 1968; Jensen, et al., 1969; Shyamala & Gorski, 1969). The discovery of the estrogen receptor 1, commonly known as estrogen receptor alpha (ERα), from the aforementioned groups and the much later identification of a second estrogen receptor, now known as estrogen receptor beta (ERβ), from Kuiper *et al.* (1996) has led to the classic concept of estrogen receptor signaling involving ligand binding and transactivation. However, there are other signaling pathways worth mentioning: a ligand independent pathway which involves activation of ERs via kinases, a genomic pathway with indirect binding of ER to DNA sequences, non-genomic pathways which are characterized by speed incompatible with transcriptional processes (Björnström & Sjöberg, 2005) as well as “non-nuclear” pathways that came to be after the discovery of an orphan G-protein coupled receptor, the GPR30, which is associated with the cellular membrane (Zimmerman, et al., 2016).

This thesis focuses only on the classical ligand signaling pathway involving ERs, which will be explained in detail during the following sections.

2.1.1.1. Estrogen receptors

ERs, along with the androgen, progesterone, glucocorticoid and mineralocorticoid receptors, are part of the nuclear hormone receptor (NHR) family. The two main ERs found in mammalian cells, either in the cytoplasm or nucleus, are ERα and ERβ. They are encoded by the genes *ESR1* and *ESR2* located on the human chromosomes 6 and 14, respectively (Enmark, et al., 1997). Like all members of the NHR family, the ERs share a common structure composed of the domains A-F. All regions are characterized by differing functions.

Firstly, the A/B domain is situated at the NH_3-terminus and known as the N-terminal domain (NTD). This region includes one of the activation function (AF) regions, the AF1, which regulates transcription in a ligand-independent way. Between the NHRs, this domain is the least homologous one possibly due to the amino acid sequences being characterized by an intrinsically disordered conformation (Kumar, et al., 2011).

The conserved "C" domain follows right after and is referred to as the DNA-binding domain (DBD). It is responsible for binding to the DNA of hormone response elements, which is the estrogen response element (ERE) in the case of ERs. This bond is facilitated by the two finger zinc structure which consists of eight cysteine residues coordinated with two Zn^{2+} ions. The first finger (proximal-box region or P-box) recognizes and interacts with the nucleotides in the ERE sequence, while the second finger (distal-box region or D-box) is involved in the dimerization process of the receptor (Kumar, et al., 2011). "C" also contains a nuclear localization signal (NLS) that allows the transport of proteins from the cytoplasm to the nucleus (Mueller & Korach, 2005).

The D/E/F domain is known as the ligand-binding domain (LBD) and sits at the COOH-terminus. Unlike DBD, it is much less conserved. Looking at each region separately, the "D" domain serves as a flexible hinge that connects the two binding domains, "C" and "E", in order to stabilize DNA binding. "E" contains the LBD, a structure made of 12 α-helices that moderates the functions connected to ligand binding. Those include the interactions with co-regulatory proteins, an NLS, receptor dimerization and transactivation of gene expression. Also located here is the AF2, which is formed by the helices 3, 4, 5 and 12 (Ceccarelli, et al., 2022). Unlike AF1, it functions in a ligand dependent manner while interacting with co-regulators, such as activators or repressors. A synergism of the two AFs is needed for a complete transcription activity (Kumar, et al., 2011). Lastly, the "F" region modulates ligand

specific gene transcription (Koide, et al., 2007) and has been shown to partake in distinguishing estrogen agonists from antagonists (Montano, et al., 1995).

Although this basic structure is common between the two ERs, there are notable distinctions in the amino acid sequences. First, the primary structure of ERβ (59 kDa) is made of a shorter amino acid sequence than ERα (67 kDa). A homology of over 90% is shown for the DBD yet only 60% of the LBD is homologous between the two receptors. This highlights a key difference in the affinity the two receptors may have for a specific ligand. Isoforms also exist for the two ERs. They usually lack specific exons, thus being shorter in length than their wild type counterparts. The existence of these variants greatly influences estrogen responsiveness as most of them suppress ER activity and inhibit gene transcription (Al-Bader, et al., 2011).

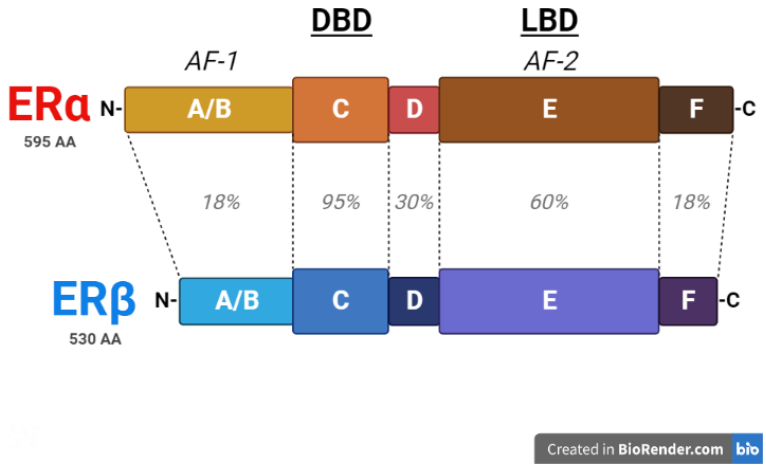

Figure 2: Schematic representation of the ERα and ERβ structures.

Starting from the N-terminus, the A/B domain contains the AF-1 which regulates transcription in a ligand-independent way, followed by the C domain that includes the DBD. A hinge region, the D domain, connects the DBD with the LBD which is situated in the E domain. Here also the AF-2 can be seen, which is responsible for ligand-dependent transcriptional activation. Lastly, the F domain is situated at the C-terminus. The percentages denote the homology in the amino acid sequences between the two receptors (Biason-Lauber & Lang-Muritano, 2022).

2.1.1.2. Classic ligand dependent pathway

After having a better understanding of the different ER domains, it is easier to explain the estrogenic mechanism which involves ligand binding. In their inactive form, the ERs located in the cytosol form a chaperone complex with the heat shock protein 90 (Hsp90). The name denotes the size of the protein being 90 kDa. Hsp90 is a highly expressed receptor-associated protein (RAP) which exists in two isoforms, Hsp90α and Hsp90β. The interactions between ER and Hsp90 are stabilized via the LBD, specifically regions “D” and “E”. This bond serves to mask amino acids of the receptor’s DBD, keeping it in a stable, inactive state (Aumais, et al., 1997).

Historically seen, Hsp90 has been the main RAP investigated, yet it is worth mentioning that recent findings have shown the significance of another family, the heat shock protein 70 (Hsp70). Hsp70 has been found associated with ERα in higher levels compared to Hsp90. However, its role is still unclear and speculated to be significantly different given that an association with the steroid receptor remains even in the presence of hormones (Dhamad, et al., 2016).

Additionally, in the absence of a ligand or until an appropriate ligand enters the cell, co-repressors are just as responsible for halting transcription of the ERs located in the nucleus. Their function includes recruiting proteins and forming a complex with histone deacetylase (HDAC) activity. Repression of gene expression is theorized to be facilitated by keeping chromatin in a condensed state that is inaccessible to transcription factors (TF). Notable co-repressors include the general silencing mediator of retinoic acid and thyroid hormone receptors (SMRT) and nuclear co-repressor (NCoR) (Varlakhanova, et al., 2010). The repressor of ER activity (REA) is much more specific (Montano, et al., 1999).

If an estrogenic ligand (e.g., E2) enters the cell, it interacts with the LBD of the receptor. This induces LBD-associated conformational changes (e.g., protein folding) and receptor modifications, such as phosphorylation, that allows the dissociation of Hsp90 or co-repressors. In addition to this, exposure of dimerization, nuclear translocation and DNA-binding sequences takes place. As a result, an E2-liganded ER is formed (Beekman, et al., 1993).

The E2-ER complex then translocates inside the nucleus of the cell where it dimerizes and uses its DBD to bind directly to a specific DNA sequence, the ERE. Unlike the other steroid receptors which link to derivatives of common response elements (Klinge, 2001), ER binds to a minimal ERE consensus sequence which consists of a 13 base pair perfect palindromic inverted repeat sequence separated by three variable bases (denoted with ‘n’), the 5’-GGTCAnnnTGACC-3’ (Klein-Hitpaß, et al., 1986). However, it should be mentioned that most estrogen responsive genes contain imperfect and non-palindromic ERE sequences, which are also recognizable by the ER (Dahlman-Wright, et al., 2006).

In order for the transcription to be initiated, a variety of factors at the target gene promoter must cooperate to form and stabilize a preinitiation complex as well as modify histones of DNA’s chromatin structure to make it accessible for the RNA polymerase II. Those include basal TFs, specifically TFIIB and TFIID. The latter consist of diverse tightly associated factors (TAFs) and the TATA box binding protein (TBP), a TF that binds specifically to the

consensus sequence of alternating thymine (T) and adenine (A) base pairs in the core promoter region (Klinge, 2000).

Primary steroid receptor co-activators (SRC) belonging to the p160 family (namely SRC-1, SRC-2 and SRC-3) are then recruited via interactions between their conserved LXXLL (amino acid sequence with L: leucine and X: any amino acid) motifs and the hydrophobic groove of AF-2 of the receptor formed during ligand-binding. Various secondary co-activators are afterwards recruited by the SRC, with the most notable example being the p300/ CREB-binding protein. Like most co-activators, it exerts a histone acetyltransferase (HAT) activity. These are responsible for altering the conformation and stability of nucleosomes, enhancing the formation of a stable preinitiation complex and facilitating transcriptional activation by RNA polymerase II (Yi, et al., 2015).

After initiation has been successful, the genes are transcribed to their respective mRNA. This is then translocated to the ribosomes where translation to proteins takes place, concluding the cell- or promoter-specific estrogenic response (Björnström & Sjöberg, 2005). Notable example is alkaline phosphatase (ALP) which is coded by the gene ALPL and up-regulated in the presence of E2 (Krum, et al., 2008).

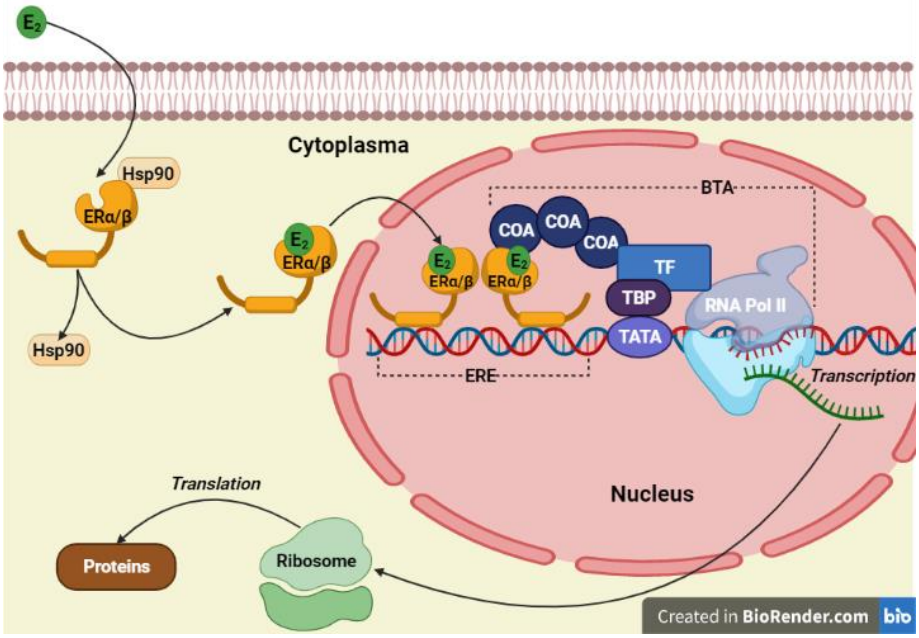

Figure 3: A simplified depiction of the main mechanism of ligand dependent ER action.

A lipophilic estrogen like E2 passes through the cell's membrane via diffusion. The inactive ERs in the cytoplasm are bound via LBD to Hsp90 which dissociates and is replaced by E2. The complex translocated in the nucleus, dimerizes and binds to the ERE of the target gene promoter via DBD. This recruits a basal transcription apparatus (BTA) to the TATA box of the promoter. The BTA consist of the TBP, various TFs, co-activators (CoA) and the RNA polymerase II (RNA Pol II) and facilitates the transcription of the specific gene to its respective mRNA. Translation takes place outside the nucleus in the ribosomes which results in the production of specific proteins (Ceccarelli, et al., 2022).

2.1.2. Tissue distribution and effects

The receptors can be found in diverse abundances in different regions of the brain. ERα is involved in the regulation of reproduction while both - ERβ more so - have a role in cognitive behavior. E2 is a powerful regulator for neural mechanisms, thus affecting memory formation, mood and pain sensitivity (Baber, 2013; Ceccarelli, et al., 2022).

Estrogens are also capable of decreasing plasma concentrations of total low-density lipoprotein (LDL) cholesterol while increasing high-density lipoprotein (HDL) cholesterol (Wakatsuki, et al., 2001). These changes correlate to prevention of atherosclerosis thus reducing the incidents of heart attacks and strokes (Florian & Magder, 2008). Cardiovascular diseases are uncommon in pre-menopausal women, yet rise significantly after menopause. One reason for this is ovarian failure during which E2 production declines drastically, therefore inducing a change in the lipidogram. An increase in serum lipids could also potentially be associated with a gain in body mass and weight (Leeners, et al., 2017).

Another issue that arises with estrogen deficiency is osteoporosis. The skeleton is constantly being remodeled based on the ratio between osteoclasts and osteoblasts. Osteoclasts are responsible for excavating the bone matrix while osteoblasts lay down a new matrix (Manolagas, et al., 2013). E2 has been shown to have protective effects towards bone-forming osteoblasts while causing apoptosis of bone-resorbing osteoclasts, the latter relating to repression of pro-inflammatory cytokines. As a result, bone mineral density is increased. Therefore, a lack of E2 could lead to the loss of bone mass and bone strength, something that is observed in post-menopausal women, who are at a higher risk of bone fracture and musculoskeletal injuries (Krum, et al., 2008).

Estrogens are critical for the normal operation of the reproductive tract in females with ERβ being the dominant receptor form in ovaries (Schüler-Toprak, et al., 2018) while ERα is mainly expressed in the uterus (Biason-Lauber & Lang-Muritano, 2022). In the early stages of life, estrogens coordinate the development and function of female genitalia. Later on, they regulate the menstrual cycle and contribute to hormonal regulation of pregnancy. As mentioned above, the production of estrogen in the ovaries halts during menopause leading to complications involving anxiety, hot flashes, palpitations and brittle bones (Hiller-Sturmhöfel & Bartke, 1998). The most common clinical condition of menopause directly related to the female reproductive organs is senile vaginitis. Pathological changes in the vagina, including its atrophy, thinning of the mucosa and pH imbalance, result in decreased defense ability against bacterial infections and increased occurrences of inflammation (Sun, et al., 2022).

Hormone replacement therapy could alleviate all the symptoms mentioned so far. However, the well-established role of E2 and ERs in breast and ovarian cancer is a major risk. Breast cancer is the most prevalent form of cancer in women and roughly 80% is ER positive, with ERα dominating as the main mediator of action. Upon its activation by an estrogenic ligand, transcriptional regulation of oncogenic genes and suppression of cell cycle inhibitors or pro-apoptotic genes results in massive proliferation of cancer cells (Choo, et al., 2022). On the other hand, the significance of ERβ is less clear. Studies have shown a down-regulation of this receptor in preinvasive mammary tumors (Roger, et al., 2001). Together with its response to antihormonal therapy (Mann, et al., 2001) and the observation of cell growth inhibition when transfected in the MCF-7 breast carcinoma cell line suggest that it may have tumor suppressive effects (Behrens, et al., 2007). Additionally, findings by the group of Schüler-Toprak *et al*. (2018) showcased that ERβ induces a reduction in proliferation and migration of ovarian cancer cells as well as an activation of their apoptosis. That being said, a continuous effort is made to research alternative methods of hormonal therapy based on receptor selectivity.

2.2. Isoflavones

IFs, alongside lignans, coumestans and stilbenes belong to the category of phytoestrogens and are plant-derived, polyphenolic, non-steroidal compounds with a structural similarity to E2. Although they have been explored for their chemo-preventive properties, particularly for breast cancer, controversy arises due to their estrogen-like activity which may pose a health risk for certain individuals (Ceccarelli, et al., 2022). IFs are mainly found in fruits, vegetables and whole grains, yet amounts that are physiologically relevant are more present in soybeans and red clover. The consumption of such products is prevalent in Asian and Central American communities and starts from an early age. However, more recently with the rise of vegetarian and vegan diets, soy protein is seen as a meat alternative and soybeans are also a preferred protein source in animal feed (Grgic, et al., 2021). In order to better understand their effects, numerous studies have been conducted. However, interpretation and comparison of the results tend to be difficult, especially for clinical studies. A reason for this is inter-individual variability regarding bioavailability and metabolism of IFs. This denotes how important it is to investigate the biological activities of the metabolites themselves to elucidate the actions of IFs (Soukup, et al., 2016).

2.2.1. Properties

2.2.1.1 Structure and biochemistry

IFs are formed by the same biosynthetic pathway as flavonoids. As depicted in Figure 4, the basic backbone of IFs (3-phenyl-1,4-benzopyrone) is composed of one benzene ring (A) next to a heterocyclic one (C), the two of them forming a benzopyran ring system with a ketone residue at C4 of the pyran ring and an additional benzene ring (B) at C3 (Squadrito & Bitto, 2013).

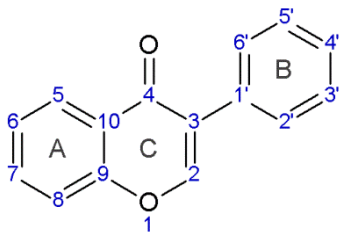

Figure 4: Main scaffold of IF structure.

Twelve dietary IFs are produced almost exclusively by legumes and can be categorized into four different groups: aglycones (genistein (GEN), daidzein (DAI), glycitein (GLY)), β-glucosides (genistin, daidzin, glycitin), acetylglucosides (acetylgenistin, acetyldaidzin, acetylglycitin) and malonylglucosides (malonylgenistin, malonyldaidzin, malonylglycitin). The highly polar, water soluble conjugated forms with the sugar moiety and their esterified versions are as such seen as biologically inactive and mostly found in plants and unprocessed foods. The chemical form of IFs influences their bioavailability and is susceptible to change during different processing methods (Kao, et al., 2004). This thesis focuses on the aglycones and their mammalian metabolites. The latter will be discussed in detail in 2.2.3. Metabolism.

The aglycones GEN (4’,5,7-trihydroxyisoflavone) and DAI (4’,7-dihydroxyisoflavone) are most relevant. When compared, GEN is characterized by an additional hydroxy group in C5, which makes it slightly more hydrophilic than DAI. This has also been associated with an increase in antioxidant activity (Rüfer, et al., 2006). GLY (4’,7-dihydroxy-6-methoxyisoflavone), biochanin A (5,7-dihydroxy-4′-methoxyisoflavone) and formononetin (7-hydroxy-4′-methoxyisoflavone) are all methylated derivatives, with the latter two being plant precursors of GEN and DAI respectively (Squadrito & Bitto, 2013).

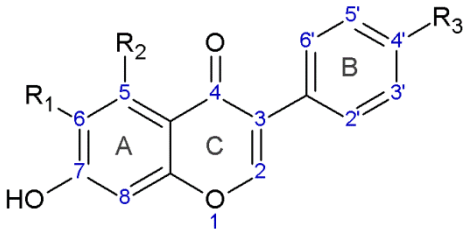

Isoflavones	R_1	R_2	R_3
Genistein	H	OH	OH
Daidzein	H	H	OH
Glycitein	OCH_3	H	OH
Biochanin A	H	OH	OCH_3
Formononetin	H	H	OCH_3

Figure 5: Chemical structures of five known IFs in their aglycone forms.

Despite being a metabolic product of DAI from gut bacteria, equol (EQ) is very often added to the group of phytoestrogenic IFs. Discovered in the 1930s by Marrian & Haslewood (1932) in horse urine, it only became relevant after its relation to the "clover disease" which caused breeding issues, such as infertility, for sheep grazing subterranean clover pastures in Western Australia (Bennetts, et al., 1946).

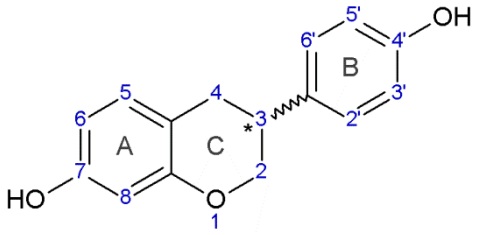

Figure 6: Chemical structure of equol. The stereocenter in C3 is denoted with '*'.

Unlike the aforementioned aglycones, EQ (7-hydroxy-3-(4'-hydroxyphenyl)-chroman) differentiates itself in the heterocyclic ring with a chiral centre on C3. Despite lacking a double bond between C2-C3 and the oxo-group in C4, EQ has been shown to have a higher antioxidant activity than DAI. Additionally, conformational difference between the two optically active isomers (R-(+)-equol and S-(-)-equol) would undoubtedly play a role when interacting with the LBD of the ER (Setchell, et al., 2005).

2.2.2. Occurrence

IFs are mainly, but not only, found in plant tissues and by-products of the *Leguminosae* (a.k.a. *Fabaceae*) family and the *Papilionidae* subfamily. Specifically, in germ/seeds and sprouts, IFs seem to participate in physiological processes regarding plant growth and act as phytoalexins and phytoanticipins, i.e. a defense mechanism against microbial plant pathogens

(Dakora & Phillips, 1996). Two notable examples rich in IFs are soybeans (*Glycine max L.*) and red clover (*Trifolium pratense L.*) (Bucar, 2013).

The predominant IF forms found stored in the vacuoles of soybeans are the malonyl derivatives of genistin, daidzin and glycitin (Cho, et al., 2020). The β-glucoside conjugates are present in non-fermented soy foods, such as soymilk, tofu, soy flour and soy protein. The conversion from IFs to their conjugates is mediated by glucosyl- and malonyltransferases respectively. The sugar moiety (mainly glucose) is lost upon fermentation (e.g., miso, tempeh) (Baber, 2013; Ghafoor, et al., 2013). The conjugated IF content can fluctuate between 1.3 and 9.5 mg IF/g soybean while the aglycone content in the order GEN>DAI>GLY ranges from 1 to 2.6 mg/g (Cho, et al., 2020). In Austrian pastures used for dairy production, Penagos-Tabares *et al.* found IFs to be the predominantly present groups but in much lower quantities of 8 to 129 μg/kg dry weight (DW). Environmental temperature was named as an influential factor for this occurrence (Penagos-Tabares, et al., 2021). Another study focused on the influence industrial treatments may have on pre-treated soybean samples (e.g., broken, flaked), dried okara using different methods and soybean oils. The general consensus was that mechanical and thermal treatments reduce the IF content of β-glucosides up to 37% yet do not impair the amount of aglycones, which are generally more stable (Privatti, et al., 2022).

Red clover is also rich in polyphenolic compounds and has thus gained interest as a novel dietary source. Formononetin and biochanin A are the main IFs found with 2-3 mg/g, followed by GEN and DAI with one tenth of these values (Krenn, et al., 2002). Another group focused on red clover sprouts due to their high nutritional value and low caloric content and compared their IFs profile with three other clover species. Quantitatively, red clover had the highest amounts of IFs between 204 and 426 mg/100 g DW while the other varieties did not go above 50 mg/100 g DW (Galanty, et al., 2022).

Looking at the aforementioned studies one can say that the composition and content of IFs in food products varies significantly. Influences include genotype, soil, altitude, temperature, postharvest processing including drying and storage conditions as well as processing techniques (e.g., heat treatment, cooking, enzymatic hydrolysis, fermentation, extraction methods) (Ferreira, et al., 2019).

2.2.3. Metabolism

The purpose of digestion is to break down food into smaller nutrients that are easier to absorb and provide energy to support the body's functions. This begins with the accessory organs of

the digestive system, the mouth, the tongue and the salivary glands. Here, mechanical breakdown by chewing as well as enzymatic (e.g., amylase in saliva) takes place. The produced bolus then travels through the esophagus to the stomach, the small intestine (duodenum, jejunum, and ileum), the large intestine (cecum, colon and rectum) all the way to the anus for the excretion of waste. The aforementioned organs make up the gastrointestinal tract (GIT) which marks the beginning of metabolism (Rogers, 2011).

2.2.3.1. Microbial transformation

Passive diffusion in the human GIT is difficult for the glycosylated forms of IFs because of their size and hydrophilic structure. Therefore, their bioavailability depends on either specific transporters or hydrolysis of the sugar moieties. Hydrolases take on the role for the latter. The β-glucosidases can be found in the gut microflora of the intestinal lumen and possess a high specificity for the IF glycosides (Day, et al., 1998). Another example is the enzyme lactase phlorizin hydrolase in the enterocyte, which has been shown to deglycosylate genistin and daidzin to GEN and DAI respectively (Day, et al., 2000). The aglycones are absorbed faster in the gut epithelium and enter thus the bloodstream which allows them to travel to other organs and undergo further metabolization.

The aglycones may also be derived from their methoxyl derivatives. Found in the human intestinal tract, *Eubacterium limosum* is an anaerobic bacterium that has been shown to be capable of *O*-demethylation of biochanin A and formononetin to GEN and DAI. Although GLY was also found to be demethylated, no further transformation to respective metabolites was observed (Hur & Rafii, 2000).

For both GEN and DAI, reductive metabolization can be mediated by bacterial strains of the *Eggerthellaceae* and *Coriobacteriaceae* families in the human gut microbiota. Reductases can transform GEN to dihydro-GEN (DHG), followed by either 6'-hydroxy-*O*-demethyl-angolensin (6-OH-ODMA) via a ring cleavage mechanism or tetrahydro-GEN (THG), which in turn forms 5-hydroxy-EQ (5-OH-EQ), a substance that has yet to be found in human biofluids (Soukup, et al., 2021). In the case of ruminants, a ring cleavage in GEN leads to the production of organic acids and p-ethylphenol, which is considered a non-estrogenic compound (Lundh, 1995).

A similar metabolic pathway is known for DAI, which is reduced to dihydro-DAI (DHD). DHD is either degraded via ring opening to *O*-demethyl-angolensin (ODMA) or further reduced to tetrahydro-DAI (THD). Most interesting for DAI is the increase in estrogenicity due to the transformation of THD to EQ (Soukup, et al., 2021). It should be mentioned that

according to Setchell *et al.* (2005) both EQ isomers are bioavailable, but human intestinal bacterial synthesis produces exclusively S-EQ.

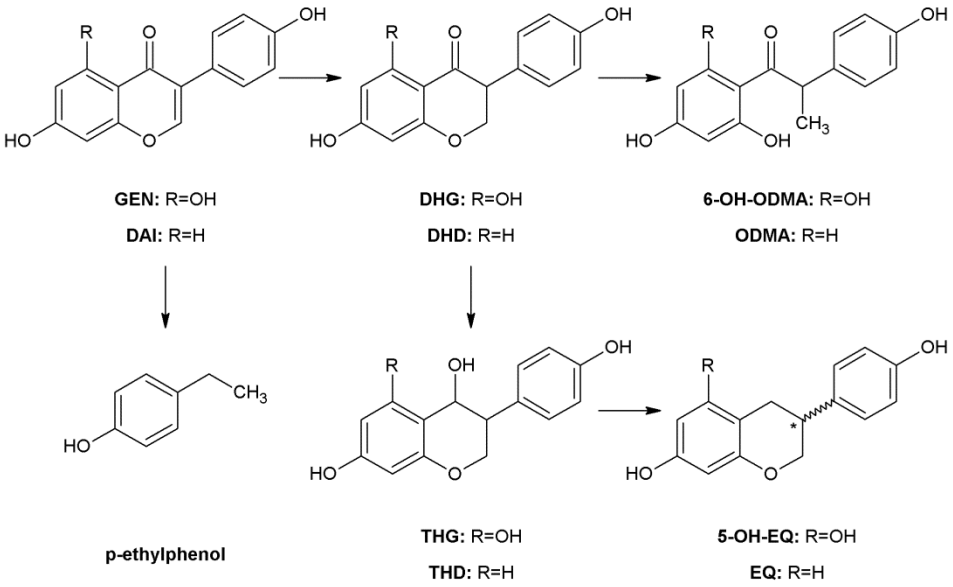

Figure 7: Possible reductive metabolization paths of GEN and DAI via gut bacteria.

Reductases mediate the formation of DHG/DHD which can either be further reduced to THG/THD or to 6-OH-ODMA/ODMA via ring opening. THG/THD is also further reduced to 5-OH-EQ/EQ. This pathway is present in humans and all livestock species with varying capacity (Soukup, et al., 2021). The pathway from GEN to p-ethylphenol is only present in ruminants (Lundh, 1995).

The ability to produce EQ is not always present and varies between species. Only about 20-35% of the Western adult population are considered to represent "equol producers" while in Asian countries, where the consumption of soy products is more common, the numbers are raised up to 50-55% (Setchell & Cole, 2006). The reason for this is attributed to differences in the compositions of each population's diets but potential non-dietary factors have also been considered, namely antibiotic use and alcohol consumption, all of which are associated with affecting the human microbiome. However, an exact explanation for the variability in EQ production remains unclear (Bolca, et al., 2007). On the other hand, almost every animal species that has been studied is capable of producing EQ (Setchell & Cole, 2006). Specifically, plasma concentrations of EQ in cattle were found to be 10 times higher than those in sheep (Lundh, et al., 1990) and very low EQ levels were found in urine samples of female pigs (Gu, et al., 2006).

2.2.3.2. Phase I

After the IF aglycones have crossed the GIT barrier, further metabolic processes take place in the intestine or liver. Phase I metabolism includes oxidative modifications which are mediated by cytochrome P450-dependent monooxygenases (CYP). The most relevant

enzyme for the hepatic metabolism of GEN and DAI has been shown to be CYP1A2, CYP2E1 to a much lesser extent and potentially the enzymes CYP1A1 and CYP1B1 (Atherton, et al., 2006).

Using rat liver microsomes, the group of Kulling *et al.* (2000) found GEN to be converted into six hydroxylated products, while DAI produced nine of them. Additionally, the monohydroxylated metabolites were themselves substrates for the enzymes, leading to the formation of di- and tri-hydroxylated compounds. Similarly for EQ, the metabolic pathway via rat liver microsomes showed the production of eleven metabolites consisting of mono- and dihydroxylated compounds, with 3'-hydroxy-EQ dominating (Rüfer, et al., 2006).

Furthermore, *in vitro* studies with human liver microsomes identified three monohydroxylated and three dihydroxylated metabolites of DAI. Significant amounts of five of them were also found in urine samples during *in vivo* experiments of the same group. GEN also transformed into six hydroxylated products, with three aromatic monohydroxylated compounds being the main metabolites. Five of them were detected in human urine samples, with an aliphatic hydroxylated metabolite being the sole exception (Kulling, et al., 2001). For EQ, six metabolites were produced by human liver microsomes, with 3'- and 6-hydroxy-EQ overpowering the rest. The 4-hydroxy-EQ, which was also present, has been detected previously in human urine samples (Rüfer, et al., 2006).

Very little information is available for the oxidative metabolism of IFs in farm animals.

2.2.3.3. Phase II

The metabolic pathways of phase II also take place in the small intestine and the liver and comprise two conjugation reactions involving enzymatic conversion. Uridine-5'-disphosphate glucuronyltransferases (UGTs) mediate glucuronidation by adding glucuronic acid from a nucleotide sugar to the IFs and forming a glycosidic bond between the two, thus creating glucuronides. Overall, fifteen UGT isoenzymes have been identified in humans and are coded by the genes UGT1 and UGT2. Sulfotransferases (SULTs) catalyze the sulfation of IFs by transferring a sulfate group from the donor substrate 3'-phosphoadenosine-5'-phosphosulfate. In human tissues, thirteen SULT isoenzymes have been detected and may be situated in the cytosol or on the membrane, with SULT1A1 and SULT1E1 playing major roles in regioselectivity of monosulfation and reaction catalysis (Nakano, et al., 2004). Both conjugation reactions are considered detoxification steps in the metabolism of IFs as they increase the polarity of the substances and make their excretion easier (Chan, et al., 2013). Overall, seven different phase II metabolites are common for GEN and DAI, consisting of

mono-, diglucuronides, mono-, disulfates and sulfoglucuronide combinations. EQ can form up to eight metabolites, however only two, a glucuronide and a sulfate, were considered in this thesis because they were commercially available. Conjugation takes place mainly in the C7 and C4' positions (Soukup, et al., 2014). Relevant for this thesis are seven GEN metabolites, namely GEN-7-sulfate (G7S), GEN-7-glucuronide (G7G), GEN-4'-glucuronide (G4'G), GEN-4',7-diglucuronide (G4',7dG), GEN-4',7-disulfate (G4',7dS), GEN-4'-glucuronide-7-sulfate (G4'G7S) and GEN-7-glucuronide-4'-sulfate (G7G4'S), seven DAI metabolites, namely DAI-4'-sulfate (D4'S), DAI-7-glucuronide (D7G), DAI-4'-glucuronide (D4'G), DAI-4',7-diglucuronide (D4',7dG), DAI-4',7-disulfate (D4',7dS), DAI-4'-glucuronide-7-sulfate (D4'G7S) and DAI-7-glucuronide-4'-sulfate (D7G4'S) and two EQ metabolites, namely EQ-7-glucuronide (E7G) and EQ-4'-sulfate (E4'S). All structures are summarized below.

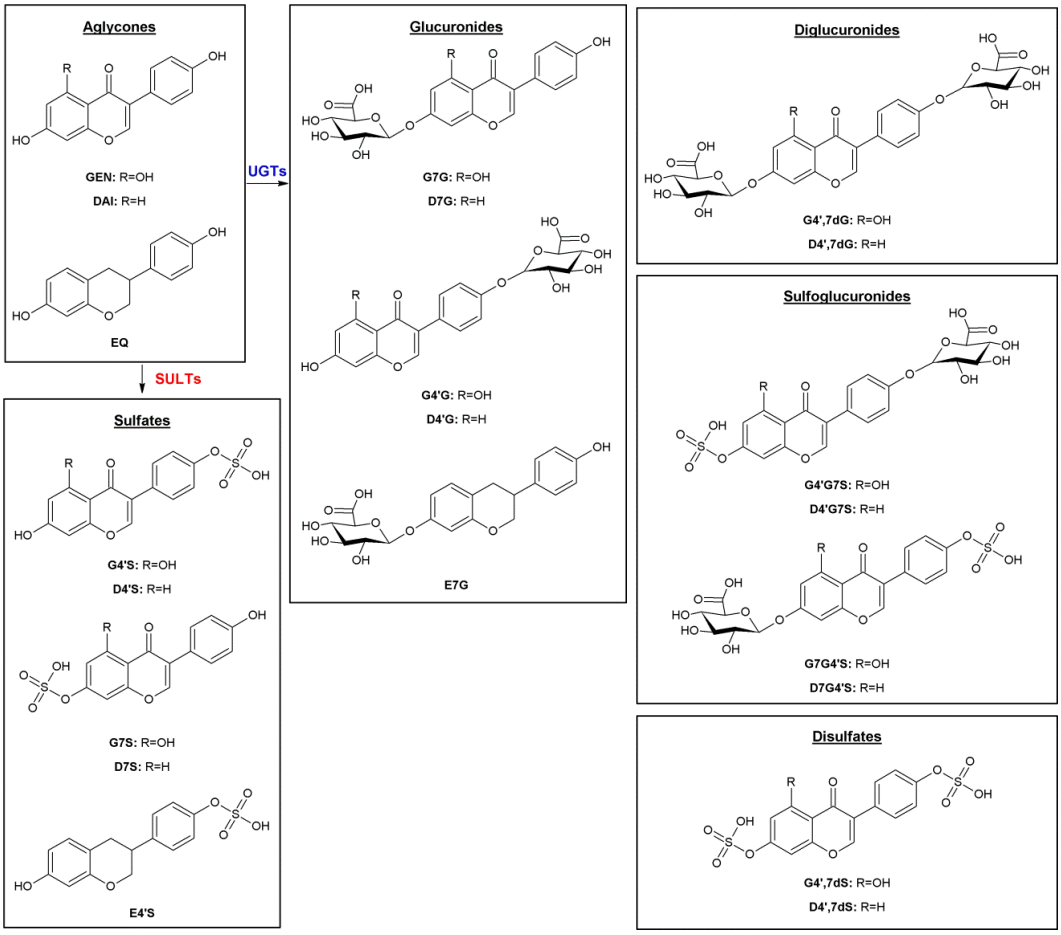

Figure 8: Summary of possible phase II metabolites of GEN, DAI and EQ.

The metabolites are categorised in groups of sulfates, glucuronides, diglucuronides, sulfoglucuronides and disulfates. To simplify the abbreviations, GEN, DAI and EQ are further abbreviated as G, D and E (always the first letter), while the glucuronide and sulfate groups are denoted with G and S respectively. Diglucuronides and disulfates are abbreviated as dG and dS.

Studies have been performed to investigate phase II metabolites of IFs in blood samples of humans and rodents. The main metabolites for GEN in human blood are G7G4'S and G4',7dG. Although there was no significant difference between female and male metabolic phenotypes, that was not the case for rodents. In female rats, G7G dominated while in male rats the G7G4'S metabolite was found in higher concentrations. Unlike humans and rats, mice exhibited more than one major metabolite. The highest concentrations were found to be the mono-conjugations of G7G and G7S for both genders, with only the female mice showing relevant concentrations of G7G4'S (Soukup, et al., 2016).

Findings for DAI and its metabolites in blood are similar to those of GEN but with some major differences. In humans, the diglucuronide was not detected in high concentrations and the only major metabolite was G7G4'S. Another difference was observed in rats, with the G4',7dS being the main metabolite, followed by G7G4'S. Lastly, only the single conjugates were present in mice with the addition of the aglycone (Soukup, et al., 2016). The observations made in humans could be explained with the specificity UGT1A10 shows for GEN, while both GEN and DAI are good substrates for UGT1A9 (Doerge, et al., 2000). SULTs however may not be responsible for the sulfation of DAI but a different enzyme that has yet to be characterized. As for rats, the increase in DAI sulfate conjugates could correlate to a higher and specific SULT activity in the liver and intestines (Ronis, et al., 2006).

Finding EQ in human plasma samples is more complicated due to the fact that not everyone is capable of producing the metabolite. Rats on the other hand produce mainly E7G, regardless of gender, and at high quantities. E4'S appears only in male rats. Both female and male mice were capable of producing the two metabolites (Soukup, et al., 2016).

With regards to farm animals, sheep show a higher conjugative activity compared to cattle in the majority of the GIT system. Overall, glucuronidation is the main conjugation reaction for DAI and EQ (Lundh, 1990; Grgic, et al., 2021).

2.2.3.4. Enterohepatic circulation and excretion

The final phase of metabolism is the excretion of the substances via bodily fluids or their transfer to different tissues. IFs may be excreted via the feces after bacterial metabolism in the colon but the majority of them and their metabolites are found in plasma or urine (Park & Ko, 2013). Yet, it is possible that a small amount undergoes enterohepatic circulation which may lead to accumulation. This has been the case for GEN and its metabolite G7G in rats. The substances were absorbed from the intestine, extracted from the portal vein blood into the liver and excreted into bile which may be reabsorbed into the small intestine and

transported back to the liver (Sfakianos, et al., 1997). However, studies are lacking in this regard and the focus remains on urinary excretion.

According to Zhang *et al.* (2003) around 70% of GEN and DAI glucuronides were found in female urine samples, followed by 20% of the sulfate conjugates and only traces of the aglycones. Excretion of the conjugated forms of IFs via urine was also observed in the case of cows, whereas the aglycones were excreted via feces. Interestingly enough, IFs have been found in milk samples of lactating ruminants with varying concentrations especially for EQ (Höjer, et al., 2012). Glucuronides of GEN and DAI were also mainly excreted via urine in pigs while rats were capable of excreting 40-50% of the aglycones as well. EQ was also found in rat urine samples mainly as glucuronide and in lower concentrations as aglycone (Gu, et al., 2006).

2.2.4. Estrogenicity and health effects

Due to of the structural similarity of IFs with E2, the substances are able to interact with ERs, alter ER structure and interact with coactivators. Based on tissue specificity as well as the ERα/ERβ ratio, they may act as partial agonists/antagonists, an ability that could potentially categorize them as natural selective estrogen receptor modulators (SERMs) (Setchell, 2001). In addition to this, IFs have been known to have a higher affinity for ERβ which is not the main receptor for e.g. the uterus. This opens up a variety of possibilities relating to targeting specific tissues while avoiding certain estrogenic effects (Kuiper, et al., 1997). Despite the 40-fold selectivity GEN has for ERβ and its binding being comparable to that of E2, it is interesting that the helix 12 conformation adopted is antagonistic rather than agonistic indicating that the transcriptional response to the bound ligand might play a bigger role (Pike, et al., 1999). EQ also has a preferential affinity for ERβ which is comparable to that of GEN. That is however only the case for the S-enantiomer as R-EQ binds much weaker and has a preference for ERα. Both of their affinities are higher than that of their precursor DAI, whereas the metabolic transformation of DAI to ODMA reduces estrogenicity greatly. This is a prime example of metabolism altering the biological activity of a substance (Muthyala, et al., 2004).

Due to the fact that phase II metabolism leads to detoxification of parent compounds, it has been assumed that IF conjugates are not estrogenic. This is the case for DAI and GEN 7-*O*-glucuronides which have been shown to exert weak estrogenic activity in mouse uterine cytosolic ERs. Specifically, the activity of G7G was higher than that of D7G (Zhang, et al., 1999). On the other hand, sulfation at the 7-position for DAI has been found to increase

estrogenic activity greatly, while sulfation in the same position for both EQ and GEN decreased said activity in MCF-7 human breast cancer cells (Pugazhendhi, et al., 2008). Yet very little information is available for the majority of the metabolites and the effects they may exert with regards to estrogenic activity.

2.2.4.1. Humans

Much like estrogens, phytoestrogens may increase the risk of cancer in estrogen-sensitive tissues, something that *in vitro* animal and epidemiological studies suggest. Clinical studies on the other hand focus mainly on positive effects IF may have on bone metabolism, cardiovascular diseases, obesity, brain function and different types of cancer (Ceccarelli, et al., 2022).

A randomized controlled one-year trial in postmenopausal women was conducted to investigate whether soy protein with IFs improves cognitive function, bone mineral density (BMD) and plasma lipids. However, no improvement was observed (Kreijkamp-Kaspers, et al., 2004). Similarly, another one-year trial found no positive effects of consuming IF rich products relating to BMD, bone metabolism and hormonal status in early postmenopausal women (Brink, et al., 2008). Trials that have showcased favorable results involve Asian populations, something that is usually associated with the intake of a long-term soy diet, especially in early childhood as well as the ability to metabolize DAI to EQ (Chen, et al., 2016).

Long term studies have been performed on rodents to assess the influence of IFs on breast cancer using rodent tumor models and are reviewed in Hüser *et al.* (2018). IFs may affect tumor initiation, development and manifestation. The majority of those studies found no noteworthy adverse effects when compared to control animals and some even showed preventive effects when IF exposure was during prepubescence. On the other hand, studies regarding the influence in pre-existing tumors and cancer cells were contradictory and highly dependent on parameters such as soy processing of the animal feed used and cultivation conditions of the MCF-7 cells implanted. Only GEN appeared to stimulate the growth of pre-existing ER positive breast cancer cells (Hüser, et al., 2018).

However, a comparison to human studies is not possible without taking into consideration the different physiologies, and most importantly, the role of metabolism. Rodents and humans differ mainly in the ability to produce EQ from DAI as well as the absorption and distribution of the different metabolites (see 2.2.3. Metabolism), once more denoting the importance of

investigating said substances to better elucidate the effects, they may exert in different cancerogenic cells.

2.2.4.2. Farm Animals

Studies on the effects IFs may have on farm animals have also been conducted over the past few decades and are summarized in the review of Grgic *et al.* (2021). To name a few examples, positive effects correlate an increase in antioxidant capacity in tissues of pigs with a high DAI dosage. However, this also induced pro-oxidant changes in liver and fat tissues (Chen, et al., 2016). Growth performance of pigs was observed to increase upon supplementation of IFs in the animal's diet yet compared to previous studies, the results differed (Li, et al., 2020). Similar growth improvement has been investigated in ruminants with positive results specifically for red-clover fed lambs (Speijers, et al., 2005). Despite the aforementioned studies showcasing some positive effects, the most common adverse effects are related to reproductive abilities. Amongst ruminants, cattle are less sensitive when exposed to IF, with sterility being only a temporary effect that is reversed after a change in diet (Lundh, et al., 1990). On the other hand, sheep that grazed clover pastures showed signs of infertility in what later became known as the "clover disease" (Bennetts, et al., 1946). All these different effects highlight the complexity of investigating how IFs affect different farm animals. Physical attributes (e.g. weight differences between cattle and sheep), ER ratios in different tissues, diet composition with regards to IFs and feeding times to name a few may influence results.

3. Aim of the thesis

Legumes and especially soybeans are rich in the phenolic phytoestrogens isoflavones. Due to the similarities between the steric structure of these compounds to the major female sexual hormone 17β-estradiol, isoflavones can bind to human estrogen receptors and thus exert estrogenic properties (Grgic, et al., 2022). Over the past two decades, research has focused on their possible influence on the prevention of hormone sensitive breast cancers (Hüser, et al., 2018), as well as various effects on cardiovascular and skeletal health (Chen, et al., 2016), cognitive function and others. Isoflavones have additionally been marketed as food supplements to alleviate menopausal symptoms. However, the concentration of the substances in these products far exceeds those accompanying a soy-rich diet and should be used with caution. The last published risk assessment of EFSA (2015) rejected the hypothesis of adverse effects on the thyroid and mammary glands as well as the uterus of post-menopausal women because of inconclusive animal studies. Despite this, the parameters of animal experiments do not necessarily correspond to the complex interactions in humans, since the metabolism between the two differs significantly and the duration of intakes investigated (three months up to a year) were too short. Due to the aforementioned characteristics, the purpose behind this thesis is to investigate the estrogenic potential of known isoflavones and their phase II metabolites *in vitro*.

The thesis was funded by the Austrian Research Promotion Agency (FFG) and is conducted in cooperation with the company DSM-BIOMIN, which specializes in animal nutrition and feed additives with mycotoxin risk management as one of their focus areas. Additionally, all the substances were provided by Prof. Dr. Sabine E. Kulling from the Max Rubner-Institut situated in Karlsruhe, Germany.

The experiments were conducted using the human endometrial adenocarcinoma cell line Ishikawa, which expresses both estrogen receptor α and β. Overall, the isoflavones genistein, daidzein and equol alongside 16 metabolites (glucuronides, diglucuronides, sulfates, disulfates and the glucuronide-sulfate-modification) were tested on their estrogenic activity via alkaline phosphatase (ALP) assay. To exclude a decrease in said activity caused by cytotoxicity, research was conducted with cytotoxicity assays, such as the CellTiter-Blue® (CTB) and the sulforhodamine B (SRB) assay. With regards to concentrations, we tested a range from 0.001 to 10 μM which includes both concentrations that might be present systematically and concentrations which exert high estrogenicity. Furthermore, we

investigated possible conversions of the aforementioned compounds to the aglycones and the metabolites using liquid chromatography coupled to tandem mass spectrometry.

The outcomes of this master thesis will provide important information for the risk assessment and risk evaluation of isoflavones and their phase II metabolites as well as metabolic pathways within an endometrial cancer cell line.

4. Materials and methods

4.1. Materials

4.1.1. Chemicals

The chemicals used during the experiments are listed in Table 1.

Table 1: Chemicals and corresponding production companies.

Name	Company
4-Nitrophenyl phosphate (4-NPP)	Sigma Aldrich Chemie GmbH, Schnelldorf, DE
Acetic acid	Carl Roth GmbH + Co. KG, Karlsruhe, DE
Acetonitrile (ACN) (≥99.9%)	CHROMASOLV™ LC-MS, Honeywell Riedel-de Haën™, Seelze, DE
CellTiter-Blue® (CTB) Cell Viability Assay Kit	Promega Corporation, Madison/ WI, USA
Charcoal stripped FBS (CD-FBS)	Gibco, Thermo Fisher Scientific, Waltham/ MA, USA
Dimethyl sulfoxide (DMSO)	Carl Roth GmbH + Co. KG, Karlsruhe, DE
Dulbecco's modified Eagle medium /F12 (DMEM/F-12) (1x), w/o: phenol red	Gibco, Thermo Fisher Scientific, Waltham/ MA, USA
Ethanol	Brenntag Austria GmbH, Vienna, AT
Fetal bovine serum (FBS), South America origin	Gibco, Thermo Fisher Scientific, Waltham/ MA, USA
L-Glutamine	Gibco, Thermo Fisher Scientific, Waltham/ MA, USA
Methanol	CHROMASOLV™ LC-MS, Honeywell Riedel-de Haën™, Seelze, DE
Minimal essential medium (MEM) (1x)	Gibco, Thermo Fisher Scientific, Waltham/ MA, USA
Penicillin-streptomycin (P/S)	Gibco, Thermo Fisher Scientific, Waltham/ MA, USA
Phosphate buffered saline (PBS)	Carl Roth GmbH & Co., Karlsruhe, DE
Sulforhodamine B (SRB)	Sigma Aldrich Chemie GmbH, Schnelldorf, DE
Trichloroacetic acid (TCA)	Carl Roth GmbH + Co. KG, Karlsruhe, DE
Tris (hydroxymethyl-) aminomethane (Tris)	Carl Roth GmbH + Co. KG, Karlsruhe, DE
Trypan blue	Sigma Aldrich Chemie GmbH, Schnelldorf, DE
Trypsin, 5 000 USP-U/mg, free from salt, from porcine pancreas, lyophilized	Carl Roth GmbH + Co. KG, Karlsruhe, DE
Water, distilled	Faculty line, Department of Chemistry, University of Vienna, Vienna

4.1.2. Consumables

All consumables used during the experiments are listed in Table 2.

Table 2: Consumables and their corresponding companies.

Name	Company
96-well plate, black	Sarstedt AG & Co, Nümbrecht, DE
96-well plate, standard (red), sterile	Sarstedt AG & Co, Nümbrecht, DE
Cell culture flasks, standard (red), sterile; sizes T-75/T-175	Sarstedt AG & Co, Nümbrecht, DE
Crimp vial caps	11 mm, TEF, Bruckner Analysentechnik GmbH, Linz, AT
Crimp vials	1.5 mL, brown or transparent glass, Bruckner Analysentechnik GmbH, Linz, AT
Falcon tubes; sizes 15 mL, 50 mL	Sarstedt AG & Co, Nümbrecht, DE
Gloves	KIMTECH™, Kimberly-Clark Worldwide Corporation, Dallas/ TX, USA
HPLC column	Ascentis Express C18 column, 10 cm × 2.1 mm, 2.7 µm, Supelco, Munich, DE
HPLC guard column	SecurityGuard™ C18 Cartridges, 4 × 2.0 mm ID, Phenomenex Ltd. Deutschland, Aschaffenburg, DE
Light-duty tissue wipers	VWR International, Radnor/ PA, USA
Microscope cover glasses	24 x 24 mm, thickness 0.17 ± 0.005 mm, VWR Austria, Wien, AT
Pasteur pipettes	Carl Roth GmbH + Co. KG, Karlsruhe, DE
Pipette tips, non-sterile; sizes 10 µL, 200 µL, 1000 µL, 5 mL	VWR Austria, Vienna, AT
Reaction tubes; sizes 0.5 mL, 1.5 mL, 2 mL	Sarstedt AG & Co, Nümbrecht, DE
Serological pipettes; sizes 15 mL, 25 mL	Sarstedt AG & Co, Nümbrecht, DE
Vacuum filtration unit	Filtropur V50, 500 ml, membrane: PES, Ø membrane: 90 mm, pore size: 0.2 µm, sterile, Sarstedt AG & Co, Nümbrecht, DE

4.1.3. Cell Line

The cell line used during the experiments was the human adenocarcinoma cell line Ishikawa, purchased from the European Collection of Authenticated Cell Cultures (ECACC) purchase number 99040201 (Public Health England, Salisbury, UK).

4.1.4. Instruments

The instruments used during the experiments are listed in Table 3.

Table 3: Instruments and their corresponding companies.

Name	Company
Autoclave	Systec DX-150, Systec GmbH, Weltenberg, DE
Balance	Adventurer™, AX224, OHAUS, Greifensee, CH Excellence Plus Micro Balance XP26, Mettler-Toledo GmbH, Gießen, DE KB 3600-2N, Kern & Sohn GmbH, Balingen, DE NewClassic MF, ML6001/01, Mettler-Toledo GmbH, Gießen, DE NewClassic MF, ML204/01, Mettler-Toledo GmbH, Gießen, DE
Centrifuge	Z 326 K, Hermle Labortechnik GmbH, Wehingen, DE
Crimper 11 mm	Supelco, Munich, DE
Decapper 11 mm	Supelco, Munich, DE
Dispenser Pipette	BRAND™ HandyStep™, BRAND GMBH + CO KG, Wertheim, DE
Drying and heating oven	ED115, BINDER GmbH, Tuttlingen, DE
Fridge/Freezer	Liebherr Premium Comfort (4°C, -20 °C, -80 °C), Liebherr, Bulle, CH
HPLC system	1260 Infinity II Prime LC System, Agilent, Santa Clara/CA, USA
Ice machine	MF 46, Scotsman Frimont, Mailand, IT
Incubator	Heracell 240 L CO_2-Incubator, Thermo Fisher Scientific, Waltham/ MA, USA
Inverse microscope	Axiovert 40C, Zeiss Objective: A-Plan, Carl Zeiss Microscopy GmbH, Jena, DE
Laminar flow hood	Hera Safe KS 18, Thermo Fischer Scientific, Waltham/ MA, USA
Magnetic Stirrer	IKA® RCT basic safety control, IKA-Werke GmbH & Co KG, Staufen, DE
Microbalance	DeltaRange, XP26, Mettler Toledo, Greifensee, CH
Multichannel pipette	10 – 100 µL (8-channel), Eppendorf Research, Hamburg, DE 50 – 300 µL (8-channel), Labemate Pro, Corning HTL SA, Warszawa, PL
Neubauer counting chamber	Paul Marienfeld GmbH & Co. KG, Lauda-Königshofen, DE
pH-meter	PC 8 + DHS, XS Instruments, Carpi MO, IT

Table 3: continued

Name	Company
Pipettes	10 µL, 20 µL, 100 µL, 200 µL, 1 000 µL, 5 mL, Eppendorf Research, Hamburg, DE Labemate Pro, Corning HTL SA, Warszawa, PL
Pipetting device	Pipetus® Akku, Hirschmann Laborgeräte, Eberstadt, DE
Plate Reader	Victor3V, 1420 Multilabel Counter, Perkin Elmer, Waltham/ MA, USA Synergy H1 Plate Reader, BioTek, Winooski/ VT, USA Cytation 3 Cell Imaging Multi-Mode Reader, BioTek, Winooski/ VT, USA
Plate Shaker	MS 3 control, IKA®-Werke GmbH & Co. KG, Staufen, DE
Pump Vacuum Aspiration System	Vacusafe, INTEGRA Biosciences AG, Zizers, CH
MS System	QTRAP® 6500+, Sciex, Framingham/MA, USA
Vortexer	Lab dancer S40 VWR Deutschland, Darmstadt, DE
Water bath	GD 100 Grant Instruments, Cambridge, UK

4.1.5. Programs

The programs and softwares used for the experiments are listed in Table 4.

Table 4: Programs used and their corresponding companies.

Name	Company
Analyst v. 1.7	Sciex, Framingham/ MA, USA
BioRender (biorender.com)	BioRender, Toronto/ OH, USA
Gen5™ Version 3.08	BioTek Instruments, Winooski/ VT, USA
Microsoft® Excel® 2010	Microsoft Corporation, Redmond/ WA, USA
Origin Pro® 2019	OriginLab Corporation, Northampton/ MA, USA
Skyline v. 22.2	MacCoss Lab Software, University of Washington, Seattle/ WA, USA
Wallac 1420 Workstation	Perkin Elmer, Waltham/ MA, USA

4.1.6. Test substances

The test substances, which were provided by Prof. Dr. Sabine E. Kulling from the Max Rubner-Institut situated in Karlsruhe, Germany and used for the experiments are listed in Table 5.

Table 5: Test substances including, if available, purities and corresponding origins.

Name	Company
(S)-Equol (EQ) (99.3%)	LC Laboratories®, Woburn/ MA, USA
(S)-Equol-4'-sulfate (E4'S) (90%)	Santa Cruz Biotechnology Inc.
(S)-Equol-7-glucuronide (E7G) (98%)	Santa Cruz Biotechnology Inc.

Table 5: continued

Name	Company
17β-Estradiol (E2)	Sigma Aldrich Chemie GmbH, Schnelldorf, DE
Daidzein (DAI) (99.2%)	LC Laboratories®, Woburn/ MA, USA
Daidzein -4',7-diglucuronide (D4',7dG) (93%)	Toronto Research Chemical Inc., Toronto/ON, CA
Daidzein -4',7-disulfate (D4',7dS) (99.5%)	Max Rubner Institute, Karlsruhe, GE
Daidzein -4'-glucuronide-7-sulfate (D4'G7S) (98.7%)	Toronto Research Chemical Inc., Toronto/ON, CA
Daidzein -4'-sulfate (D4'S)	Toronto Research Chemical Inc., Toronto/ON, CA
Daidzein -7-glucuronide (D7G) (99.2%)	Toronto Research Chemical Inc., Toronto/ON, CA
Daidzein -7-glucuronide-4'-sulfate (D7G4'S) (100%)	Toronto Research Chemical Inc., Toronto/ON, CA
Daidzein-4'-glucuronide (D4'G) (94.4%)	Toronto Research Chemical Inc., Toronto/ON, CA
Genistein (GEN) 100%)	LC Laboratories®, Woburn/ MA, USA
Genistein-4',7-diglucuronide (G4',7dG) (90.8%)	Toronto Research Chemical Inc., Toronto/ON, CA
Genistein-4',7-disulfate (G4',7dS) (99.4%)	Max Rubner Institut, Karlsruhe, GE
Genistein-4'-glucuronide (G4'G) (99%)	Toronto Research Chemical Inc., Toronto/ON, CA
Genistein-4'-glucuronide-7-sulfate (G4'G7S) (98.9%)	Toronto Research Chemical Inc., Toronto/ON, CA
Genistein-7-glucuronide (G7G) (95%)	Toronto Research Chemical Inc., Toronto/ON, CA
Genistein-7-glucuronide-4'-sulfate (G7G4'S) (99%)	Toronto Research Chemical Inc., Toronto/ON, CA
Genistein-7-sulfate (G7S)	Toronto Research Chemical Inc., Toronto/ON, CA

4.2. Methods

4.2.1. Cell culture

The Ishikawa human cancer cell line was established in 1985 by the group of Nishida *et al.* in Japan (Nishida, et al., 1985). The cells were isolated from a 39-year-old Japanese female patient, who was diagnosed with endometrial adenocarcinoma stage 2. Culturing the adherent cell line forms a monolayer of botryoidal appearing cells and notable dome structures, as can be seen in Figure 9.

The doubling time of the population is approximately 36 hours till the 9th passage, and is reduced to 29 hours at the 40th passage. After the 45th passage, undifferentiated cells are built (Nishida, 2002). Therefore, only cells until passages 30-35 were used in this thesis.

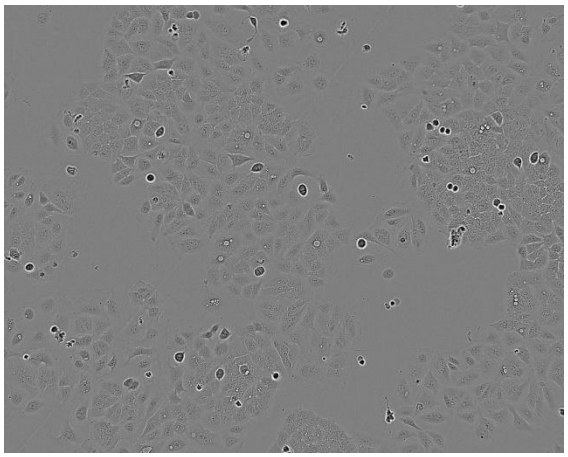

Figure 9: Ishikawa cells 48 hours post seeding (UK Health Security Agency, n.d.).

The major characteristic of this cell line, are the estrogen (both α and β) and progesterone receptors, which makes them suitable for the investigation of compounds with possible estrogenic effects. However, these receptors are no longer detectable after the 50th passage (Nishida, 2002).

4.2.1.1. Cell cultivation

Sterilization

During work in cell culture, protective gloves and lab coat were worn. The gloves, work surface, i.e. the laminar hood, as well as all objects placed inside (e.g. falcon tubes, serological pipettes) were sprayed beforehand with a 70% ethanol solution in order to maintain a sterile working environment. Additionally, all used materials that came in contact with the cells (e.g. syringes, plates) were sterile.

Media preparation

For the purpose of ensuring a supply of nutrients (e.g. amino acids, vitamins, etc.) essential for the vitality and growth of the culture, MEM was used as a cultivation medium. This medium also contained Earle's salts, non-essential amino acids and sodium bicarbonate. Phenol red allowed for a visual indication of a pH change, which might occur in the case of contamination or high concentrations of metabolic compounds. In physiological pH conditions (around 7.4) the indicator had a bright cherry red color. If the pH reached above 7.6 it turned violet and below 7.2 it became yellow. Before usage, the medium bottle was supplemented with 5% FBS for additional growth factors (25 mL) and 1% L-glutamine

(5 mL) as an important energy source. Due to the instability of L-glutamine during longer exposures at 37 °C, the medium bottle was kept at 4°C in the fridge. At the beginning of each week, a falcon tube (50 mL) was prepared with MEM and 1% of the antibiotic P/S (0.5 mL) to avoid bacterial contamination (Gstraunthaler & Lindl, 2013).

Cell passaging

The cultivation took place in an incubator with the temperature setting of a mammalian body (37 °C) and an atmosphere of 5% carbon dioxide. Due to this, all solutions that came into contact with the cells were pre-warmed at the same temperature in a water bath. The time during which the cells were outside the incubator was kept at a minimum. The cells were kept in standard culture flasks (red) of sizes T-75 and T-175.

The proliferation rate decreases after a specific cell density. Therefore a regular change of medium for monolayer cell lines is necessary to guarantee a healthy growth and preservation of vitality (Gstraunthaler & Lindl, 2013). Passaging - also known as splitting- was performed twice a week (every 3-4 days) for the Ishikawa cells.

First, the confluence was examined under a microscope and was around 70-80%, with few exceptions. After the medium was aspirated with a Pasteur pipette connected to the vacuum pump in the laminar hood, pre-warmed PBS (5 mL for T-75; 9 mL for T-175) was added to the flask and equally distributed along the surface using a westward-southward motion to thoroughly rinse any remaining serum. The FBS contains protease inhibitors that inactivate trypsin and interfere with the splitting process (Gstraunthaler & Lindl, 2013). PBS was aspirated and pre-warmed trypsin (1.5 mL for T-75; 2.5 mL for T-175) was added to the flask which was moved around as described above to dissociate the cells from the surface. This process took place in the incubator for the duration of 5-7 minutes, since more than 10 minutes could result in irreversible damages to the cells. Afterwards, free movable cells were observed under the inverse microscope and to enhance the success of the process, the flask was tapped gently multiple times. Adding MEM supplemented with serum (4-5 mL for T-75; 6-9 mL for T-175) with a serological pipette stopped the trypsination and allowed transferring of the cell suspension to a falcon tube. At later passages (above 25) it was observed that the cells adhered to each other. To avoid this, a pipette was used to withdraw 4-5 mL of the suspension and gently release them at the side of the tube, providing mechanical force for separation. This was repeated a couple of times before the cells were counted.

Cell counting

The number of cells plays an important role for the speed with which they grow. If the cells are seeded thinly they grow very slowly and if they are densely packed they reach high confluence too quickly and must be sub-cultivated. With each sub-cultivation, the lifespan of the cells is also shortened (Gstraunthaler & Lindl, 2013). Therefore, cell counting must be done routinely, accurately and in a manner that allows for determination of cell vitality.

For this, the cell suspension (20 µL) was mixed with a trypan blue solution (80 µL) in a microliter tube. Trypan blue is an acidic, dark blue coloring agent, which as an anion easily binds to proteins that are only accessible in dead cells that have lost the integrity of their membrane. Living cells on the other hand remain uncolored (Gstraunthaler & Lindl, 2013).

After vortexing the tube, 10 µL of the blue solution were applied between the Neubauer counting chamber -a precision optical device- and its corresponding cover slip. The base plate is made of thick, special glass with two counting nets etched upon it, each consisting of 3x3 large squares (each with an area of 1 mm^2) as depicted in Figure 10.

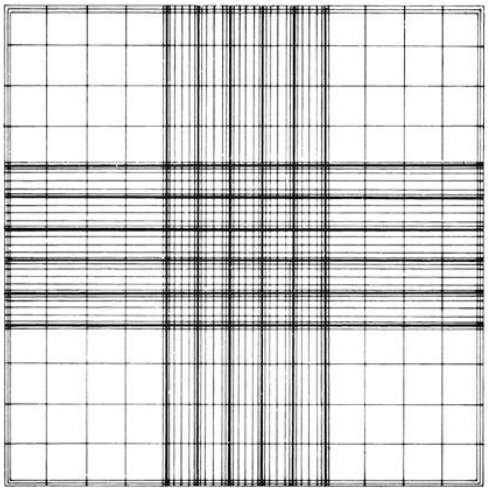

Figure 10: One counting net of the Neubauer counting chamber (Gstraunthaler & Lindl, 2013).

The four corner squares (each 4x4) were used for the counting of cells and observed under an inverse microscope. Cells outside of this area were not accounted for with the exception of cells found in the lines of 2/4 square sides (always the same sides for all 4 corners). To derive the cell number, the dilution factor (1:5) and the conversion of microliter to millilitre is incorporated per following equation.

$$\#cells/mL = \frac{1}{4} \cdot \sum (\#cells\ in\ 4\ compartments) \cdot 5 \cdot 10000$$

If dead cells (blue colored) were present, they were counted as well. To determine the vitality, the following equation was used.

$$\%\ living\ cells\ = \frac{uncolored\ cells}{uncolored + colored\ cells} \cdot 100\%$$

The lowest vitality observed was 94%, meaning that there was never a need to thaw new cells based on this aspect alone.

After counting, the calculated amount was used to divide the desired cell amount to derive the volume that would be added back to the flask, alongside MEM. Both quantities depended on flask size and growth period, which are summarized in Table 6. Each flask would be used for passaging subcultures for a maximum of three times and labelled with cell type (ISHI), passage number (PX+Y; X: passage before freezing; Y: passage after thawing), cells seeded, abbreviation of experimentator's name and date. After making sure that the flask contained cells by using the microscope, it was returned in the incubator till the next splitting day. The rest of the cell suspension was used in section 4.2.1.2. Cell seeding for estrogenicity and cytotoxicity assays.

Table 6: Cells seeded and medium volume needed for splitting based on growth period and flask size.

Growth Period	Flask Size	Seeded Cells	MEM [mL]
3 days	T-75	400 000	10-15
	T-175	500 000	
4 days	T-75	800 000	30-35
	T-175	1 000 000	

4.2.1.2. Cell seeding for estrogenicity and cytotoxicity assays

The remaining cell suspension in the falcon tube was centrifuged at a speed of 300 g and acceleration of 9 for 10 minutes. Theoretically, the temperature of the centrifuge should be at 37 °C, however due to unknown malfunctions of the machine that temperature was never reached. After enrichment, the supernatant was aspirated in the laminar hood and the pellet containing the cells was re-suspended in 5 mL of a different medium, namely DMEM/F-12. This modified version contains 1-4 times the concentration of amino acids, alongside other components like pyruvate, and is combined with a ham F-12 nutrient mixture. New 50 mL of the medium is prepared at the beginning of each week and supplemented with 5% charcoal stripped FBS (2.5 mL), which reduces the availability of hormones by binding to activated charcoal (Gstraunthaler & Lindl, 2013), and 1% P/S (0.5 mL). The reason the medium is changed, is because the indicator phenol red has been found to be a weak estrogen since it is structurally similar to nonsteroidal estrogens, like cyclofenil (Berthois, et al., 1986).

At this point, the cells are counted as described in 4.2.1.1. Cell cultivation. The amount depended on incubation time and was 150 000 cells/mL for 24 hours and 100 000 cells/mL for 48 hours.

For the three assays performed, the cells were seeded in sterile 96-well plates. Each week 2-8 plates were prepared, always in duplicates, as one was used for ALP and the other for CTB/SRB. Only the 60 inner wells of the plate were seeded with cells, each with 100 µL of the prepared DMEM/F-12 solution. Therefore, 7 mL were prepared for each plate (or 14 mL since the plates were prepared in duplicates; the calculated cell volume was multiplied with 14, added to a falcon tube and filled up to 14 mL with DMEM/F-12). The outer wells are subject to yielding varying results due to evaporation, commonly known as the edge effect (Mansoury, et al., 2021). These wells were filled with PBS (100 µL). In both cases a multistep pipette with a 2.5 mL syringe was utilized.

Lastly, the plates were labelled with cell type (ISHI), passage number, cells seeded, name, date, a unique number (e.g., E001). At the end of the day, they were placed in the incubator for 24 or 48 hours.

4.2.2. Incubation with test substances

After the cells were incubated for either 24 or 48 hours, it is necessary to make sure they appear healthy and are homogenously distributed before continuing with the experiments. This is done by observing randomly chosen wells under an inverse microscope, where the cells appear round in form and their surrounding background is light and lacks texture. If their environment looks grainy, almost like sand, this would be an indication of a contamination. Additionally, if one well is contaminated it might appear outside the microscope as cloudy or milky white in color, unlike the usual transparent liquid of the medium. In those cases, the wells are noted and excluded from calculations. If there are multiple contaminations in one plate, it may be disregarded completely and all chemicals used are to be closely inspected as possible sources, especially those that have been in falcon tubes for longer periods of time (e.g., PBS).

The incubation of the test substances begins with a layout. Overall, there are three IFs and 16 of their metabolites to be investigated (listed in Table 5). Each biological replicate contains a solvent control, a positive control and three test substances in five different concentrations, all of which are measured in triplicates, ergo three technical replicates per plate, to obtain mean values and standard deviations. Given that well position has been shown to influence

results (Mansoury, et al., 2021), the layout of each biological replicate was changed frequently to exclude this effect. An example of a layout is depicted in Figure 11.

	1	2	3	4	5	6	7	8	9	10	11	12
A	PBS no cells	PBS no cells	PBS no cells	PBS no cells	PBS no cells	PBS no cells	PBS no cells	PBS no cells	PBS no cells	PBS no cells	PBS no cells	PBS no cells
B	PBS no cells	E2 [1 nM]	E2 [1 nM]	E2 [1 nM]	GEN [10]	GEN [10]	GEN [10]	DAI [0.001]	DAI [0.001]	DAI [0.001]		PBS no cells
C	PBS no cells	DMSO [1%]	DMSO [1%]	DMSO [1%]	EQ [0.001]	EQ [0.001]	EQ [0.001]	DAI [0.01]	DAI [0.01]	DAI [0.01]		PBS no cells
D	PBS no cells	GEN [0.001]	GEN [0.001]	GEN [0.001]	EQ [0.01]	EQ [0.01]	EQ [0.01]	DAI [0.1]	DAI [0.1]	DAI [0.1]		PBS no cells
E	PBS no cells	GEN [0.01]	GEN [0.01]	GEN [0.01]	EQ [0.1]	EQ [0.1]	EQ [0.1]	DAI [1]	DAI [1]	DAI [1]		PBS no cells
F	PBS no cells	GEN [0.1]	GEN [0.1]	GEN [0.1]	EQ [1]	EQ [1]	EQ [1]	DAI [10]	DAI [10]	DAI [10]		PBS no cells
G	PBS no cells	GEN [1]	GEN [1]	GEN [1]	EQ [10]	EQ [10]	EQ [10]					PBS no cells
H	PBS no cells	PBS no cells	PBS no cells	PBS no cells	PBS no cells	PBS no cells	PBS no cells	PBS no cells	PBS no cells	PBS no cells	PBS no cells	PBS no cells

Figure 11: Example of an incubation plan of the 96-well plate.

The depiction includes the positive control (E2), solvent control (DMSO) and test substances (GEN, DAI, EQ) with varying concentrations in µM (unless stated otherwise in the brackets).

The solvent control utilized was 1% DMSO, as it was the solution used to dissolve the test substances and further dilute them to achieve the desired concentrations. E2 was used as a positive control with a concentration of 1 nM. According to Holinka *et al.* (1986) an E2 concentration of 1-100 nM yields a maximum response of ALP activity. Additionally, 1 nM was chosen as a realistically physiological concentration due to E2 serum values during the menstrual cycle of women being shown to vary between 0.147 nM and 1.47 nM (Bruhn, et al., 2011).

Procedure

The stocks of the test substances were prepared according to the following equation,

$$c = \frac{n}{V} = \frac{m}{M \cdot V} \rightarrow m = c \cdot M \cdot V$$

with *m* the mass of each substance, *c* the concentration, *M* the molar mass of each substance and *V* the volume of the solvent (1% DMSO). All stocks corresponded to a concentration of 10 mM and were stored in the freezer at -80 °C. Since each plate consisted of three technical replicates (100 µL each) and from the same passage two plates were prepared (one for ALP

and one for CTB/SRB), 700 µL of the substance to be incubated were prepared. The serial dilution with DMSO is shown in Table 7.

Table 7: Serial dilution of 10 mM stock of test substance with DMSO in five different concentrations.

S	Concentration [µM]	Volume (Substance) [µL]	Volume (DMSO) [µL]
1	1000	1 (Stock)	9
2	100	1 (S1)	9
3	10	1 (S2)	9
4	1	1 (S3)	9
5	0.1	1 (S4)	9

Table 8 shows how the substances were further diluted (1:100) using the assay medium that was previously prepared using DMEM/F-12, CDFBS and P/S.

Table 8: Preparation of the concentrations of test substances for ALP and CTB/SRB using the assay medium (AM).

ALP, CTB/SRB	Concentration [µM]	Volume (Substance) [µL]	Volume (AM) [µL]
1	10	7 (S1)	693
2	1	7 (S2)	693
3	0.1	7 (S3)	693
4	0.01	7 (S4)	693
5	0.001	7 (S5)	693

It is of importance to note that during this procedure both DMSO and the pre-warmed assay medium were placed first in the corresponding, labelled micro tubes. This was done in order to avoid leaving the stocks outside the freezer for longer periods of times and to speed up the dilution process.

Once the concentrations have been prepared, the plate seeded with cells was removed from the incubator and placed in the laminar hood, where the medium was aspirated with a yellow tip connected to a vacuum pump. Using a micropipette, 100 µL of each concentration of the isoflavones or metabolites was transferred to their perspective wells according to the layout. This process was done in rows of three to avoid leaving the cells too long in an environment lacking medium. After the final concentration has been added to the plate, it was returned to the incubator. Similarly, the other plate of the same passage was prepared. The incubation of the cells with the test substances lasted approximately 48 hours.

4.2.3. Estrogenicity assay

4.2.3.1. Alkaline phosphatase assay

In order to investigate the estrogenicity of IFs and their metabolites, the biological, *in vitro* ALP assay was chosen (Littlefield, et al., 1990).

If a molecule is structurally similar to estrogen, it may enter the cell and activate ERs, leading to the production of different enzymes, like ALP. This process is explained in detail in 2.1.1.2. Classic ligand dependent pathway. The activity of ALP has been shown to be stimulated by human endometrial cancer cells, like the Ishikawa, which makes them suitable for this experiment (Holinka, et al., 1986).

Principle

ALPs are a group of homodimeric enzymes. Their catalytic sites contain three metal ions, two zinc and one manganese, which are vital for their enzymatic activity. These enzymes are capable of catalyzing the hydrolysis of monoesters of phosphoric acid in alkaline conditions, thus working as phosphohydrolases and phosphodiesterases (Millán, 2006). Therefore, the principle of the assay (depicted in Figure 12) is based on the cleavage of a phosphate group from the colorless, light-sensitive 4-NPP. The yellow product, para-nitrophenol, is then photometrically measured at 405 nm to determine its amount and consequently the quantity of ALP.

Procedure

The ALP-assay was conducted according to Lehmann *et al.* (2006) and optimized by Vejdovszky *et al.* (2016). A graphic representation of the different steps, alongside the principle of the assay is found in Figure 12.

The chemicals listed in Table 9 have been used during this experiment. All chemicals that come into contact with the cells were pre-warmed at 37 °C in a water bath.

Table 9: ALP-assay chemicals and their method of preparation.

Chemical	Preparation
ALP-Buffer	Magnesium chloride (0.24 mM; 11.3 mg), diethanolamine (1 M; 52.7 g) and para-nitrophenyl phosphate (5 mM; 928.6 mg) were dissolved in autoclaved water (ca. 350 mL) and the pH was adjusted with 37% hydrochloric acid to 9.81. Preparation of the chemical was conducted in the dark. The flask was filled up to 500 ml in a volumetric flask, aliquoted in 50 mL brown falcon tubes and stored at -20 °C.

Following 4.2.1.2. Cell seeding for estrogenicity and cytotoxicity assays and 4.2.2. Incubation with test substances, the plate was removed from the incubator and placed under the inverse microscope to detect possible morphological changes or contaminations. If no such observations were made the assay medium was aspirated in the laminar hood with a yellow tip connected to the vacuum pump. The inner wells were then washed one to three times with 100 µL PBS using the multichannel pipette and after the PBS has been sucked off for the last time, the plate was placed at -80 °C for a minimum of 20 minutes. During this time cell lysis took place and the produced ALP was released. Afterwards the plate was left for 5 minutes in the laminar hood to thaw and 50 µL of the ALP-buffer was added to the wells using a multichannel pipette. Due to the light sensitivity of para-nitrophenyl phosphate, the lights were switched off when the buffer was used. After 5 more minutes, the plate was placed inside a metal box and transferred to a plate reader, where the absorbance at 405 nm was measured in 3 minute gaps for 1 hour. The plate reader was heated beforehand at 37 °C.

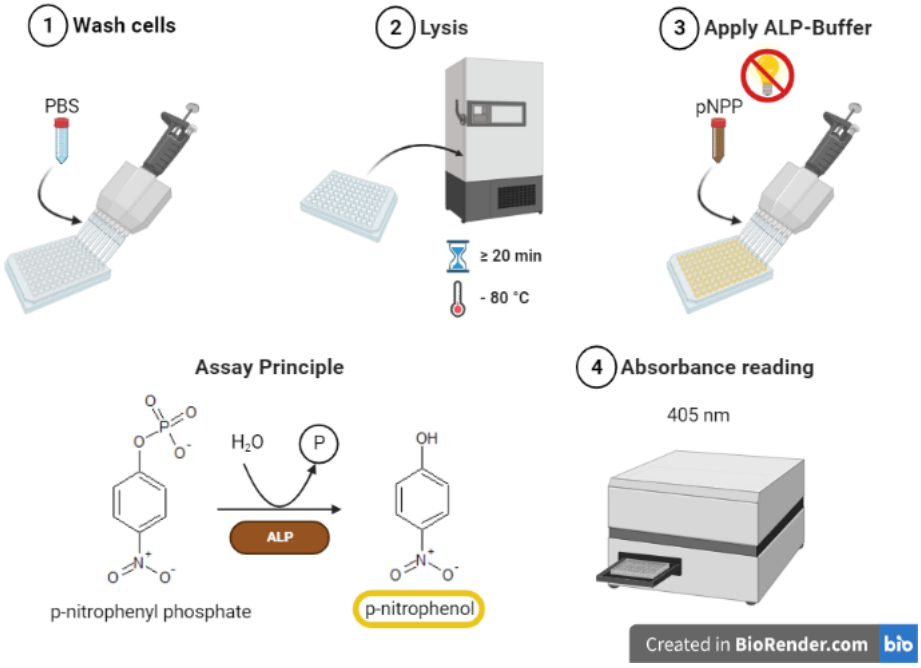

Figure 12: ALP assay procedure and principle.

Data evaluation

The final results were presented as percentage of relative ALP activity against the varying concentrations, whereas the mean values of the technical replicates were calculated alongside their standard deviations. These results were then related to the measurements of the solvent control (1% DMSO) that was set at a 0% estrogenic effect and the data derived from 1 nM E2, which represented a 100% ALP induction.

4.2.4. Cytotoxicity assays

Although estrogenic activity may be observed with the ALP-assay in Ishikawa cells, it is important that these results are verified. Cytotoxicity may be the reason for a low estrogenicity and must therefore be excluded. Due to this, the second plate that was prepared during 4.2.1. Cell culture and 4.2.2. Incubation with test substances was used to investigate any cytotoxic effects, utilizing two assays, namely CTB and SRB.

4.2.4.1. CellTiter-Blue® assay

The CTB assay is a photometric method used to estimate the number of viable cells in a multiwell plate. The buffer contains highly purified resazurin, alongside other ingredients for optimization, and is commercially available via Promega (Promega Corporation, 2016).

Resazurin is used as an indicator of cell viability based on cellular metabolism. Enzymes like mitochondrial reductases, NAD(P)H: quinone oxidoreductases and flavin reductases, which are found in the cytoplasm and mitochondria, may be able to reduce resazurin, thus signifying cellular impairment (Rampersad, 2012). As an electron acceptor, the dark blue dye changes from its oxidized state to the reduced, highly fluorescent, pink state, known as resorufin (depicted in Figure 13). The absorbance maximum of resazurin is 605 nm and that of resorufin is 573 nm. Due to this, the presence of viable cells causes the visible light absorption properties of the reagent to undergo a "blue shift". On the other hand, dead cells do not have the capacity for this reductive reaction, thus generating no fluorescent signal. Although it is possible to measure either absorbance or fluorescence, the latter is preferred due to higher sensitivity (Promega Corporation, 2016).

Procedure

The CTB-assay was conducted according to the protocol from Promega (Promega Corporation, 2016). A graphic representation of the different steps, alongside the principle of the assay is found in Figure 13. The chemicals listed in Table 10 have been used during this experiment.

Table 10: CTB-assay chemicals and their method of preparation.

Chemical	Preparation
CTB-Buffer	Since the buffer is stored at -20 °C, it is first left to thaw in a drawer. DMEM/F-12 (6.3 mL), which has been previously warmed at 37 °C, is added to a 15 mL falcon tube. CTB-buffer (0.7 mL) is then mixed with the assay medium. Preparation of the chemical is conducted in the dark.

The plate for the CTB-assay was prepared similarly and simultaneously as the one for the ALP-assay (described in detail in 4.2.1.2. Cell seeding for estrogenicity and cytotoxicity assays and 4.2.2. Incubation with test substances), where the cells were seeded and incubated with the test substances. Before beginning, the cells were checked for any contaminations or changes in morphology under an inverse microscope. Afterwards, the medium was aspirated using a yellow tip on the vacuum pump of the laminar hood and 100 µL from the CTB-buffer were added to the 51 test wells and 6 wells that contained no cells using a multistep pipette. This step was performed in rows of three instead of removing the medium and adding the buffer on all test and empty wells at once. Working with the CTB-buffer was performed in the dark, as the reagent is sensitive to light (Promega Corporation, 2016). The plate was then returned to the incubator for the duration of 50 minutes, followed by careful transfer -in order to avoid creating bubbles- of 90 µL of each well with a multichannel pipette to a new, black 96-well plate. This step was of importance as fluorescence of neighbouring wells could influence the results. Meanwhile, the transparent plate with the cells was used for the SRB-assay (see 4.2.4.2. Sulforhodamine B) and the black plate was placed inside a transfer box. The measurements were conducted with a plate reader at an excitation wavelength of 560 nm and an emission wavelength of 590 nm using two different gains to obtain usable data.

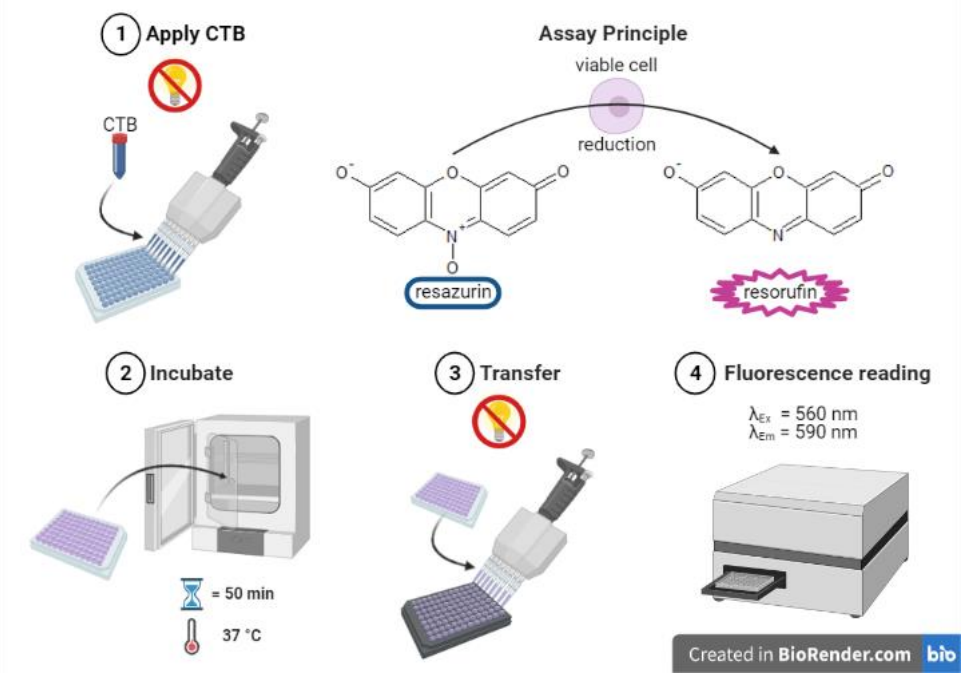

Figure 13: CTB assay procedure and principle.

Data evaluation

The results were presented as percentage of metabolic activity against the varying concentrations of each substance. The average and standard deviation of the six wells without

cells was calculated as blank. From the technical replicates the mean values and standard deviations were also derived and from them, the blank was subtracted. Lastly, the results were related to that of the solvent control (1% DMSO in assay medium) which has been set to represent cell viability of 100%.

4.2.4.2. Sulforhodamine B assay

The SRB-assay was developed in 1990 as method of determining the viability of cells based on their protein content (Skehan, et al., 1990). Nowadays, it is widely used to investigate cytotoxicity in cell-based studies due to being inexpensive and sensitive.

SRB is a bright pink, aminoxanthene dye with two sulfonic groups depicted in Figure 14. It has the ability to bind to basic amino acid residues because of the two sulfonic groups in its structure, thus forming an electrostatic complex.

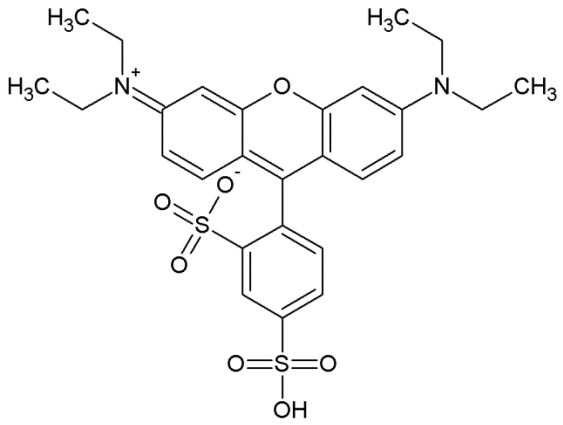

Figure 14: Molecular structure of sulforhodamine B.

For this to occur, the cells must first be fixed to the well plate. Mild acidic conditions are necessary for binding, while basic conditions allow for dissociation and solubilization of the fixed dye. The following measurements are photometrical. The binding of SRB to proteins is stoichiometric, thus the amount of dye extracted from stained cells is directly proportional to cell mass. This allows for observations on cell proliferation and cytotoxicity (Skehan, et al., 1990).

This assay is independent from cell metabolic activity. Therefore, it is possible to perform it alongside the CTB-assay to investigate different parameters that relate to cytotoxicity and enhance the validity of the results. During this thesis, CTB was performed first on a biological replicate, the solution from that assay was transferred to a different plate and the original plate was experimented on using SRB.

Procedure

The SRB-assay was conducted according to the protocol of Vejdovszky *et al.* (2016). A graphic representation of the different steps, alongside the principle of the assay is found in Figure 15. The chemicals listed in Table 11 have been used during this experiment.

Table 11: SRB-assay chemicals and their method of preparation.

Chemical	Preparation
TCA	The fixing reagent (50% w/v) is prepared by solving TCA (12.5 g) in 25 mL distilled water.
Acetic acid	The solution (1% v/v) to achieve acidic conditions is prepared by mixing acetic acid (20 mL) in 2 L of autoclaved water.
SRB dye	The dye (0.4% w/v) is prepared by dissolving SRB (4 g) in 1 L of acetic acid (1% v/v).
Tris-buffer	The dissolving solution is prepared by dissolving tris (hydroxymethyl-) aminomethane (0.5 g) in 250 mL of distilled water.

The plate used for the SRB assay was the same, transparent one in which the CTB was performed. Therefore, the remaining solution was first sucked off using a yellow tip connected to the vacuum pump in the laminar hood. The cells were then fixed to the plate with a 50% TCA solution, where 50 µL were given directly in the middle of the well with a multistep pipette. The plate was then labelled with its unique number on the side and placed in the fridge at 4 °C for a minimum of 1 hour. Afterwards, all wells were washed four times using a distilled water bottle. It is of importance that the washing steps are conducted carefully, as a stronger input of a solution in the well could dislocate the fixed cells and lead to false results. The plate was lastly placed upside down inside a drawer to dry overnight.

The experiment was continued the following week, during which 50 µL of the SRB solution were added to the inner wells utilizing a multistep pipette. The staining took place in the course of an hour, after which the wells were washed twice with a distilled water bottle and twice with 1% acetic acid to improve binding conditions. The plate was left once more in the drawer to dry overnight.

During the final day the bound dye was solubilized in alkaline conditions by adding 100 µL of the Tris-buffer and by shaking for 5 minutes in the plate reader. Lastly, the absorbance was measured at 570 nm.

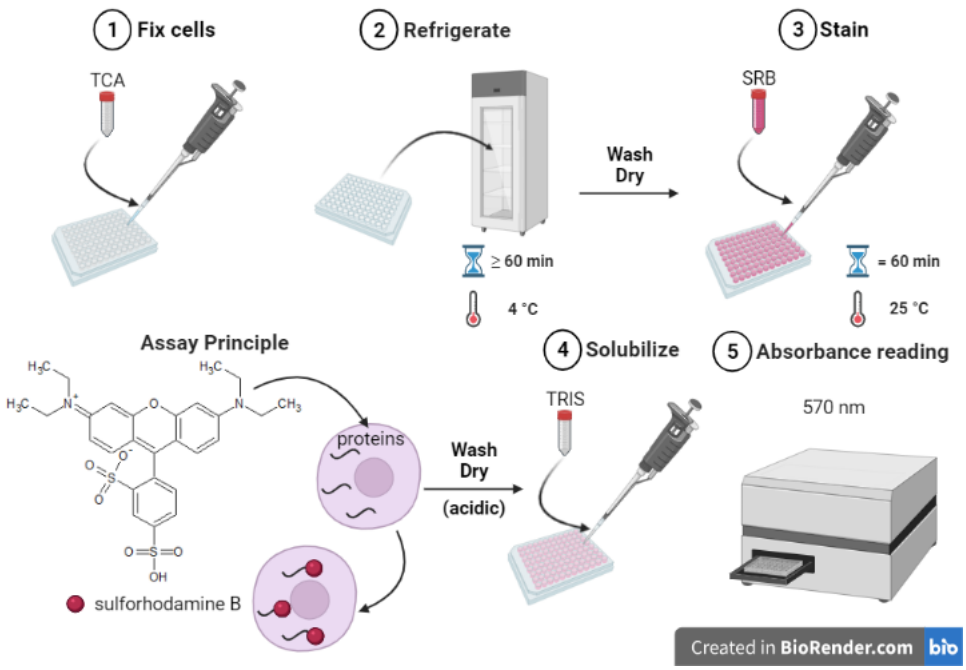

Figure 15: SRB assay procedure and principle.

Data evaluation

The results were presented as percentage of protein content against the varying concentrations of each substance. The mean value and standard deviation of the six wells without cells were calculated as blank. From the three technical replicates the mean values and standard deviations were also derived. From them, the blank value was subtracted. Lastly, the results were related to that of the solvent control (1% DMSO in assay medium) which has been set to represent cell viability of 100%.

4.2.5. High performance liquid chromatography - mass spectrometry

Two indispensable tools have become a staple in the scientific field of analytical chemistry with varying applications. The method of chromatography was invented at the beginning of the 20th century by the Russian botanist Mikhail T. Tswett who used the separation technique on plant pigments (Tswett, 1906; Sakodynskii, 1972). Mass spectrometry (MS) emerged from the works of Joseph J. Thomson, the discoverer of atoms and isotopes (Thomson, 1911), as well as Francis W. Aston who first provided the atomic characterization of many elements (Aston, 1920) as a means to separate ions by mass to charge ratio (Gross, 2017).

HPLC-MS/MS as a hyphenated technique is widely used in the analysis of phytochemicals (Verma, et al., 2020; Martínez-Ávila, et al., 2022). Although the possible estrogenic and cytotoxic effects of IFs and their metabolites have been investigated, little is known about how those substances may be metabolized within Ishikawa cells and whether the observed

effects truly correspond to the seeded compounds. Therefore, a qualitative and quantitative analysis of select IFs and metabolites was conducted

4.2.5.1. Analyte separation via HPLC

In high performance liquid chromatography (HPLC) the separation relies on equilibrium of adsorption and desorption of compounds between a mobile and a stationary phase, defined as the distribution coefficient. Depending on polarity and interactions of a compound with the stationary phase, analytes may adsorb more strongly and reside longer in the column. Others which adsorb weakly may move and eluate faster. The time needed for a component to pass through the column is the retention time, a characteristic value that remains invariable for each chromatographic setup with unchanged conditions (Gross, 2017).

The choices of stationary and mobile phase are crucial for a successful separation. The oldest stationary phases in HPLC are made of silica or alumina, and the associated technique is "normal phase" chromatography. However, nowadays the most used technique is the so-called reversed phase chromatography (RP). In this case the stationary phase includes an additional, organic layer by coating with hydrophobic groups (e.g. alkyl, aryl) that are covalently bound to the silica support. Such chains can be long (octadecyl; C_{18}) to better bind molecules of low polarity or shorter (octyl; C_8) which are less retentive (Dong, 2019). The mobile phase is usually a mixture of two or more solutions, of which one is water and the other an organic solvent such as acetonitrile or methanol. The ratio of eluents varies depending on the experiment. It can either be held constant (i.e. isocratic operation) or the composition can be programmed in a gradient manner to increase the fraction of organic solvent and better mobilize molecules of decreasing polarity. In RP-systems elution follows the order of ionic>polar>nonpolar molecules (Gross, 2017).

An HPLC instrument begins with the eluents of the mobile phase in their respective reservoirs. These are connected to a multisolvent pump and a manual injector valve or automated system for the samples, a column inside an oven and a detector with a data system. A control panel attached to the instrument is responsible for the input of the experimental parameters, such as pressure (usually up to 400 bar) or flow rate (0.01-10 mL/min). These variables have been improved by Jorgenson *et al* (1997) who introduced the ultra-high performance liquid chromatography (UHPLC). With pressures between 1000 and 1500 bar as well as flow rates of 0.001-2.5 mL/min, separation of complex mixtures is faster and more efficient (Dong, 2019). As the mobile phase flows through the column, the injector is responsible for introducing the sample. An autosampler allows for better precision and

productivity as the automated system can inject multiple samples over longer periods of time without the interference of the operator. Separation takes place in the column which holds the stationary phase. Choosing an appropriate column depends on its parameters, such as dimensions (e.g., length and width) and packing characteristics (e.g., particle size and pore size). Preferable are short, narrow columns with smaller particles, something that increases analysis speed and resolution while it decreases the amount of solvent (Dong, 2019).

Following the separation, the analytes go to the detector which measures concentration or mass based on physical or chemical properties. Detectors can be universal (e.g., refractive index, nuclear magnetic resonance, mass spectrometer) or specific (e.g., UV/Vis, fluorescence) (Dong, 2019).

4.2.5.2. Analyte detection and quantification via MS

The combination of UHPLC with a sensitive and specific detection method like MS ensures accuracy and reliability of analytical information (Dong, 2019).

The basic principle of MS revolves around the measurement of fragments of inorganic or organic molecules that have been broken down after a bombardment. Generating a charged form of the analyte is achieved via a suitable ionization method, followed by the deflection of ions based on charge, mass and velocity. Lastly, separation takes place according to *mass-to-charge ratio* (*m/z*) and the quantitative detection is proportional to ion abundance (Ahamad, et al., 2022).

A mass spectrometer begins with the injection of the sample through an inlet. In the case of this hyphenated method, the problem originally was bringing the analytes from the high pressure environment of UHPLC to a system utilizing atmospheric pressure without disrupting the flow of the eluent. This was solved with the introduction of electrospray ionization (ESI) as an interface/ion source. Used for large, non-volatile and chargeable molecules (e.g., proteins) all the way to smaller molecules with hydrocarbons, ESI is a soft ionization technique that allows the transfer of ions from the liquid to the gas phase. The eluent with the sample is pumped through a small electrical capillary of high potential, thus creating an electrostatic aerosol with many charged droplets. The droplets shrink in the countercurrent of a heated inert gas, which works as a heat supply for the rapid vaporization of the solvent. Further shrinkage causes electrostatic repulsion of the same charges to overcome the surface tension that holds the droplet together, resulting in coulombic fission. Ionized analytes are thus created in the gas phase and focused on the mass analyzer (Gross, 2017).

The ions that leave the interface are separated by an electric or magnetic field based on *m/z*. Mass analyzers include ion trap, Orbitrap and time of flight but most commonly used are triple quadrupole (Q) mass spectrometer. One quadrupole consists of four cylindrical shaped rod electrodes in a parallel arrangement with space in the middle (z-axis). The opposing rods form pairs which are electrically connected and held at the same potential. In order to generate an oscillating electric field, radio frequency (RF) voltage and direct current (DC) voltage is applied between opposing rods. In the example of positive ions entering the quadrupole in the z-axis, they travel towards the rod that is negatively charged. However this trajectory is complicated due to the positive polarity of the other pair. Controlling the RF/DC voltage ratio allows the trajectory to be stable for specific *m/z* ions. The specifically chosen ions then reach the detector (e.g., a photomultiplier) while the rest collide with the rods. An improvement to this ion-guiding ability has been made with the use of hexapoles or octapoles, which consist of six and eight rods respectively (Ahamad, et al., 2022)

Nowadays hybrid MS are popular due to the advantage they provide with different application modes. Tandem MS utilizes a triple quadrupole (QqQ) structure, which is made of three quadrupoles arranged one after the other. Q_1 and Q_2 can be operated independently as MS_1 and MS_2 and filter ions depending on desired application while the q in-between is a fragmentation compartment with an inert gas that operates by collision induced dissociation (CID). One of the most popular methods involving QqQ is targeted analysis, during which the *m/z* values are predefined for both Q_1 and Q_2 to gain information about ionic fragmentation pathways. Targeted analysis can involve a single transition, namely selected reaction monitoring (SRM) or the observation of several SRM during one cycle, thus being called multiple reaction monitoring (MRM) (Gross, 2017; Shandilya, 2022). The different triple quad modes and applications are summarized in Table 12.

Table 12: Scan modes and different applications of triple quadrupole mass spectrometer.

Scan Mode	Q1	q	Q2	Application
Product ion	*m/z* selection	CID	scan	Identification
Precursor ion	scan	CID	*m/z* selection	Analyte screening
Neutral loss	scan	CID	scan	Analyte screening
SRM	*m/z* selection	CID	*m/z* selection	Single transition analysis
MRM	*m/z* selection	CID	*m/z* selection	Multiple transition analysis

A simplified depiction of the UHPLC-MS/MS used during the experiments is in Figure 16.

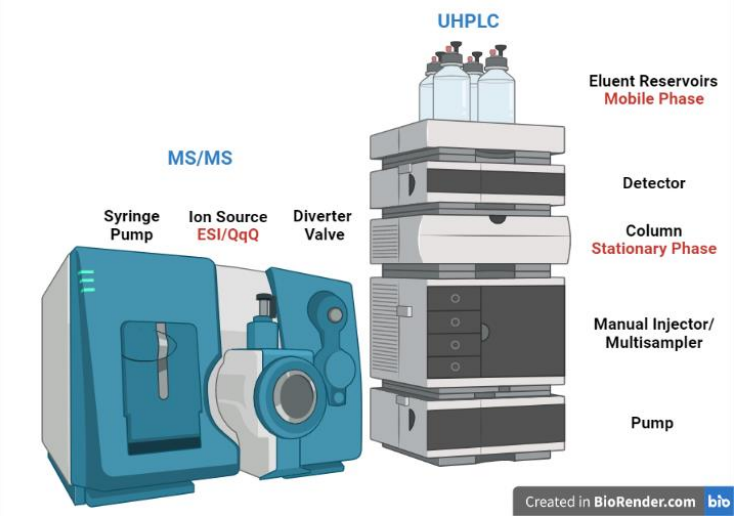

Figure 16: An UHPLC-MS/MS system with specific compartments of each method.

4.2.5.3. Workflow

Sample preparation

Cell cultivation and seeding with substances was performed according to 4.2.1. Cell culture and 4.2.2. Incubation with test substances in order to keep the same conditions as the ones for the assays. IFs and metabolites for UHPLC-MS/MS experiments were investigated according to their estrogenicity. Non-estrogenic compounds were prepared only at the highest concentration of 10 µM while estrogenic compounds were prepared in two different concentrations, namely 1 µM and 10 µM. Additionally, cells with no test substance and cells with solvent control (DMSO 1%) were prepared. Figure 17 depicts an example of one biological replicate with two technical replicates of each substance prepared for UHPLC-MS/MS. Overall, four replicates were prepared to ensure reproducibility of the results.

	1	2	3	4	5	6	7	8	9	10	11	12
A	PBS no cells	PBS no cells	PBS no cells	PBS no cells	PBS no cells	PBS no cells	PBS no cells	PBS no cells	PBS no cells	PBS no cells	PBS no cells	PBS no cells
B	PBS no cells			**G7G [10]**	**G7G [10]**	G7G4'S [10]	G7G4'S [10]	D4',7dG [10]	D4',7dG [10]	**EQ [1]**	**EQ [1]**	PBS no cells
C	PBS no cells	DMSO [1%]	DMSO [1%]	**G4',7dG [1]**	**G4',7dG [1]**	G4'G7S [10]	G4'G7S [10]	**D4'S [1]**	**D4'S [1]**	**EQ [10]**	**EQ [10]**	PBS no cells
D	PBS no cells	**GEN [1]**	**GEN [1]**	**G4',7dG [10]**	**G4',7dG [10]**	**DAI [1]**	**DAI [1]**	**D4'S [10]**	**D4'S [10]**	E7G [10]	E7G [10]	PBS no cells
E	PBS no cells	**GEN [10]**	**GEN [10]**	**G7S [1]**	**G7S [1]**	**DAI [10]**	**DAI [10]**	D4',7dS [10]	D4',7dS [10]	**E4'S [1]**	**E4'S [1]**	PBS no cells
F	PBS no cells	G4'G [10]	G4'G [10]	**G7S [10]**	**G7S [10]**	D4'G [10]	D4'G [10]	D7G4'S [10]	D7G4'S [10]	**E4'S [10]**	**E4'S [10]**	PBS no cells
G	PBS no cells	**G7G [1]**	**G7G [1]**	G4',7dS [10]	G4',7dS [10]	D7G [10]	D7G [10]	D4'G7S [10]	D4'G7S [10]			PBS no cells
H	PBS no cells	PBS no cells	PBS no cells	PBS no cells	PBS no cells	PBS no cells	PBS no cells	PBS no cells	PBS no cells	PBS no cells	PBS no cells	PBS no cells

Figure 17: Example of an incubation plan of the 96-well plate.

The depiction includes the Ishikawa cells (grey), solvent control (DMSO) and test substances (GEN, etc.) with varying concentrations in µM (unless stated otherwise in the brackets). Colored substances were found to be estrogenic and were tested in two concentrations.

After 48 hours of incubation with the test substances, from each well 80 µL supernatant were transferred to microtubes, which already contained 80 µL of ice cold ACN (resulting in a 1:2 dilution), and mixed. Lastly the microtubes were kept at -80°C until further processing (about 72 hours later).

In the following, the test substances were taken out of the freezer and thawed, followed by 10 minutes of centrifugation at 4 °C and 18620 rcf. Lastly, 100 µL from the supernatant were transferred to HPLC vials containing microinserts and measured.

Matrix effects

To check whether the mass spectrometric results are significantly influenced by matrix effects and to calculate the recovery rates, four different spiking solutions were prepared. These solutions consisted of the three IFs, the metabolites of GEN, the metabolites of DAI and the metabolites of EQ (see Table 28 in Appendix). A biological replicate was prepared using only DMSO (1%) instead of the test substances. After 48 hours of incubation, the following solutions were prepared in microtubes:

1. For recovery calculations: 80 µL supernatant from a well incubated with DMSO 1% + 10 µL spiking solution + 70 µL ACN

2. For the assessment of matrix effects: 80 µL supernatant from a well incubated with DMSO 1% + 80 µL ACN
3. As solvent control: 150 µL MeOH:H_2O (30:70) + 10 µL spiking solution

The solutions were then stored at -80°C until further processing. After more than 72 hours, the test samples were taken out of the freezer and thawed, followed by 10 minutes of centrifugation at 4°C and 18620 rcf. From solutions 1 and 3, 140 µL of the supernatant were transferred to HPLC vials containing micro inserts. From solution 2, 140 µL were spiked with 10 µL of the aforementioned spiking solution.

UHPLC-MS/MS calibration and parameters

Standards

Stocks of 100 mg/L were used to prepare the calibration standards. The stock of each of the 19 test substances was first diluted 1:20 in DMSO (1%) to create new stocks of 5 mg/L (= 5000 µg/L). These stocks were then further diluted with DMSO (1%) according to the following equation to create two stocks of 1 mg/L and 3 mg/L.

$$c_1 \cdot V_1 = c_2 \cdot V_2$$

$$V_1 = \frac{c_2 \cdot V_2}{c_1}$$

With c_1 the 5 mg/L stock, c_2 the desired mg/L amount (1 or 3), V_1 the volume used from the 5 mg/L stock and V_2 the end volume of 200 µL. The aforementioned equation is then transformed to the following.

$$V_{3\ mg/L} = \frac{3\ mg/L \cdot 200\ \mu L}{5\ mg/L} = 120\ \mu L (+80\ \mu L\ solvent)$$

$$V_{1\ mg/L} = \frac{1\ mg/L \cdot 200\ \mu L}{5\ mg/L} = 40\ \mu L\ (+160\ \mu L\ solvent)$$

As solvent, a solution of MeOH:H_2O (30:70) was used. The rest of the calibration standards were prepared according to Table 13 in a serial dilution manner of 1:10.

Table 13: Serial dilution of 1 and 3 mg/L stocks with solvent.

S	Concentration [µg/L]	Volume (Substance) [µL]	Volume (MeOH:H_2O) [µL]
1	1000	-	-
2	100	20 (S1)	180
3	10	20 (S2)	180
4	1	20 (S3)	180
5	0.1	20 (S4)	180

Table 13: continued

S	Concentration [µg/L]	Volume (Substance) [µL]	Volume (MeOH:H_2O) [µL]
1	3000	-	-
2	300	20 (S1)	180
3	30	20 (S2)	180
4	3	20 (S3)	180
5	0.3	20 (S4)	180

Therefore, the calibration series for the UHPLC-MS/MS experiments consisted of eleven standards ranging from 0.1 to 5000 µg/L.

Eluents

Following eluents were prepared for the mobile phase.

- Eluent A: Ammonium carbonate (25 mL) + H_2O (2475 mL)
- Eluent B: ACN (700 mL) + MeOH (1750 mL)

Method Parameters

The samples in the HPLC vials were placed in the autosampler of the hyphenated UHPLC-MS/MS system. The method was developed and applied by DI Dr. Elisabeth Varga using the following parameters.

Table 14: Pump, autosampler and column parameters for the UHPLC-MS/MS experiments.

Pump			
Flow rate [mL/min]	0.5		
Gradient	**Time [min]**	**A [%]**	**B [%]**
	0.0	97	3
	2.6	97	3
	10.7	44	56
	11.0	5	95
	14.0	5	95
	14.1	97	3
	16.5	97	3
Autosampler			
Temperature [°C]	5		
Injection volume [µL]	2		
Column			
Temperature [°C]	40		

Data were acquired in MRM mode applying negative electrospray ionization and the specific transitions are listed in the Appendix in Table 27. Qualitative analysis was performed using

the Analyst (v. 1.7) software while the analytes were quantified by external calibration using the Skyline (v. 22.2) software.

Data evaluation

Firstly, the calculations for the spiked samples were conducted in order to evaluate recovery and matrix effects. For this, the same method as for the test substances was used and the results are summarized in the Appendix in Table 28 and Table 29. Due to the fact that the recovery rates were between 80 and 120%, as shown in Table 30, no corrections of the results were necessary.

The data of the prepared standards for each sequence were observed separately to ensure whether the program integrated the peaks correctly. Adjustments were made in the case of peak shifts. Certain standards were not considered in the calibration if they were outside the linear range or, in the case of lower concentrations, no peaks were detectable. The coefficient of determination R^2 was always between 0.98 and 0.99, with few exceptions.

Quantification involved investigating each substance for its subsequent metabolites. In the case of DAI, its metabolite EQ and metabolites thereof were also considered. Overall, four biological replicates were prepared, each consisting of two technical replicates in order to acquire reproducible data and calculate mean values and standard deviations. Limit of detection (LOD) and limit of quantification (LOQ) were obtained using the following equations,

$$LOD = 3 * \frac{S}{N}$$

$$LOQ = 10 * \frac{S}{N}$$

with *S/N* being the signal to noise ratio. If an observed signal was below the LOQ, it was not taken into consideration in the statistics. Via means of external calibration, the concentration in µg/L was directly calculated in the utilized software by integrating peak areas. To obtain absolute values of the concentrations, the following equations were used,

$$\beta\ [ng/80\ \mu L] = \frac{\beta\ [\mu g/L] * V\ [\mu L] * DF}{1000}$$

$$c\ [nmol/80\ \mu L] = \frac{\beta\ [ng/80\ \mu L]}{M\ [g/mol]}$$

with, β the absolute mass concentration in 80 µL, *V* the volume of the sample (=80 µL), *DF* the dilution factor, *c* the absolute molar concentration in 80 µL and *M* the molar mass of the

substance. Lastly, a sum of the concentrations of the substances found in each tested sample was calculated and set as 100% in order to obtain the percentages of each IF and each metabolite found and graphically represent them in pie charts.

4.2.6. Evaluation and statistics

ALP, CTB/SRB

The estrogenic and cytotoxic measurements of IFs and metabolites were performed each in three technical triplicates and a minimum of three independent biological replicates.

For the evaluation, Microsoft Excel® 2010 was used. For each biological replicate, the mean values of the three technical replicates were calculated and for the final values of each substance the mean values of the biological replicates were used. As a precondition, the results were tested for outliers according to Nalimov. If any outliers were identified, they were excluded from the calculations of the mean values and the standard deviations.

A normality test according to Shapiro-Wilk as well as the statistical analysis was performed with Origin Pro® 2019. The significance levels were 5% (#,* = $p < 0.05$), 1% (##,** = $p < 0.01$) and 0.1% (###,*** = $p < 0.001$). The evaluation for the significant differences was performed with one-way analysis of variance (ANOVA) followed by Fisher's least significant difference (LSD) post hoc test.

UHPLC-MS/MS

For the quantification, which was performed with the software Skyline (v. 22.2), mean values and standard deviations were calculated from four biological replicates, each with two technical replicates. As a precondition, the results were tested beforehand for outliers according to Nalimov when necessary. If any outliers were identified, they were excluded from the statistical calculations.

5. Results and discussion

5.1. Estrogenicity of IFs measured via ALP

The estrogenic activities of the substances of interest were investigated in Ishikawa cells utilizing the ALP assay. Overall, the estrogenicity of three IFs and 16 metabolites ranging from 0.001 to 10 µM, were considered for these experiments. The concentrations related to physiological amounts found in human plasma (Soukup, et al., 2014). A minimum of three biological replicates were investigated per compound, with each containing three technical replicates for reproducibility. The results are separated into four sections, each containing a specific IF (GEN, DAI or EQ) with their perspective metabolites, followed by a summary of all the substances found to induce estrogenicity in the Ishikawa cell line.

5.1.1. GEN and metabolites

The results for GEN and seven of its metabolites are depicted in Figure 18.

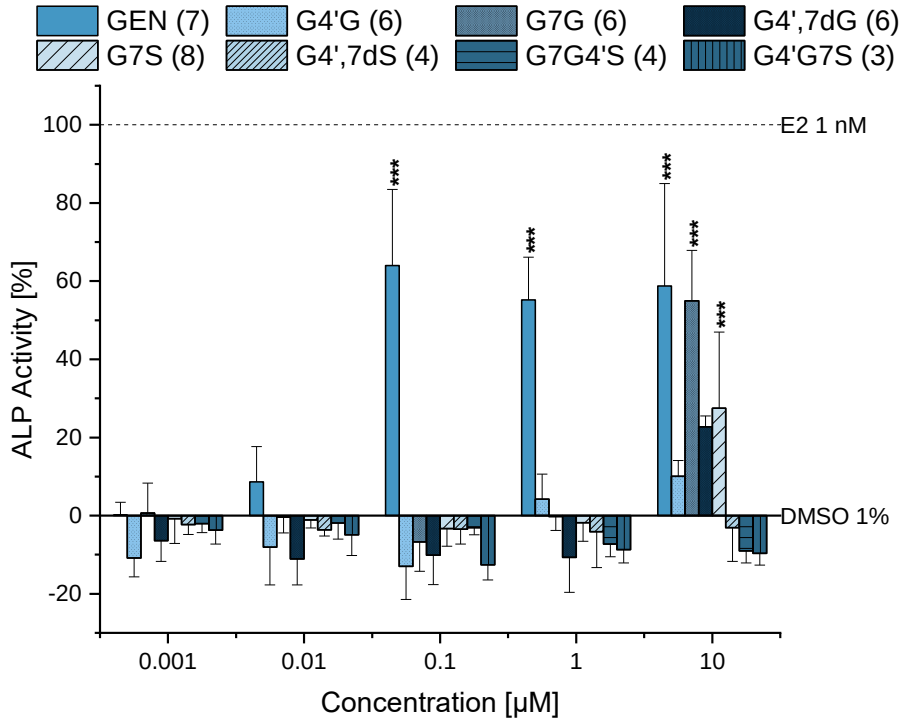

Figure 18: Graphic depiction of the estrogenic induction of GEN and seven of its metabolites in Ishikawa cells. The ALP activity [%] after 48 hours incubation is provided against the concentration [0.001 – 10 µM], with DMSO (1%) as solvent control and 17β-estradiol (1 nM) as positive control representing 0 and 100% respectively. Results are depicted as bars of mean ± standard deviation values. The biological replicates of each substance (ranging from 3 - 8) are shown in the parentheses next to the abbreviated names in the legend above the graph. Outliers after Nalimov outlier test were excluded. Significant differences of effects between solvent control and the incubated compounds were calculated by one-sample Student's *t*-test and were indicated with * ($p < 0.05$), ** ($p < 0.01$) and * ($p < 0.001$).**

Human plasma concentrations of the aglycone relate to roughly 0.001 μM (Soukup, et al., 2014), however, neither GEN nor its metabolites were found to be significantly estrogenic in their lowest concentrations of 0.001 and 0.01 μM. A minor exception was GEN with a very weak estrogenic effect of 9 ± 9% at 0.01 μM.

The IF showed a significant increase in estrogenicity at 0.1 μM with 64 ± 19%, which was then lowered to 55 ± 11% at 1 μM and remained relatively stable with 59 ± 26% at the highest concentration of 10 μM. Interestingly enough, GEN does not follow the traditional dose-response effect, where the ALP activity would be expected to increase with increasing concentration. This decrease has also been observed previously by Vejdovszky *et al*. (2016) which utilized the same cell line and assay. However, in their case the estrogenicity of GEN decreased from 80% (1 μM) to 60% (10 μM) and further to 40% at a higher concentration (20 μM) while here, a 10% decrease was already observed from 0.1 μM to 1 μM. It is worth mentioning that the results of each biological replicate for these three concentrations of GEN varied so, that the standard deviations, especially for the highest concentration, were high. Additionally, the origin of GEN for the experiments of Vejdovszky *et al*. (2016) was different than the one used in this thesis and impurities might play a role.

Both glucuronides have been found in human plasma, with twofold amounts of the 4'-*O*-glucuronide (0.15 μM) variant compared to that of the 7-*O*-glucuronide (0.07 μM) (Soukup, et al., 2014). In addition to this, the same group in a different study found roughly three times higher amounts of the diglucuronide (0.54 – 0.62 μM) when compared to a sum of the glucuronides in both male and female human plasma. None of the three substances show estrogenic activity at the relevant concentrations of 0.001 to 1 μM. In fact, glucuronidation appears to work as a detoxification process for GEN up to the concentration of 1 μM, which has been previously observed (Beekmann, et al., 2015; Islam, et al., 2015). That was not the case with the highest concentration in our work. The ALP activity of G7G at 10 μM with 55 ± 13% is comparable to that of GEN and about two and a half times higher than that of G4',7dG (23 ± 3%) at the same concentration. G4'G followed, showing the weakest estrogenicity of the three of 10 ± 4% at 10 μM. Our results differ from those of Kinjo *et al.* (2004), whose group showed that the two isomers have similar binding effects with regards to ERβ yet G4'G bound better than G7G with regards to ERα. However, this might be explained with their utilized cells, the breast cancer MCF-7 cell line, or the competition assay they used compared to our single exposure. The diglucuronide has not been previously studied.

Most interesting would be the sulfoglucuronides which represent the major metabolites in both female and male human plasma (Soukup, et al., 2016), with the G7G4'S isomer

dominating tenfold (0.77 μM) (Soukup, et al., 2014). In the tested concentrations, neither of the combined glucuronide-sulfate metabolites showed estrogenic activity, meaning that this metabolic pathway also possibly reduces the biological activity of GEN.

The percentage of the sulfate metabolites of GEN found in human plasma is comparable to that of the glucuronides (Soukup, et al., 2016). The position of the functional group also plays a role, as the G7S isomer was found in much higher concentrations (0.14 μM) compared to G4'S (0.006 μM). Much like the glucuronides, we found out that the G7S increased the ALP activity by 28 ± 19%. Yet when compared to the aglycone, the estrogenicity decreased, something that has been previously observed in an MCF-7 cell line (Pugazhendhi, et al., 2008). Although not investigated in this thesis, it is worth mentioning that such a decrease in biological activity was not observed by the same research group for the 4'-sulfate isomer. The importance of the positioning of a functional group is thus once more highlighted.

5.1.2. DAI and metabolites

The results for DAI and its metabolites are depicted in Figure 19.

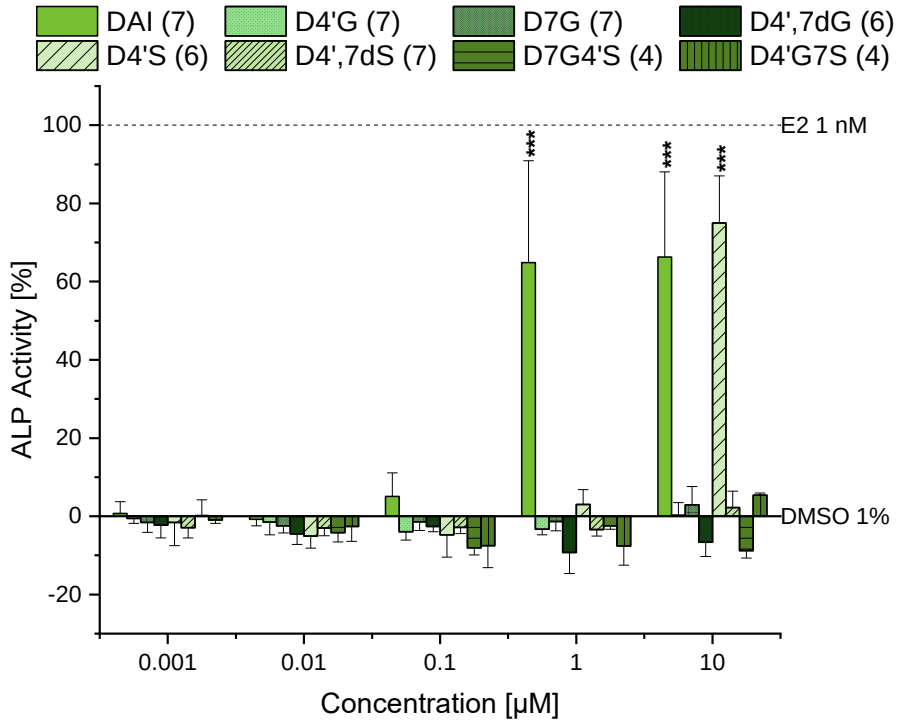

Figure 19: Graphic depiction of the estrogenic induction of DAI and seven of its metabolites in Ishikawa cells
The ALP activity [%] after 48 hours incubation is provided against the concentration [0.001 – 10 µM], with DMSO (1%) as solvent control and 17β-estradiol (1 nM) as positive control representing 0 and 100% respectively. Results are depicted as bars of mean ± standard deviation values. The biological replicates of each substance (ranging from 3 - 8) are shown in the parentheses next to the abbreviated names in the legend above the graph. Outliers after Nalimov outlier test were excluded. Significant differences of effects between solvent control and the incubated compounds were calculated by one-sample Student's *t*-test and were indicated with * ($p < 0.05$), ** ($p < 0.01$) and * ($p < 0.001$).**

Much like GEN, DAI also occurs mainly conjugated in human plasma, as the aglycone represents only around 1% (Soukup, et al., 2016). It was found in very low concentrations of roughly 0.02 µM by the same group (Soukup, et al., 2014). During our experiments, the aglycone and its seven metabolites showed no estrogenic activity for the concentrations of 0.001 to 0.1 µM, with the exception of a very weak one (5 ± 6%) for DAI at 0.1 µM. This is in agreement with previous studies conducted utilizing the same cell line and estrogenicity assay, however in that work the activity of DAI at 0.1 µM was four times higher than in this study (Grgic, et al., 2022). One possible explanation for this could be that the IFs used were of different origin and impurities played a role.

A significant increase was observed for the 1 µM concentration. The ALP activity reached 65 ± 26% and remained relatively stable for the highest concentration with 66 ± 22%. This

increase was also observed in the work of Grgic *et al.* (2022). In this case, DAI reached a higher activity of 80% and showcased an immediate decrease at the higher concentration, once more falling out of the typical dose-response scheme. It is important to mention that the effects of DAI on the estrogenicity fluctuated between the biological replicates (ranging from 29 to 88% at 1 μM), resulting in a higher standard deviation.

The 4'-*O*- and 7-*O*-glucuronide represent around one fifth of the DAI substances found in human plasma, unlike the diglucuronide which amounts to one tenth (Soukup, et al., 2016). G4'G and G7G can be found in similar concentrations of 0.16 and 0.15 μM respectively (Soukup, et al., 2014). No estrogenicity was induced by any of the glucuronides or the diglucuronide metabolites of DAI for the tested concentrations. The effect of glucuronidation on the biological activity of DAI is in agreement with previous studies. Islam *et al.* (2015) investigated to what extent DAI glucuronides themselves were biologically active in normal rat and human breast tissues and showed that estrogenic activity was a result of intracellular deconjugation to the aglycones. It can be assumed, that this metabolic pathway works as a detoxifying process for the aglycone.

The main DAI metabolites found in human plasma are the sulfoglucuronide combination, rounding up to 50% for both men and women (Soukup, et al., 2016). Specifically, D7G4'S has been found in amounts of 0.6 μM (Soukup, et al., 2014). Much like the glucuronides, no effects have been observed with regards to the estrogenic activity for either D7G4'S or D4'G7S in our experiments. This leads to the hypothesis, that a metabolism of DAI to the sulfoglucuronides inactivates its biological activity. This work appears to be the first of its kind to investigate this effect of the combination metabolites.

Lastly, the sulfates of DAI made up about 22% and 16% of the possible substances found in human plasma of females and males, respectively. The amounts of the disulfate were negligible (≤ 0.5%) (Soukup, et al., 2016). Interestingly, the concentrations of D7S were almost twice as high when compared to those of D4'S (0.14 and 0.06 μM) (Soukup, et al., 2014). Although at those concentrations no induction in ALP activity was observed, the most interesting finding was for D4'S at the highest concentration of 10 μM. It appears that the estrogenicity of this metabolite is 10% higher than that of DAI at the same concentration, reaching levels of 75 ± 12. These results contradict the works of Pugazhendhi *et al.* (2008) and Totta *et al.* (2005), both of which have shown that sulfation of DAI in the 4' position leads to a decrease in estrogenicity in the MCF-7 cell line. The significant increase of estrogenicity surpassing that of the aglycone was instead associated with a sulfation in the 7 position of DAI. Unfortunately, a comparison with D7S was not possible in our work due to

the lack of availability but this contradiction raises the question of whether and how the Ishikawa cells metabolize the incubated IFs. This will be further explored in the HPLC-MS/MS experiments.

5.1.3. EQ and metabolites

The results for EQ and its two metabolites, E7G and E4'S, are depicted in Figure 20.

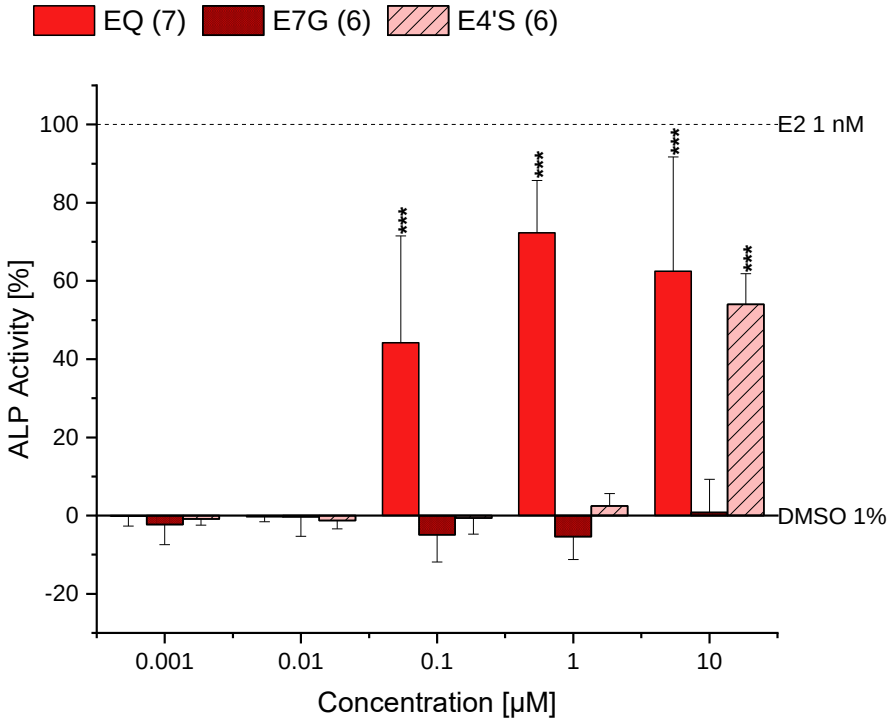

Figure 20: Graphic depiction of the estrogenic induction of EQ and two of its metabolites in Ishikawa cells. The ALP activity [%] after 48 hours incubation is provided against the concentration [0.001 – 10 µM], with DMSO (1%) as solvent control and 17β-estradiol (1 nM) as positive control representing 0 and 100% respectively. Results are depicted as bars of mean ± standard deviation values. The biological replicates of each substance (ranging from 3 - 8) are shown in the parentheses next to the abbreviated names in the legend above the graph. Outliers after Nalimov outlier test were excluded. Significant differences of effects between solvent control and the incubated compounds were calculated by one-sample Student's *t*-test and were indicated with * ($p < 0.05$), ** ($p < 0.01$) and * ($p < 0.001$).**

In view of biological activity, EQ is considered the most important metabolite. Its detection in plasma however is complicated by the fact that not everyone is capable of producing the microbial metabolite. For example, in the work of Soukup *et al.* (2016), EQ was detected in urine samples of only 36% of women and 20% of men. All rats and mice however possessed EQ producing capabilities regardless of sex. Therefore, its quantification is not an easy task. Still, in one of their previous studies, the metabolite was detected in human plasma samples (Soukup, et al., 2014). This was in agreement with Obara *et al.* (2019), who focused

specifically on using two EQ producers. Both works denoted the possibility of further metabolic processes for EQ, tissue distributions and the significance of investigating their biological activities.

None of the three substances showed any changes in ALP activity till the concentration of 0.1 μM, when the aglycone presented a 44 ± 27% increase compared to the solvent control. A higher estrogenicity was observed for 1 μM, reaching 77 ± 13%, which subsequently was reduced to 63 ± 29% at the highest concentration of 10 μM. The results of the 1 μM EQ showing the highest induction in ALP activity are comparable with previous works (Grgic, et al., 2022). EQ was the only IF in our work whose estrogenicity was reduced at higher concentrations. The reason for this remains unknown. Like GEN and DAI, the different biological replicates for the highest concentration fluctuated so, that the resulting standard deviation was high.

Traces of the EQ glucuronide, E7G, have been detected at low concentrations (0.004 μM) (Soukup, et al., 2014) and represented the second major metabolite according to Obara *et al.* (2019). Glucuronidation of EQ appears to inactivate the biological ability of the aglycone as no induction of ALP activity was observed for any concentration. Due to the fact that no previous research has been conducted for the effects of E7G on estrogenicity, these results lead to the hypothesis that this might be a detoxification pathway for EQ.

That was not the case for the sulfate. Despite showing no changes in estrogenicity for the majority of the concentrations, E4'S depicted a significant increase of 54 ± 8% which was only 10% less than that of EQ at the same concentration of 10 μM. However, like DAI and D4'S, this effect on estrogenicity has been attributed to sulfation in the 7 position. Sulfation in the 4' position has been previously shown to reduce, but not fully abolish, the biological activity in MCF-7 cells (Pugazhendhi, et al., 2008). Unfortunately, E7S was not available and a comparison was not possible. Although this difference may be attributed to the differing cell lines, it is of utmost importance to investigate whether the Ishikawa cell line is capable of metabolizing the incubated compounds and which metabolites it may form. Only then is it possible to fully elucidate which substances are responsible for an induction in ALP activity.

5.1.4. Comparison of major estrogenic IFs and metabolites

The compounds found to exert a significant estrogenic activity via ALP assay in Ishikawa cells are summarised in Figure 21.

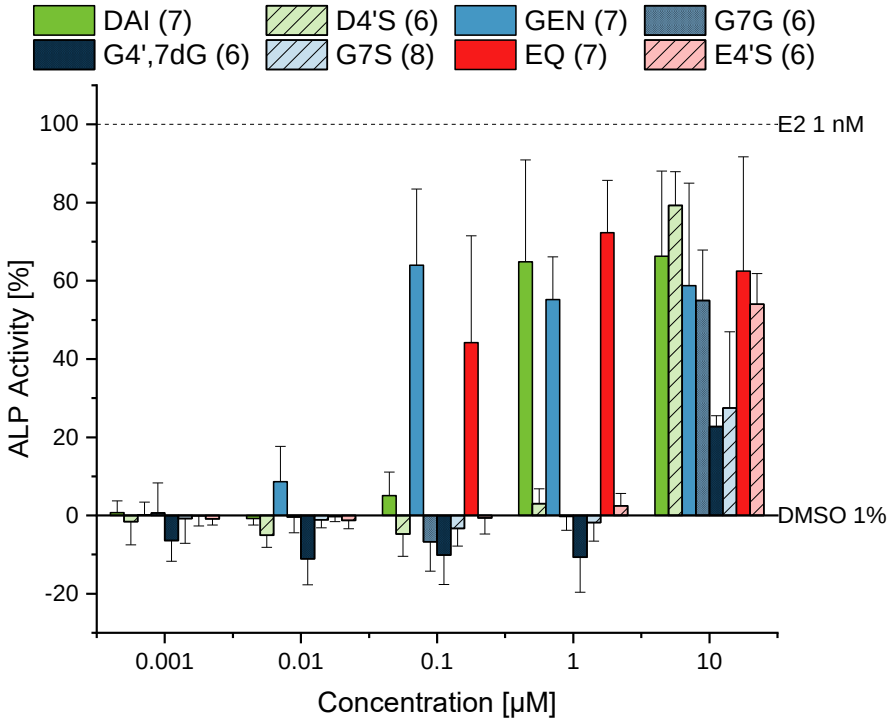

Figure 21: Graphic depiction of the significantly estrogenic IFs and metabolites in Ishikawa cells.
The ALP activity [%] after 48 hours incubation is provided against the concentration [0.001 – 10 µM], with DMSO (1%) as solvent control and 17β-estradiol (1 nM) as positive control representing 0 and 100% respectively. Results are depicted as bars of mean ± standard deviation values. The biological replicates of each substance (ranging from 3 - 8) are shown in the parentheses next to the abbreviated names in the legend above the graph. Outliers after Nalimov outlier test were excluded.

All three IFs were found to be estrogenic at concentrations above 1 µM. DAI was the only one to show a very weak induction in ALP activity at 0.1 µM, which is in accordance with previous research (Pugazhendhi, et al., 2008). At that concentration, GEN was found to be more estrogenic than EQ, something which Grgic *et al.* (2022) also observed. However, the current data set differed at the next tested concentration, where EQ was found to be more estrogenic, followed by DAI and lastly GEN whereas the order reported by Grgic *et al.* (2022) began with GEN, EQ and ended with DAI. Given that the parameters of the experiments were the same, it is hard to explain why this disparity occurs but could be attributed to the differing origins of the IFs or impurities. A decrease in estrogenicity was also observed in our work with regard to the highest concentration. This has been previously

reported (Grgic, et al., 2022; Vejdovszky, et al., 2016) yet in our case it was no more than 10%.

Another difficulty arises in comparing our results to other research groups, as the IF with the maximal achieved ALP induction at each of the three highest concentrations is different. GEN reached its maximum at 0.1 μM but at higher concentrations began declining, while DAI showed weak estrogenicity at 0.1 μM and was comparable to that of EQ at the two highest concentrations. EQ has been previously shown to be more estrogenic than DAI and GEN, as its binding affinity to ERs is higher (Morito, et al., 2001). However, the use of different cell lines, assays and incubation times renders a comparison difficult, especially since most groups tend to research individual compounds, instead of all three IFs. Even in the case of Lehmann *et al.* (2005), who utilized Ishikawa cells and an ALP assay, EQ was still found to be more estrogenic. However, their concentrations for the positive (10 nm E2) and solvent (0.1 % DMSO) control differed to ours. Therefore, when conducting a comparison with other studies, it is of utmost importance to take these details into considerations.

With regards to the phase II metabolites, interesting data was obtained for the glucuronides and sulfates. Due to their size, it has been hypothesized that glucuronides do not fit in the ER pockets and thus cause no alterations in the estrogenic activity, not to mention their hydrophilicity hinders a passing through the cell membrane (Zhang, et al., 1999). However, in the case of GEN the glucuronides exerted an ALP induction. At a concentration of 10 μM, the ALP activity of G7G was close to that of GEN itself. A weak estrogenic activity has been reported previously for G7G (Beekmann, et al., 2015), yet another group explained this effect as a result of deconjugation to the aglycone (Islam, et al., 2015). The weak estrogenicity of G4',7dG, which was threefold lower to that of GEN at 10 μM, has been reported for the first time.

All of the tested sulfate metabolites were proven to be estrogenic at the highest concentration, following the order of D4'S>E4'S>G7S. Most interesting was D4'S, whose ALP induction overcame the one of DAI while the one for E4'S was close to EQ. In contradiction, this effect was reported for the 7-sulfation for both IFs, while sulfation in the 4'-position actually decreased estrogenicity in MCF-7 cells (Pugazhendhi, et al., 2008) and in human cervix epitheloid carcinoma cells HeLa cells transfected with human ERβ (Totta, et al., 2005). G7S, which was much weaker in comparison to the other sulfates, was also threefold lower than its aglycone. This significant reduction in estrogenic activity because of a 7-sulfation has been previously reported for GEN, while a 4'-sulfation only showed a minor reduction (Pugazhendhi, et al., 2008). Regardless, in both cases, the position of the sulfate group did

influence the resulting ALP induction differently for DAI and EQ when compared to GEN, yet in no case did it abolish all activity. Hydroxy groups in the 4’ and 7 positions of the phytoestrogens play a significant role in their interactions with the LBD of ERs, especially since they form hydrogen bonds with the different amino acids (Pugazhendhi, et al., 2008). Another possible explanation for this could be given to the mode in which the three IFs bind into the LBD of the ER, something that can be investigated using crystallographic studies (Manas, et al., 2004). Additionally, without looking at HPLC-MS/MS data, a deconjugation to the aglycones should not be excluded.

5.2. Cytotoxicity of IFs measured via CTB and SRB

When observing toxicological effects of substances in cell lines, it is of utmost importance to simultaneously conduct assays like CTB and SRB to exclude cytotoxicity. Given that a lot of the tested metabolites did not show any estrogenic activity, this could be a side-effect attributed to a decrease in cell viability and thus was investigated for the three IFs and the 16 metabolites. Once more, the results are separated into three sections, each containing a specific IF (GEN, DAI or EQ) with their perspective metabolites.

5.2.1. GEN and metabolites

Figure 22 depicts the CTB and SRB results for GEN and its seven metabolites.

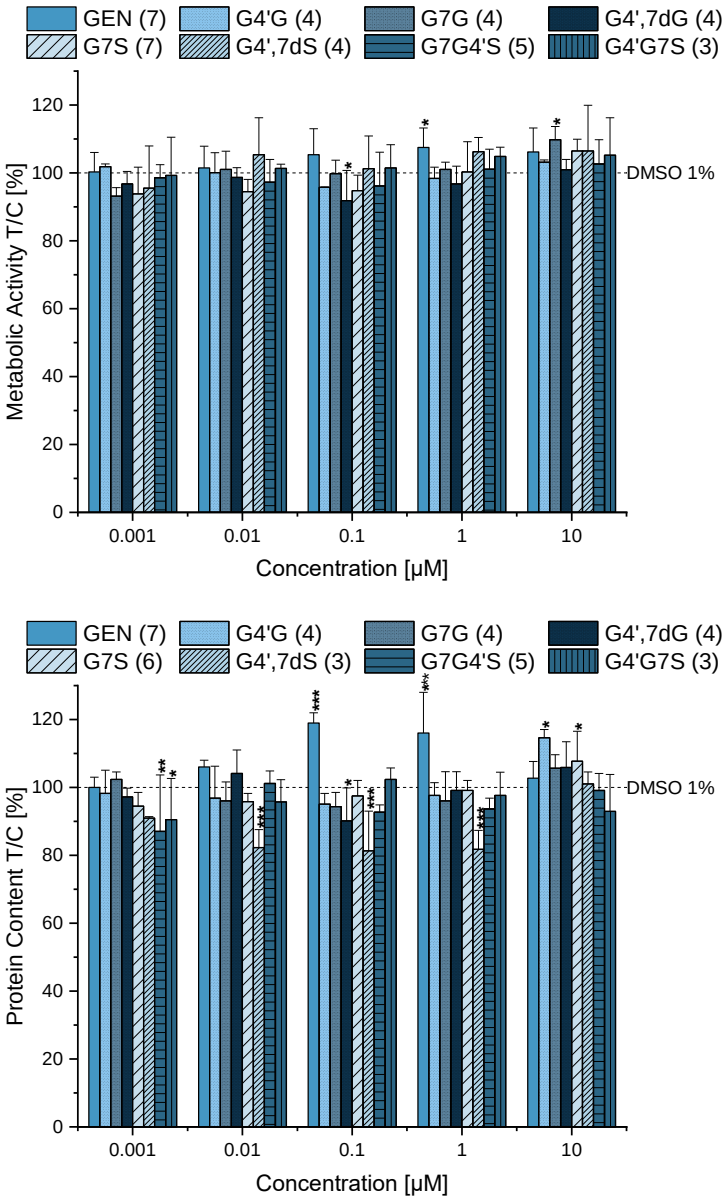

Figure 22: Graphic depiction of the effects of GEN and its metabolites on cytotoxicity in Ishikawa cells.

The cell viability after 48 h incubation is provided as metabolic activity [%] measured by CTB assay (top) and as cell protein content [%] measured by SRB assay (bottom) against the concentrations of the substances [0.001 – 10 µM]. The values were referred to DMSO (1%) as solvent control represented as 100%. Results are depicted as bars of mean ± standard deviation values. The biological replicates of each substance (ranging from 3 - 7) are shown in the parentheses next to the abbreviated names in the legend above the graphs. Outliers after Nalimov outlier test were excluded. Significant differences of effects between solvent control and the incubated compounds were calculated by one-sample Student's *t*-test and were indicated with * ($p < 0.05$), ** ($p < 0.01$) and * ($p < 0.001$).**

Overall, very few changes have been observed with regards to cytotoxicity when looking at the CTB data. The metabolic ability of the majority of the substances remained similar to that of the solvent control. A slight decrease in viability was observed at the lowest concentration of G7G, G7S and G4',7dS. The lowest metabolic ability reached in all GEN data-sets was for G4',7dG with 92 ± 9% at the concentration of 0.1 µM. Grgic *et al.* (2022) showed a decrease of cell viability to about 90%, yet we found no alteration in cell viability with regards to the highest concentration of GEN, something that could offer a possible explanation for the decrease in ALP activity in 5.1.1. GEN and metabolites. On the contrary, for the concentrations of 0.1 and 1 µM a slight increase in the metabolic activity was observed, something that was also shown for the highest concentration of G7G.

Interestingly, certain effects were far more visible in the SRB data. The proliferative action of GEN for the concentrations of 0.1 and 1 µM were present with 119 ± 3% and 116 ± 12% protein content each, followed by a reduction of those numbers at 10 µM. Proliferation was also observed for G4'G at the highest concentration with 115 ± 2%. On the contrary, the most notable decrease in cell viability was for G4',7dS at concentrations of 0.01, 0.1 and 1 µM with about 82% each. Similar data was derived for the lowest concentrations of the sulfoglucuronides. Compared to CTB, the SRB results (with the exception of GEN) pointed overall to slight cytotoxic effects for a few substances. However, the amount of washing steps required for SRB should be taken into consideration as a dislocation of the cells could take place and yield misleading results. Generally, CTB is more trustworthy than SRB.

GEN has been previously shown to inhibit cell growth in a dose- and time-dependent manner in both ERα dependent (Ishikawa) and ERα independent (KLE) endometrial cancer cell lines, specifically by inducing cell cycle arrest in G2/M and apoptosis. However, these cells were treated with 20 µM of GEN for the duration of 6 days, parameters which differ to ours (Yoriki, et al., 2022). In fact, the majority of the anti-proliferative effects for GEN have been associated with high treatment doses (> 20 µM) and independent of ER, e.g. the work of Peterson & Barnes (1991) for both ER negative (MDA-468) and ER positive (MCF-7) breast cancer cell lines. Additionally, GEN is a known inhibitor for tyrosine kinases, which are

responsible for the phosphorylation of other proteins (Mitropoulou, et al., 2002), for DNA topoisomerases (Russo, et al., 2012) and for modulation of mitogen-activated protein kinase (MAPK) signalling (Li, et al., 2006). The aforementioned inhibitory actions are related to mechanisms that could exert GEN's anticancer properties. Numerous cases showcased these effects but also showed ER mediated proliferative effects at lower doses (0.01 to 10 μM) in MCF-7 cells (Hsieh, et al., 1998; Choi & Kim, 2013; Choi, et al., 2014), which are in agreement with our own.

Unfortunately, no research has been conducted so far for the cytotoxicity of the GEN metabolites. Xiong *et al.* (2015), who synthesized GEN analogues, correlated cytotoxic and anti-proliferative effects to the hydroxy groups of C5 and C7. Substitution in those positions showed a lower potency for cell growth inhibition in HeLa cervical cancer cells at 1 and 10 μM. Given that cell proliferation in our experiments was not caused by any of the metabolites, with the exception of G4'G at the highest concentration and only in SRB, these effects could be related.

5.2.2. DAI and metabolites

Figure 23 depicts the CTB and SRB results for DAI and its seven metabolites.

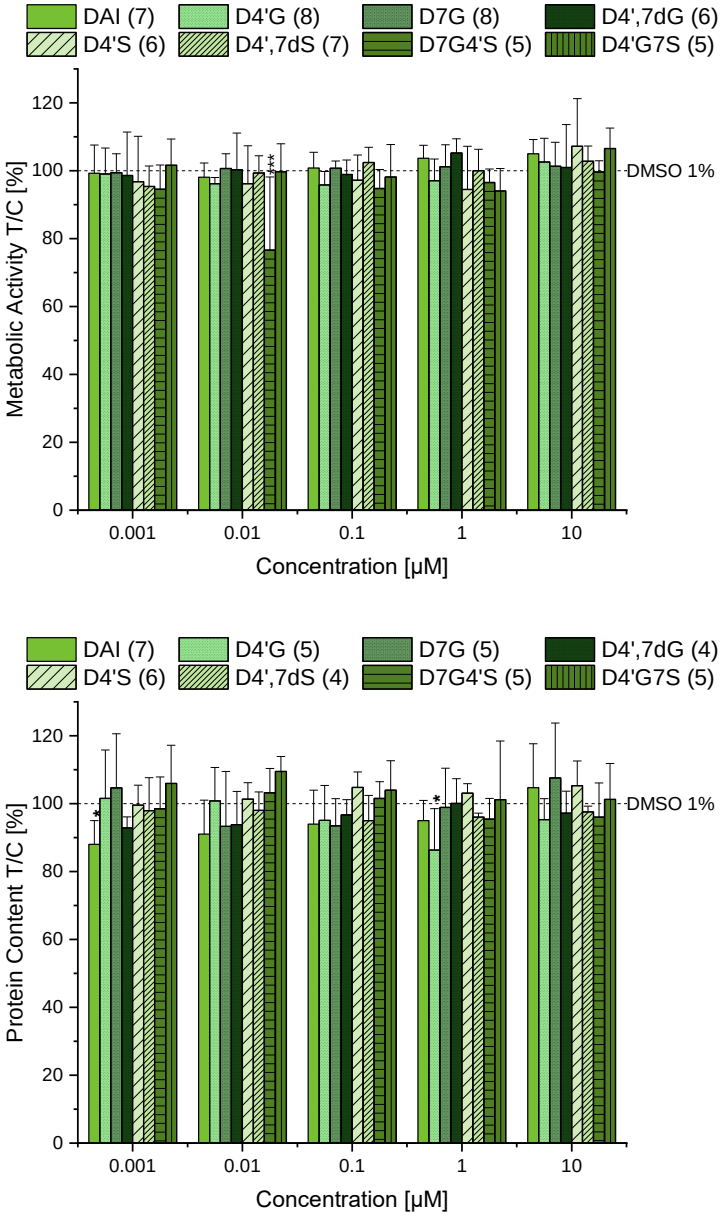

Figure 23: Graphic depiction of the effects of DAI and its metabolites on cytotoxicity in Ishikawa cells. The cell viability after 48 h incubation is provided as metabolic activity [%] measured by CTB assay (top) and as cell protein content [%] measured by SRB assay (bottom) against the concentrations of the substances [0.001 – 10 µM]. The values were referred to DMSO (1%) as solvent control represented as 100%. Results are depicted as bars of mean ± standard deviation values. The biological replicates of each substance (ranging from 4 - 8) are shown in the parentheses next to the abbreviated names in the legend above the graphs. Outliers after Nalimov outlier test were excluded. Significant differences of effects between solvent control and the incubated compounds were calculated by one-sample Student's *t*-test and were indicated with * ($p < 0.05$), ** ($p < 0.01$) and * ($p < 0.001$).**

Much fewer observations are to be made for DAI and its metabolites. Unlike GEN, no significant proliferation was observed for DAI with regards to metabolic activity, although a

slight but not significant increase was observed at higher concentrations. This did not agree with a previous research, which showcased a minor decrease instead (Grgic, et al., 2022). No other effects were derived from the CTB data with the exception of the sulfoglucuronide D7G4'S, which exhibited anti-proliferation for the concentrations 0.001 to 1 μM. It reached a minimum for 0.01 μM with 77 ± 22%. However, the standard deviation for this singular case was high. This effect was not observed for the other sulfoglucuronide.

Much like with GEN, anti-proliferative effects were observed only in the SRB data. DAI contradicted the results of CTB and showed a decrease in cellular protein content for all concentrations except the highest one. Similarly, D4'G for 0.1-10 μM, D7G for 0.01-0.1 μM and D4',7dG for 0.001-0.1 μM exhibited slight anti-proliferative effects. Given that CTB is a more trustworthy assay, this data may relate to loss of cells due to the various washing steps of SRB and may not represent true results.

Unlike its hydroxylated form, DAI is much less potent with regards to cytotoxicity when compared to GEN. Concentrations above 50 μM were needed for a variety of cancer cell lines in order to display cytotoxic effects and differed depending on the used cell line (Han, et al., 2015). Similar findings were yielded for the MCF-7 and other breast cancer cell lines in the study of Lin *et al.* (2009). Specifically, they showed that DAI (and other IFs) induced cell apoptosis via a caspase-3-dependent pathway and mediated cell cycle arrest in the G2/M phase. Unlike GEN, DAI displays little to no activity towards topoisomerase II (Bandele & Osheroff, 2007) and tyrosine kinases (Du, et al., 2004).

Lin *et al.* (2009) treated MCF-7 cells with serum metabolites (sulfates/glucuronides) of DAI extracted from rats, which resulted in inhibition of cell proliferation at a much lower concentration than that of the aglycone, namely 2.35 μM. This was explained by an upregulation of apoptotic proteins, such as p21, p53 and caspase-9. Given that they used a mixture and not individual metabolites plus the longer incubation times (72 h) and a different assay, a comparison with our data is not possible. Otherwise, not much research has been conducted on the cytotoxic effects of the DAI phase II metabolites. However, few researches have shown that oxidative metabolism increases not only cytotoxicity (Lo, 2013), but also genotoxicity (Baechler, et al., 2014), specifically with a possible interference of topoisomerase II. If the presence of hydroxy groups is necessary for such effects, then a substitution, which occurs with phase II metabolism, could potentially nullify this biological activity. However, for such a hypothesis to be proven, more research is needed.

5.2.3. EQ and metabolites

Figure 24 depicts the CTB and SRB results for EQ and its two metabolites.

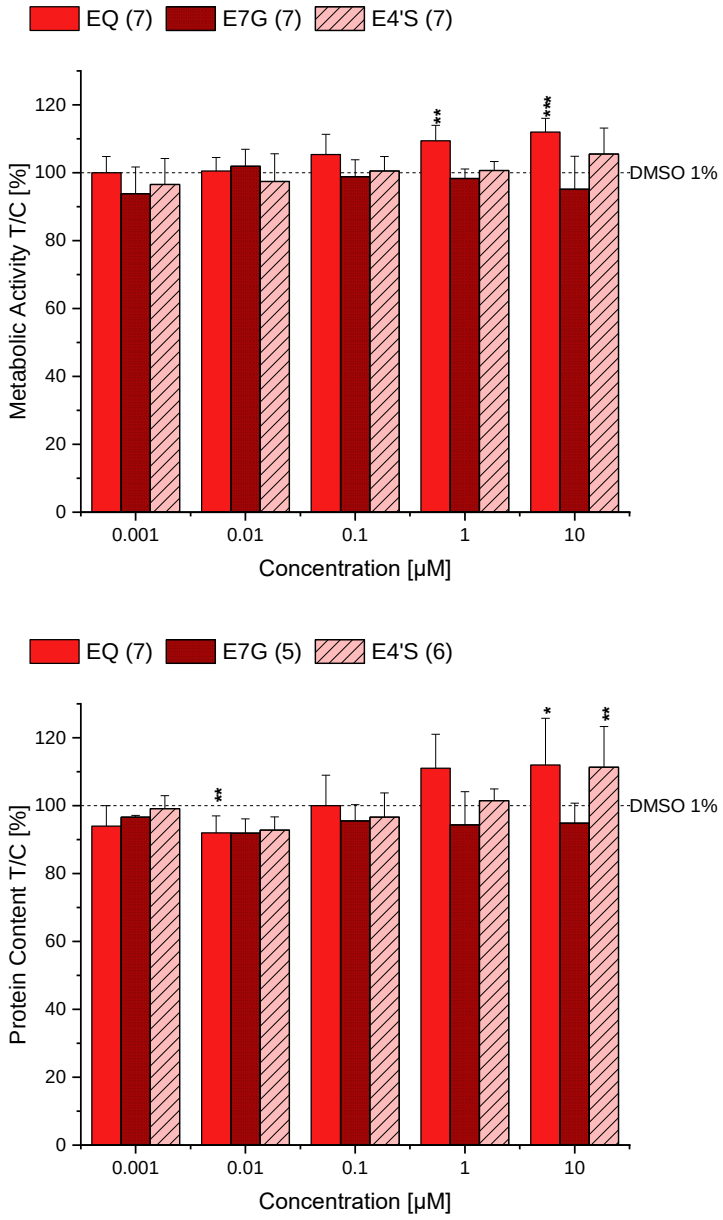

Figure 24: Graphic depiction of the effects of EQ and its metabolites on cytotoxicity in Ishikawa cells. The cell viability after 48 h incubation is provided as metabolic activity [%] measured by CTB assay (top) and as cell protein content [%] measured by SRB assay (bottom) against the concentrations of the substances [0.001 – 10 µM]. The values were referred to DMSO (1%) as solvent control represented 100%. Results are depicted as bars of mean ± standard deviation values. The biological replicates of each substance (ranging from 5 - 7) are shown in the parentheses next to the abbreviated names in the legend above the graphs. Outliers after Nalimov outlier test were excluded. Significant differences of effects between solvent control and the incubated compounds were calculated by one-sample Student's *t*-test and were indicated with * ($p < 0.05$), ** ($p < 0.01$) and * ($p < 0.001$).**

The phytoestrogen metabolite EQ weakly increased cell proliferation in a concentration-dependent manner in both assays. Especially in CTB, the gradual increase was observed till it

reached a 112 ± 4% of metabolic activity for the highest concentrations. Although the same occurred for the concentrations 0.1-10 μM in SRB, slight but not significant anti-proliferation was observed for the lowest concentrations, reaching a minimum of 92 ± 5% protein content. Just like before, this could be explained with a dislocation of the cells during the multiple washing steps of SRB. This proliferative effect has also been previously observed (Grgic, et al., 2022).

With regards to the metabolites, differing data were observed. Overall, E7G appeared to have a tendency towards decreasing cell viability, especially during SRB yet the opposite was observed for E4'S, which followed a similar to EQ concentration-dependent increase of cell proliferation. This contrasting effect was mainly highlighted at the highest concentration of 10 μM.

Anti-proliferative effects of EQ have been previously investigated in the MDA-MB-453 human breast cancer cell line. According to Choi *et al.* (2009), a significant decrease in cell proliferation was observed for concentrations above 10 μM after 48 h incubation. However, this was already shown for lower concentrations (1 μM) when the incubation time was raised to 72 h. The apoptotic effects have been associated with the mitochondrial-mediated pathway, specifically due to activation of caspase 3 and 9. The inhibition of cell growth was also investigated in prostate cancer cells, where the required concentrations were lower than 10 μM (Magee, et al., 2006). Cell cycle arrest of MCF-7 cells was observed in G1/S, unlike GEN and DAI, which occured in G2/M (Ono, et al., 2017). Not much is known for the effects EQ has on tyrosine kinases and DNA topoisomerases. However, together with GEN and DAI, the three of them have been found to be potent inhibitors of leukocyte functions, since T cells and natural killer cells both express ERs (Gredel, et al., 2008).

Unfortunately, nothing is known for the phase II metabolites of EQ with regards to their cytotoxic effects. Here we report for the first time slightly different effects in cell proliferation when considering position and type of substitution groups. However more data are required to adequately form and prove a hypothesis.

5.3. HPLC-MS/MS

A preface to the results was the discussion of sulfation. Unfortunately, for all three IFs, only one sulfate was available at the time of the study. Therefore, for the sake of accuracy, the results regarding sulfation are denoted as GS, DS and ES with each of them representing a "summary" of the possible 4'- and 7-sulfate metabolites of GEN, DAI and EQ respectively instead of the individual isomers. Indeed, in some cases a split peak was present, possibly suggesting that both 4'- and 7-sulfates were produced by the cells. In no case however a distinct peak separation was possible. Therefore, the choice to represent sulfation as a summary was taken.

Overall, three sequences were utilized with the UHPLC-MS/MS. Only the last sequence showed an overall peak shift, with a 0.2-0.6 minutes difference. For the same sequence, tailing and fronting of the peaks were in some cases visible, meaning that the quantification was not entirely accurate and several results show high standard deviations. Additionally, there were issues when investigating the recovery rates and matrix effects, all of which are summarized in the Appendix. For some reason, the quantification of the spiked solvent showed lower concentrations when compared to the DMSO control spikes. Due to this fact, the recovery rates were considered as a means of correction of the results. All were between 80 and 120%, thus no corrections were necessary.

5.3.1. GEN and metabolites

GEN itself had a retention time of 11 min. The metabolites followed the order of G4',7dG (4.5 min), G7G4'S (5.8 min), G4'G7S (6.3 min), G7G (7.2 min), G4',7dS (7.5 min), G4'G (7.8 min) and G7S (9.1 min).

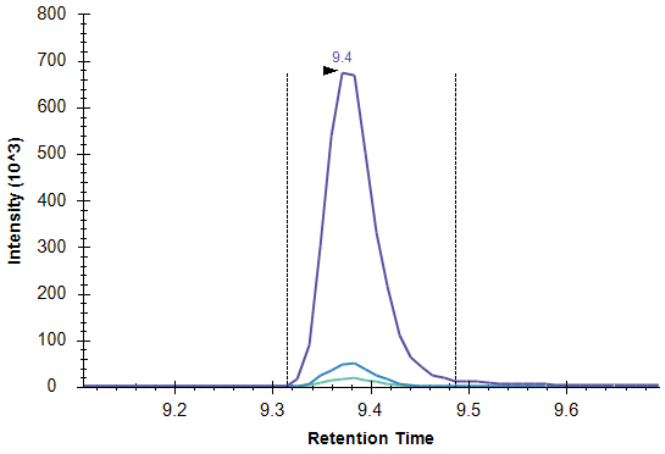

Figure 25: Chromatogram of a G7S sample denoting the retention time [min] of the metabolite.

In Figure 25 the retention time visible for one of the G7S samples belonged to the sequence that was characterized by a slight peak shift. No split peak was visible in this or any other case, leading to the assumption that only one isomer was present, yet the existence of both in the tested samples should not be entirely excluded. Figure 26 represents the percentage of the produced substances when the Ishikawa cell line was incubated with two different concentrations of GEN for 48 h.

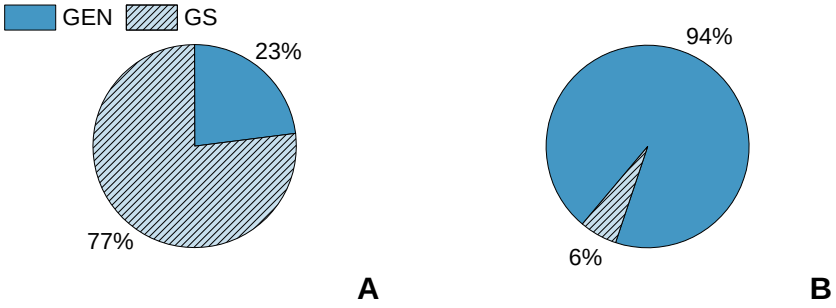

Products of GEN	1 µM [nmol/80 µL]	Theor. (1 µM) [nmol/80 µL]	10 µM [nmol/80 µL]	Theor. (10 µM) [nmol/80 µL]
GEN	0.02 ± 0.01	0.08	0.75 ± 0.44	0.8
GS	0.07 ± 0.01	-	0.05 ± 0.03	-
Sum	0.1 ± 0.02	-	0.8 ± 0.44	-

Figure 26: Pie charts representing the metabolites present after incubating Ishikawa cells for 48 h. Graphs A and B correspond to incubations with 1 and 10 µM GEN, respectively. The table denotes the incubated concentrations (1 and 10 µM) of the test substances, the produced concentrations of the aglycones or metabolites in nmol per 80 µL and the theoretical values.

The most notable changes occurred overall for the IFs. When the cells were incubated with a concentration of 1 µM GEN, the majority of that substance was metabolized to a sulfate counterpart, rounding up to 77% hence only 23% of the aglycone was present after 48h of incubation. In contrast to this, incubation with a higher concentration (i.e. 10 µM) did not show such a preference for metabolization, rather 94% of the substance was detected as the IF itself. This, according to Michaelis-Menten kinetics, would mean that between 1 and 10 µM of GEN, a saturating substrate concentration is achieved and the system with the sulfotransferases reaches its maximum reaction rate, thus halting any further metabolization. Such an observation is of utmost importance, as it showcases that conjugation with sulfates does not nullify the biological activity of GEN, rather the previous observation with regard to estrogenicity at 1 µM could be partially attributed to the metabolite instead.

According to Nishiyama *et al.* (2002), all four major recombinant human SULTs (SULT1A1, SULT1A3, SULT1A2 and SULT1E1) are capable of sulfating this phytoestrogen. The highest catalytic efficiency however was shown for SULT1E1 and SULT1A1, with the

former being more active for GEN (with the Michaelis constant K_m being 0.7 and 0.3 µM respectively). Nakano *et al.* (2004) also reported similar results. In addition to this, both genes are expressed by the Ishikawa cell line, with the mRNA levels of SULT1E1 being twofold those of SULT1A1 (Hevir-Kene & Rižner, 2015). The presence of these SULTs allows for a conjugation to take place and explains our UHPLC-MS/MS results.

Although not possible to observe with our tested substances, regioselectivity should still be considered. The group of Nakano *et al.* (2004) utilized purified recombinant human SULTs and showed not only that SULT1E1 catalyzed the 4'- and 7-sulfation of GEN with similar efficiencies, but also that no inhibition by the substrate took place at high concentrations. However, already at concentrations above 5 µM, the formation of the sulfate slowly began reaching a maximum, something that is in accordance with our results. In contrast to this, substrate concentrations higher than 1 µM inhibited the formation of both isomers by SULT1A1, which showed a clear preference for the formation of G7S with an 8.8 ratio. Interestingly enough, by considering gene expression in the human breast cancer cell line MCF-7, the mRNA expression of SULT1E1 is undetectable and only SULT1A1 was present (Fu, et al., 2010). This core difference between the two cell lines could explain some differing results we saw when it came to the estrogenic activities.

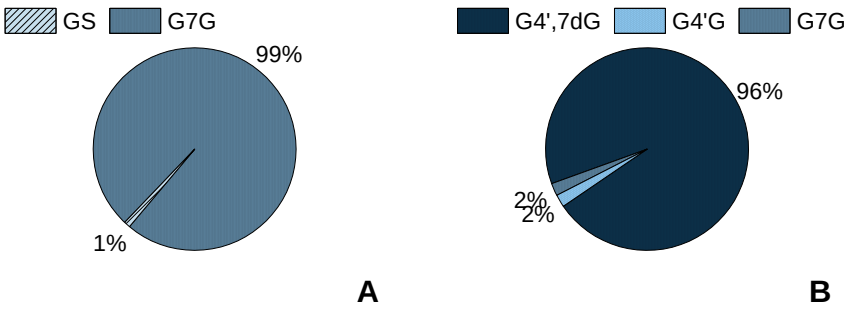

Products of G7G	1 µM [nmol/80 µL]	Theor. (1 µM) [nmol/80 µL]	10 µM [nmol/80 µL]	Theor. (10 µM) [nmol/80 µL]
G7G	0.14 ± 0.4	0.08	0.84 ± 0.13	0.8
GS	0.0007 ± 0.0003	-	-	-
Sum	0.14 ± 0.4	-	-	-
Products of G4',7dG	**1 µM [nmol/80 µL]**	**Theor. (1 µM) [nmol/80 µL]**	**10 µM [nmol/80 µL]**	**Theor. (10 µM) [nmol/80 µL]**
G4',7dG	0.13 ± 0.05	0.08	1.22 ± 0.26	0.8
G4'G	-	-	0.03 ± 0.01	-
G7G	-	-	0.02 ± 0.01	-
Sum	0.13 ± 0.05	-	1.27 ± 0.26	-

Figure 27: Pie charts representing the metabolites present after incubating Ishikawa cells for 48 h. Graphs A and B correspond to incubations with G7G (1 µM) and G4',7dG (10 µM), respectively. The table denotes the incubated concentrations (1 and 10 µM) of the test substances, the produced concentrations of the aglycones or metabolites in nmol per 80 µL and the theoretical values.

With regards to the metabolites of GEN, no significant observations were made. The only two metabolites that showed a miniscule difference were G7G at 1 µM and G4',7dG at 10 µM. The former showed the formation of 1% of GS. The diglucuronide began breaking down into its individual glucuronides in almost equal amounts to a small extent (4%). Both substances presented in Figure 27 are of interest, as they showcased estrogenic activities at 10 µM. Although it is possible that the metabolic effects were more present at lower concentrations, those were not relevant to estrogenicity and were therefore not investigated. Unfortunately, there was no research regarding which enzymes were capable of altering the metabolites themselves, therefore no further explanations can be provided. With the resulting UHPLC-MS/MS data however, it can be assumed that the estrogenicity at 10 µM is a direct result of the metabolites themselves, as none of the substances were deconjugated to the aglycone. Further experiments based on how these two molecules fit in the hydrophobic groove of ERs are necessary in order to better elucidate these results, especially for G7G, whose activity overcame that of the IF itself at that concentration.

Table 15: Concentrations (1 or 10 µM) of the test substances G4',7dS, G7S, G4'G7S, G7G4'S, G4'G and G7G, the produced concentrations of the aglycones or metabolites in nmol per 80 µL after 48 h incubation in Ishikawa cells and the theoretical values.

Products of G4'7dS	**1 µM [nmol/80 µL]**	**Theor. (1 µM) [nmol/80 µL]**	**10 µM [nmol/80 µL]**	**Theor. (10 µM) [nmol/80 µL]**
G4',7dS	-	0.08	1.53 ± 0.29	0.8
Products of G7S	**1 µM [nmol/80 µL]**	**Theor. (1 µM) [nmol/80 µL]**	**10 µM [nmol/80 µL]**	**Theor. (10 µM) [nmol/80 µL]**
G7S	0.07 ± 0.05	0.08	1.36 ± 0.14	0.8
Products of G4'G7S	**1 µM [nmol/80 µL]**	**Theor. (1 µM) [nmol/80 µL]**	**10 µM [nmol/80 µL]**	**Theor. (10 µM) [nmol/80 µL]**
G4'G7S	-	0.08	1.99 ± 1.11	0.8
Products of G7G4'S	**1 µM [nmol/80 µL]**	**Theor. (1 µM) [nmol/80 µL]**	**10 µM [nmol/80 µL]**	**Theor. (10 µM) [nmol/80 µL]**
G7G4'S	-	0.08	1.90 ± 0.97	0.8
Products of G4'G	**1 µM [nmol/80 µL]**	**Theor. (1 µM) [nmol/80 µL]**	**10 µM [nmol/80 µL]**	**Theor. (10 µM) [nmol/80 µL]**
G4'G	-	0.08	1.95 ± 1.32	0.8
Products of G7G	**1 µM [nmol/80 µL]**	**Theor. (1 µM) [nmol/80 µL]**	**10 µM [nmol/80 µL]**	**Theor. (10 µM) [nmol/80 µL]**
G7G	0.14 ± 0.4	0.08	0.84 ± 0.13	0.8

The rest of the metabolites of GEN in Table 15, namely G4',7dS, G7S, G4'G7S, G7G4'S, G4'G and G7G (at 10 µM) did not appear to be transformed by the Ishikawa cell line or revert back to the aglycone. Interestingly enough, G7S was found to be estrogenic at the highest concentration. This along with the resulting UHPLC-MS/MS data of GEN allow for the hypothesis that the sulfate metabolite might be a good ligand for ERs and is responsible

for such a biological activity. It should be noted, that with the lack of G4'S in our laboratories, it is not possible to assess whether this result corresponds to one or the other isomers or a mixture of both. In general, there is little to no information on whether any of these molecules are substrates for enzymes and, to our knowledge, this is the first available information about whether any further metabolism or deconjugation of phase II metabolites takes place in an endometrial cancer cell line.

Another distinct observation was that for GEN and all its metabolites, an unknown peak belonging to a singular transition of DS (*m/z*=116.9) was detectable at 8.8 or 9.2 min. Given that this did not equate to any of the known and available DAI metabolites and because the concentrations were low and differed significantly between biological replicates, it was not considered for our results.

5.3.2. DAI and metabolites

DAI itself was characterized by a retention time of 10.1 min. Its metabolites followed the order of D4',7dG (3.8 min), D7G4'S (5.2 min), D4'G7S (5.7 min), D7G (6.4 min), D4',7dS (6.9 min), D4'G (7.1 min) and D4'S (8.4 min).

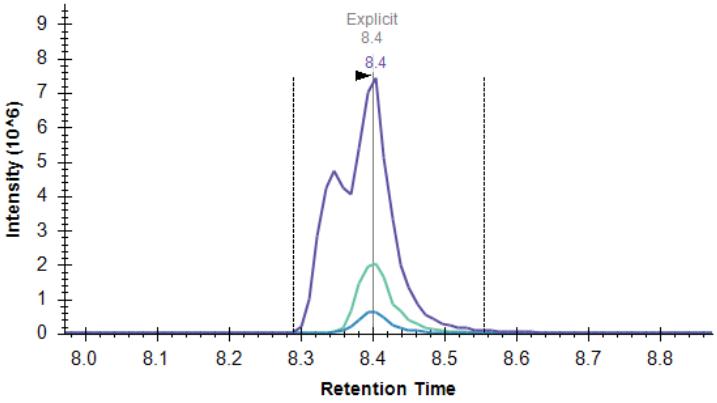

Figure 28: Chromatogram of a D4'S sample denoting the retention time [min] of the metabolite.

As already previously stated, a split peak was visible for D4'S (as depicted in Figure 28) leading us to hypothesize that both sulfate isomers could be present but were not easy to separate. It is possible, that the standard that was obtained might have been impure and contaminated with D7S. Figure 29 represents the percentage of the produced substances when the Ishikawa cell line was incubated with two different concentrations of DAI for 48 hours.

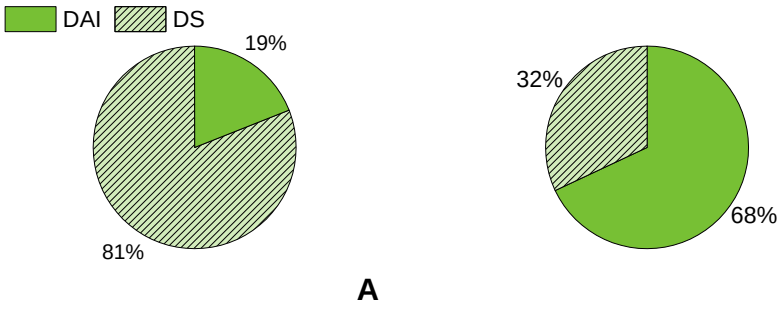

Products of DAI	1 µM [nmol/80 µL]	Theor. (1 µM) [nmol/80 µL]	10 µM [nmol/80 µL]	Theor. (10 µM) [nmol/80 µL]
DAI	0.06 ± 0.01	0.08	0.56 ± 0.29	0.8
DS	0.24 ± 0.07	-	0.26 ± 0.17	-
Sum	0.29 ± 0.07	-	0.83 ± 0.34	-

Figure 29: Pie charts representing the metabolites present after incubating Ishikawa cells for 48 h. Graphs A and B correspond to incubations with 1 and 10 µM of DAI, respectively. The table denotes the incubated concentrations (1 and 10 µM) of the test substances, the produced concentrations of the aglycones or metabolites in nmol per 80 µL and the theoretical values.

Much like GEN, DAI also appeared to be metabolized to its sulfate counterpart. At the lowest concentration, the majority of DAI formed a sulfate to 81%. In contrast to this, incubation of a higher concentration showed a much lower production of a sulfate metabolite, consisting of 32% sulfates and 68% of DAI itself. It should however be noted, that the standard deviation for the latter is quite high. In addition to this, one would expect the amount of nmol produced to be twice as high for 10 µM but that was not the case. Regardless, it appears that a saturating substrate concentration is also slowly achieved between 1 and 10 µM. This is once more of importance because at both concentrations, DAI has shown a high estrogenic activity, part of which could now be attributed to a sulfate metabolite, leading us to believe that sulfation is not necessarily a detoxifying pathway.

The effects of SULTs on DAI are quite similar to those mentioned in the case of GEN. All four major SULTs are also capable of sulfating DAI, with SULT1E1 and SULT1A1 having higher catalytic efficiencies. SULT1A1 was again inhibited by substrate concentrations above 1 µM, which was not the case for SULT1E1 (Nakano, et al., 2004). Interestingly enough, Nishiyama *et al.* (2002) observed that GEN was a much better substrate than DAI, specifically 12- and 8-fold for SULT1A1 and SULT1E1 respectively and based on catalytic efficiency. The reason for this however was attributed to a higher K_m and not because of the catalytic rate constant k_{cat}. Our results suggest that DAI was much easier metabolized to a sulfate counterpart, even at the highest concentration. Although this contradicts the aforementioned work, it is noteworthy that the level of expression of SULTs is highly

dependent on the confluency of the cell cultures, something that could also explain why in some cases significant differences were observed between the biological replicates (Fu, et al., 2010).

In the case of DAI regioselectivity plays an important role, as a distinct split peak was visible in the chromatograms and was present in most data. SULT1A1 was the only enzyme which showed regioselectivity in sulfation of DAI with a clear preference for the 7-position. This was attributed to k_{cat} instead of K_m (Nakano, et al., 2004). SULT1E1 is expressed twofold higher than SULT1A1 in the Ishikawa cell line (Hevir-Kene & Rižner, 2015) and since it lacks a regioselective preference, it can be assumed that both sulfate isomers could be present in the sample. With the presence of SULT1A1 in the Ishikawa cell line it could also be theorized, that D7S is formed and possibly dominates over its D4'S counterpart. Further investigations are however necessary for this hypothesis to be proven, especially when it comes to whether a breaking in the bond between sulfate and the aglycone is possible, followed by a reformation of the metabolite but in a different position.

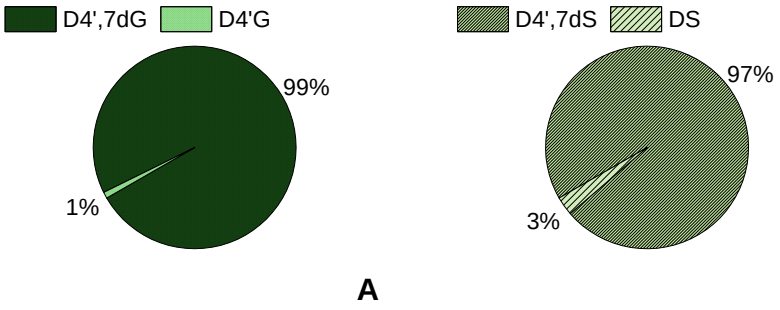

Products of D4',7dG	1 µM [nmol/80 µL]	Theor. (1 µM) [nmol/80 µL]	10 µM [nmol/80 µL]	Theor. (10 µM) [nmol/80 µL]
D4',7dG	-	0.08	0.97 ± 0.31	0.8
D4'G			0.009 ± 0.002	-
Sum			0.98 ± 0.31	-
Products of D4',7dS	**1 µM [nmol/80 µL]**	**Theor. (1 µM) [nmol/80 µL]**	**10 µM [nmol/80 µL]**	**Theor. (10 µM) [nmol/80 µL]**
D4',7dS	-	0.08	1.62 ± 0.21	0.8
DS			0.06 ± 0.02	-
Sum			1.68 ± 0.21	-

Figure 30: Pie charts representing the metabolites present after incubating Ishikawa cells for 48 h. Graphs A and B correspond to incubations with D4',7dG (10 µM) and D4',7dS (10 µM), respectively. The table denotes the incubated concentrations (1 and 10 µM) of the test substances, the produced concentrations of the aglycones or metabolites in nmol per 80 µL and the theoretical values.

Just like in the case of GEN, there are not many observations to be made with regards to the metabolites of DAI. In the case of the diglucuronide, the majority of the substance remained as such and only 1% was metabolized to a monoglucuronide counterpart. The disulfate on the

other hand appeared to be slightly deconjugated to a monosulfate by 3%. None of these metabolites showed any estrogenic effect at the tested concentration which suggests that this metabolic pathway indeed leads to a loss of the biological activity of DAI.

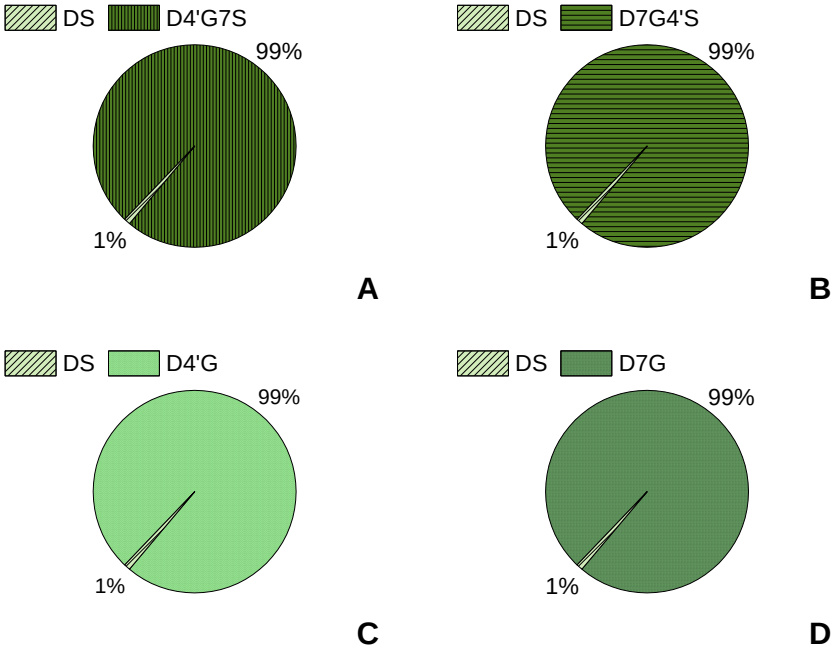

Products of D4'G7S	1 µM [nmol/80 µL]	Theor. (1 µM) [nmol/80 µL]	10 µM [nmol/80 µL]	Theor. (10 µM) [nmol/80 µL]
D4'G7S	-	0.08	1.28 ± 0.25	0.8
DS			0.008 ± 0.004	-
Sum			1.29 ± 0.25	-
Products of D7G4'S	**1 µM [nmol/80 µL]**	**Theor. (1 µM) [nmol/80 µL]**	**10 µM [nmol/80 µL]**	**Theor. (10 µM) [nmol/80 µL]**
D7G4'S	-	0.08	1.06 ± 0.22	0.8
DS			0.02 ± 0.01	-
Sum			1.08 ± 0.22	-
Products of D4'G	**1 µM [nmol/80 µL]**	**Theor. (1 µM) [nmol/80 µL]**	**10 µM [nmol/80 µL]**	**Theor. (10 µM) [nmol/80 µL]**
D4'G	-	0.08	3.13 ± 0.94	0.8
DS			0.02 ± 0.01	-
Sum			3.15 ± 0.94	-
Products of D7G	**1 µM [nmol/80 µL]**	**Theor. (1 µM) [nmol/80 µL]**	**10 µM [nmol/80 µL]**	**Theor. (10 µM) [nmol/80 µL]**
D7G	-	0.08	2.22 ± 0.24	0.8
DS			0.02 ± 0.01	-
Sum			2.25 ± 0.24	-

Figure 31: Pie charts representing the metabolites present after incubating Ishikawa cells for 48 h. Graphs A, B, C and D correspond to incubations with 10 µM of D4'G7S, D7G4'S, D4'G, and D7G, respectively. The table denotes the incubated concentrations (1 and 10 µM) of the test substances, the produced concentrations of the aglycones or metabolites in nmol per 80 µL and the theoretical values.

Similarly, the glucuronides and sulfoglucuronides showed no changes, except for the formation of 1% of the sulfate metabolite. Overall, none of these substances were found to be estrogenic, therefore one could assume that the formation of glucuronides and sulfoglucuronides works as detoxification for DAI. It should be noted, that significant differences were observed between the amounts quantified via UHPLC-MS/MS yet no explanation can be provided for this occurrence.

Table 16: Concentrations (1 or 10 µM) of D4'S, the produced concentrations of the aglycones or metabolites in nmol per 80 µL after 48 h incubation in Ishikawa cells and the theoretical values.

Products of D4'S	1 µM [nmol/80 µL]	Theor. (1 µM) [nmol/80 µL]	10 µM [nmol/80 µL]	Theor. (10 µM) [nmol/80 µL]
DS	0.18 ± 0.11	0.08	0.67 ± 0.25	0.8

The most important metabolite, namely D4'S, did not appear to be altered in its structure and remained as such. There was a high standard deviation due to differing data between the biological replicates and much like a few other substances, the amount produced by the highest concentration was not ten times the one from 1 µM. SULT1E1 was previously shown to be most efficient at catalyzing disulfation mainly of D7S. The formation of the disulfate was also possible via D4'S (Nakano, et al., 2004), something that was not observed in our experiments. However, the question remains which monosulfate we are observing.

Interestingly enough, this was the metabolite which appeared to exert higher estrogenicity than the aglycone at the highest concentration. This attribute has been previously given to sulfation in the 7-position of DAI (Pugazhendhi, et al., 2008) yet in our case, D4'S was shown to exhibit this effect during our ALP experiments. In the case of DAI, there have been no experiments observing whether a metabolite has been broken down to its aglycone and reformed with the functional group taking a different position. Such a phenomenon would explain why our estrogenicity results differ from those of Pugazhendhi *et al.* (2008). It should also be mentioned, that the gene expression of SULTs is dissimilar between the Ishikawa and MCF-7 cell lines, with the latter only expressing SULT1A1. Regardless, attention should be given to the conclusion, that the aforementioned estrogenic effects can be attributed to the monosulfate itself.

5.3.3. EQ and metabolites

The retention times for EQ, E7G and E4'S were 10.8, 7.7 and 8.9 min respectively.

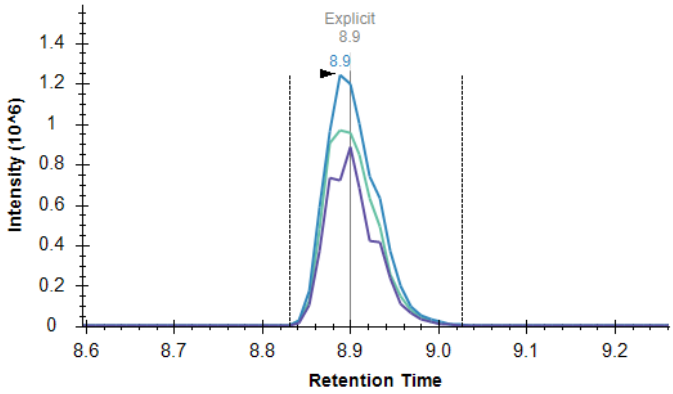

Figure 32: Chromatogram of an E4'S sample denoting the retention time [min] of the metabolite.

In Figure 32 the retention time for one of the E4'S samples is visible and unlike DAI, no split peak was observed leading to the assumption that only one isomer was present, yet the existence of both sulfates in the tested samples should not be entirely excluded. Figure 33 represents the percentage of the produced substances when the Ishikawa cell line was incubated with two different concentrations of EQ for 48 hours.

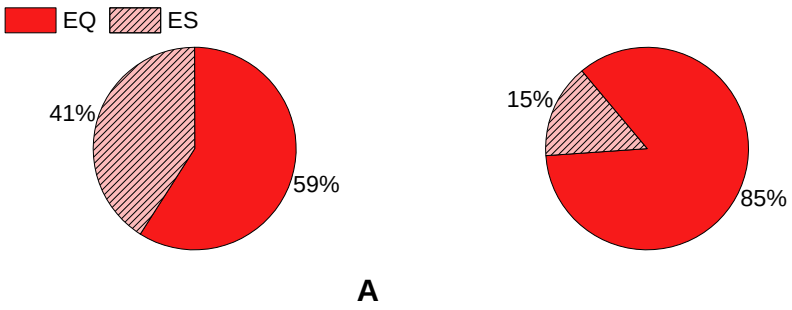

Products of EQ	1 µM [nmol/80 µL]	Theor. (1 µM) [nmol/80 µL]	10 µM [nmol/80 µL]	Theor. (10 µM) [nmol/80 µL]
EQ	0.02 ± 0.01	0.08	0.28 ± 0.22	0.8
ES	0.02 ± 0.01	-	0.05 ± 0.04	-
Sum	0.04 ± 0.02	-	0.33 ± 0.22	-

Figure 33: Pie charts representing the metabolites present after incubating Ishikawa cells for 48 h with EQ. Graphs A and B correspond to incubations with 1 and 10 µM of EQ, respectively The table denotes the incubated concentrations (1 and 10 µM) of the test substances, the produced concentrations of the aglycones or metabolites in nmol per 80 µL and the theoretical values.

EQ also followed the same trend as GEN and DAI, where the aglycone was metabolized to a monosulfate. At the concentration of 1 µM, 41% of the monosulfate was present in the samples which then reduced to 15% at a higher concentration. Unlike GEN and DAI, the majority of the molecule remained as the aglycone at both of the tested concentrations.

However, not only was the precision of the data very low, the sum of the formed amounts of each substance was much lower when compared to others. As there were no unknown peaks visible in the data, this cannot really be explained. Additionally, there is not any information regarding EQ being a substrate for SULTs yet it would appear that this is the case. Despite being a DAI metabolite, EQ is also conjugated with sulfates and this metabolic pathway could possibly lead to retaining of the biological activity, based on our ALP data.

Table 17: Concentrations (1 or 10 µM) of E7G and E4'S, the produced concentrations of the aglycones or metabolites in nmol per 80 µL after 48 h incubation in Ishikawa cells and the theoretical values.

Products of E7G	**1 µM [nmol/80 µL]**	**Theor. (1 µM) [nmol/80 µL]**	**10 µM [nmol/80 µL]**	**Theor. (10 µM) [nmol/80 µL]**
E7G	-	0.08	0.82 ± 0.19	0.8
Products of E4'S	**1 µM [nmol/80 µL]**	**Theor. (1 µM) [nmol/80 µL]**	**10 µM [nmol/80 µL]**	**Theor. (10 µM) [nmol/80 µL]**
E4'S	0.09 ± 0.05	0.08	0.26 ± 0.12	0.8

Similarly with others, the EQ metabolites, namely E4'S and E7G did not appear to be metabolized and only these molecules were present in the samples. Much like with EQ, the quantification also yielded very low concentrations when compared to the other substances. Given that glucuronidation did not change the ALP activity and since no other metabolites or the aglycone itself were present in the samples, it can be assumed that this leads to detoxification. On the other hand, E4'S was found to be estrogenic at the highest concentration. This together with the UHPLC-MS/MS data as well as the sulfation of EQ allows postulating the hypothesis, that such a metabolic pathway does not fully diminish estrogenicity. Quite like the previous metabolites, not much research has been conducted with regards to the relationship between EQ, its metabolites and different enzymes that partake in phase II metabolism.

6. Conclusion

With the present work we investigated the estrogenic effects of the IFs GEN and DAI, the gut microbial metabolite EQ and 16 phase II metabolites, comprising glucuronides, sulfates, diglucuronides, disulfates and the glucuronide-sulfate modification. Based on the results from the ALP experiments, the IFs remain as the most biologically active substances, since an ALP induction was already visible at lower concentrations. The order for the IFs was GEN>EQ>DAI. GEN's estrogenicity peaked at 0.1 μM with 64% ALP induction and only slightly decreased at higher concentrations. Although this reduction could be potentially explained with other cellular pathways relating to cytotoxicity, this was not the case based on our cell viability experiments with regards to metabolic activity and protein content. Estrogenic impact of EQ and DAI both peaked at 1 μM with an ALP induction of 72% and 65%, respectively. The estrogenic response mediated by DAI remained relatively stable at 10 μM while those by EQ decreased slightly. Also, in this case, no cytotoxic effects were observed, rather slight proliferative, dose-dependent effects with increasing concentrations of EQ.

Interestingly, at a concentration of 1 μM, GEN and DAI were primarily conjugated with sulfate, while the occurrence of this conjugation for EQ was less abundant with about 50 %. This conjugation was not observed at the highest applied concentration, meaning that somewhere between 1 and 10 μM the sulfotransferases began reaching saturation. An explanation for this was offered based on the enzyme profile of the utilized endometrial adenocarcinoma Ishikawa cell line, which expresses SULT1E1 and SULT1A1, two of the major sulfotransferases responsible for the sulfation of the IFs (Hevir-Kene & Rižner, 2015). The expression of these enzymes is also highly dependent on cell confluence (Fu, et al., 2010), something that could potentially explain the high standard deviations of certain results. None of the metabolites showed a significant biological ability with the exception of five substances which induced relatively high, medium and low ALP activities at 10 μM. Looking only at that concentration, the order follows D4'S>G7G≈E4'S>G7S≈G4',7dG for the metabolites with ALP induction of 75%, 55%, 54%, 28% and 23%, respectively. Compared to their aglycones, only D4'S appears to slightly enhance the estrogenic activity of DAI whereas the rest of the metabolites mediated a decrease instead. Although the estrogenicity of phase II metabolites, specifically monoglucuronides of GEN (Zhang, et al., 1999) and sulfates of GEN, DAI and EQ (Pugazhendhi, et al., 2008) has been studied previously, D4'S was the only case that contradicted previous studies which attributed a potential enhancement

of DAI's estrogenicity to the formation of D7S instead (Pugazhendhi, et al., 2008). Furthermore, according to the UHPLC-MS/MS results the aforementioned possibly estrogenic metabolites were not deconjugated to their respective aglycones meaning, that the high ALP activity could be attributed to the metabolites themselves. It is therefore possible that sulfation could no longer be considered a fully detoxifying metabolic pathway.

As for future perspectives of this particular work, first focus should be given to the kinetic aspect of IF metabolism. Since our incubation times were set to 48h, it would be interesting to see at which time frame the formation of sulfates takes place and whether that also influences ALP induction. Only with those experiments would it be easier to form a hypothesis surrounding the possible estrogenic activity of IF sulfates and glucuronides.

In addition to this, the investigation on different cell lines, specifically MCF-7, could be relevant since this was a major difference between our results and the cited literature. Based on the fact that the enzyme profile of sulfotransferases differs between these two cell lines, with SULT1E1 being absent in the breast cancer cell line MCF-7 (Fu, et al., 2010), it would be possible that estrogenicity experiments of IFs yield differing results. Therefore, a comparative study could prove significant not only within our project, but also to further investigate whether cell line specific metabolism plays a role and how it may affect data.

Furthermore, focus should be given to the sulfates. Acquiring the other substances that were commercially lacking, namely D7S, G4'S and E7S, and by conducting the same experiments of this work, it will be much easier to better allocate the estrogenic effects on specific substances instead of a summary of both possible sulfate isomers, not to mention explain why sulfation of DAI seems to be the only metabolic pathway that could potentially increase the estrogenic activity, unlike sulfation of GEN and DAI. This data could then be accompanied with molecular modelling, e.g., *in silico*, which has been previously utilized (Dellafiora, et al., 2018). With regard to ER expression, both Ishikawa and MCF-7 cell lines were shown to express higher mRNA levels of ERα rather than ERβ (Fu, et al., 2010; Hevir-Kene & Rižner, 2015). The IFs GEN and DAI, as well as EQ, are known to have a preference for the latter (Hwang, et al., 2006) yet this does not necessarily mean the same holds true for their metabolites. According to Beekmann *et al.* (2015) glucuronidation appears to switch the preferential activation of GEN and DAI to ERα. The work of Pugazhendhi *et al.* (2008) demonstrated the estrogenic properties of sulfated GEN, DAI and EQ in the MCF-7 human breast cancer cell line, which predominantly contains ERα yet how the levels of ERβ might influence this activity, is unknown. In addition to this, EQ and D7S have been shown to transactivate reporter gene expression in ERβ-transfected HeLa cells, yet D4'S was inactive

(Totta, et al., 2005). Overall the results of these studies suggest that structural conformation plays an important role in the estrogenic activities of IF and their sulfated counterparts yet it remains to be determined how specifically these alterations influence the observed effects.

To conclude, estrogenic activities of a few phase II IF metabolites were detected. The sulfoglucuronides, diglucuronide of DAI, disulfates and the glucuronides, with the exception of G7G, were not found to be estrogenic at any concentration. In no case were the monosulfates D4'S, G7S and E4'S capable of nullifying the estrogenic potential of their respective aglycones, with D4'S even showing a minor increase in ALP induction for 10 μM when compared DAI itself. G7G and G4',7dG were also found to exert medium and low ALP induction respectively for the highest concentration. However, the IF remained as the most biologically active substances due to an estrogenic activity at lower concentrations, starting from 0.1 μM for GEN and EQ and 1 μM for DAI. According to the UHPLC-MS/MS data none of the metabolites reverted back to their aglycones after 48 hours of incubation time. In contrast to this, the IFs were found to be mainly conjugated with sulfates at 1 μM, the content of which reduced significantly at the highest concentration. Therefore, conjugation with sulfates for the IFs could be re-considered to provide a biologically active substance for the endometrial adenocarcinoma Ishikawa cell line with regards to estrogenic activity instead of a detoxifying metabolic pathway.

7. Summary

Isoflavones are natural, non-steroidal, phenolic secondary plant metabolites primarily found in dietary sources such as soybeans and red clover. Possible chemo-preventive properties of these phytoestrogens have been of interest, as well as their relation to cardiovascular and skeletal health, cognitive function and alleviation of menopausal symptoms. However, such roles remain controversial due to the structural similarity between isoflavones and the female sexual hormone 17β-estradiol. Since this biological activity is affected by biotransformation, our aim was to investigate phase II metabolites, namely glucuronides, sulfates, diglucuronides, disulfates and sulfoglucuronides, for any possible estrogenic effects and compare those to their aglycones, the major isoflavones genistein, daidzein and the gut metabolite equol.

For this purpose, the alkaline phosphatase assay (ALP) was utilized with the human endometrial adenocarcinoma Ishikawa cell line. Additionally, CellTiter-Blue and sulforhodamine B assays were necessary to exclude cytotoxic influences because of altered cell viability. Physiologically relevant concentrations of 0.001 to 10 μM were chosen. Lastly, the content profile of the individual compounds was determined with a hyphenated ultra-high performance liquid chromatography tandem mass spectrometry system on selected concentrations based on the estrogenicity results to further determine whether the observed effects should be attributed to the metabolites themselves or whether a deconjugation or further metabolization took place.

Most biologically active were the isoflavones themselves, with the order GEN>EQ>DAI. The highest ALP induction was observed at concentrations of 0.1 μM for GEN and 1 μM for EQ and DAI. Interestingly enough, at 1 μM the majority of the aglycones were found to be mainly conjugated with sulfates after 48 hours of incubation. At a higher concentration this amount was reduced significantly. For the metabolites, ALP induction was observed only at 10 μM following the order of D4'S>G7G≈E4'S>G7S≈G4',7dG. All sulfates induced an estrogenic activity with varying percentages as well as one GEN glucuronide (G7G) and the GEN diglucuronide. D4'S was the only case where an ALP induction was slightly higher than the one of its precursor, while the rest of the metabolites were less potent. None of the metabolites appeared to be deconjugated or further metabolized in a significant amount after 48 hours of incubation. The sulfoglucuronides, glucuronides of EQ and DAI, disulfates and diglucuronide of DAI exhibited no estrogenicity at any of the tested concentrations.

Furthermore, no cytotoxic effects were observed with the minor exception of dose-dependent proliferative effects for EQ.

In conclusion, the isoflavones exhibited already established estrogenic actions. Although the majority of the metabolites were found to be biologically inactive, focus should be given on the sulfates and the complexity of sulfation on the biological activity of phytoestrogens.

8. Zusammenfassung

Isoflavone sind natürliche, nichtsteroidale, phenolische sekundäre Pflanzenmetaboliten, die hauptsächlich in Nahrungsquellen wie Sojabohnen und Rotklee vorkommen. Von Interesse sind mögliche chemopräventive Eigenschaften dieser Phytoöstrogene sowie ihre Beziehung zur kardiovaskulären und skelettalen Gesundheit, zur kognitiven Funktion und zur Verminderung von Wechseljahresbeschwerden. Diese Rollen bleiben jedoch aufgrund der strukturellen Ähnlichkeit der Isoflavonen mit dem weiblichen Sexualhormon 17β-Östradiol umstritten. Da diese biologische Aktivität durch die Biotransformation beeinflusst werden kann, war unser Ziel, Phase II Metaboliten, nämlich Glukuronide, Sulfate, Diglukuronide, Disulfate und Sulfoglukuronide, hinsichtlich möglicher östrogener Wirkungen zu untersuchen und diese mit ihren Aglyka, den wichtigsten Isoflavonen Genistein, Daidzein und dem Darmmetaboliten Equol zu vergleichen.

Zu diesem Zweck wurde der alkalische Phosphatase-Assay (ALP) mit der humanen endometrialen Adenokarzinomzelllinie Ishikawa verwendet. Zusätzlich waren CellTiter-Blue- und Sulforhodamin-B-Assays erforderlich, um zytotoxische Einflüsse aufgrund einer veränderten Zellviabilität auszuschließen. Es wurden physiologisch relevante Konzentrationen von 0,001 bis 10 µM gewählt. Schließlich wurde für die einzelne Verbindungen das Metabolitenprofil nach 48 h Inkubation mit einem Ultrahochleistungs-Flüssigkeitschromatographie-Tandem-Massenspektrometriesystem bestimmt. Die Konzentrationen wurden basierend auf den Östrogenitätsergebnissen ausgewählt. Sinn und Zweck dieser Untersuchung war festzustellen, ob die beobachteten Wirkungen den Metaboliten selbst, einer Dekonjugation oder einer weiteren Metabolisierung zugeschrieben werden sollten.

Am biologisch aktivsten waren die Isoflavone selbst, mit der Reihenfolge GEN>EQ>DAI. Die höchste ALP-Induktion wurde bei Konzentrationen von 0,1 µM für GEN und 1 µM für EQ und DAI beobachtet. Interessanterweise wurde festgestellt, dass bei 1 µM die Mehrheit der Aglyka nach 48 h Inkubation hauptsächlich mit Sulfaten konjugiert war. Bei einer höheren Konzentration wurde diese Menge deutlich reduziert. Bei den Metaboliten wurde eine ALP-Induktion nur bei 10 µM in der Reihenfolge D4'S>G7G≈E4'S>G7S≈G4',7dG beobachtet. Alle Sulfate, sowie ein GEN-Glukuronid (G7G) und das GEN-Diglukuronid, induzierten eine östrogene Aktivität mit unterschiedliche Effizienz. D4'S war der einzige Fall, in dem eine ALP-Induktion etwas höher war als die seines Vorläufers, während der Rest der Metaboliten eine verminderte Wirkung im Vergleich zum Aglykon aufwies. Keiner der

Metaboliten schien dekonjugiert oder signifikant weiter metabolisiert zu werden. Die Sulfoglukuronide, Glukuronide von EQ und DAI, Disulfate und Diglukuronid von DAI zeigten bei keiner getesteten Konzentration östrogene Eigenschaften. Darüber hinaus wurden keine zytotoxischen Wirkungen beobachtet, mit der geringfügigen Ausnahme von einer dosisabhängigen proliferativen Wirkung von EQ.

Zusammenfassend zeigten die Aglyka der Isoflavone wie bereits literaturbekannt östrogene Wirkung. Obwohl festgestellt wurde, dass die Mehrzahl der Metaboliten biologisch inaktiv ist, sollte der Fokus auf die Sulfate und die Komplexität der Sulfatierung auf die biologische Aktivität von Phytoöstrogenen gelegt werden.

9. Bibliography

Ahamad, J., Ali, F., Sayed, M. A. & Ahmad, J., 2022. Basic Principles and Fundamental Aspects of Mass Spectrometry. In: L. Nollet & R. Winkler, eds. *Mass Spectrometry in Food Analysis.* 1st ed. Boca Raton: CRC Press, p. 3–18.

Al-Bader, M., Ford, C., Al-Ayadhy, B. & Francis, I., 2011. Analysis of estrogen receptor isoforms and variants in breast cancer cell lines. *Experimental and Therapeutic Medicine,* May, 2(3), pp. 537-544.

Aston, F. W., 1920. LIX. The mass-spectra of chemical elements. *The London, Edinburgh, and Dublin Philosophical Magazine and Journal of Science,* Volume 39, pp. 611-625.

Atherton, K. M., Mutch, E. & Ford, D., 2006. Metabolism of the soyabean isoflavone daidzein by CYP1A2 and the extra-hepatic CYPs 1A1 and 1B1 affects biological activity. *Biochemical Pharmacology,* Volume 72, pp. 624-631.

Aumais, J. P., Lee, H. S., Lin, R. & White, J. H., 1997. Selective Interaction of Hsp90 with an Estrogen Receptor Ligand-binding Domain Containing a Point Mutation. *Journal of Biological Chemistry,* Volume 272, pp. 12229-12235.

Baber, R. J., 2013. Chapter 1: Phytoestrogens in Health-The Role of Isoflavones. In: P. Victor R, ed. *Isoflavones: Chemistry, Analysis, Function and Effects.* s.l.:Royal Society of Chemistry, p. 3–13.

Baechler, S. A. et al., 2014. Oxidative metabolism enhances the cytotoxic and genotoxic properties of the soy isoflavone daidzein. *Molecular Nutrition & Food Research,* Volume 58, pp. 1269-1281.

Bandele, O. J. & Osheroff, N., 2007. Bioflavonoids as Poisons of Human Topoisomerase IIα and IIβ. *Biochemistry,* May, Volume 46, p. 6097–6108.

Beekman, J. M. et al., 1993. Transcriptional activation by the estrogen receptor requires a conformational change in the ligand binding domain. *Molecular Endocrinology,* October, Volume 7, pp. 1266-1274.

Beekmann, K. et al., 2015. The effect of glucuronidation on isoflavone induced estrogen receptor (ER)α and ERβ mediated coregulator interactions. *The Journal of Steroid Biochemistry and Molecular Biology,* Volume 154, pp. 245-253.

Behrens, D., Gill, J. H. & Fichtner, I., 2007. Loss of tumourigenicity of stably ERβ-transfected MCF-7 breast cancer cells. *Molecular and Cellular Endocrinology,* Volume 274, pp. 19-29.

Bennetts, H. W., Underwood, E. J. & Shier, F. L., 1946. A specific breeding problem of sheep on subterranean clover pastures in Western Australia. *Australian Veterinary Journal,* Volume 22, pp. 2-12.

Berthois, Y., Katzenellenbogen, J. A. & Katzenellenbogen, B. S., 1986. Phenol red in tissue culture media is a weak estrogen: implications concerning the study of estrogen-responsive cells in culture. *Proceedings of the National Academy of Sciences of the United States of America,* April, 83(8), pp. 2496-500.

Biason-Lauber, A. & Lang-Muritano, M., 2022. Estrogens: Two nuclear receptors, multiple possibilities. *Molecular and Cellular Endocrinology,* Volume 554, p. 111710.

Björnström, L. & Sjöberg, M., 2005. Mechanisms of Estrogen Receptor Signaling: Convergence of Genomic and Nongenomic Actions on Target Genes. *Molecular Endocrinology,* April, Volume 19, pp. 833-842.

Bolca, S. et al., 2007. Microbial and Dietary Factors Are Associated with the Equol Producer Phenotype in Healthy Postmenopausal Women. *The Journal of Nutrition,* November, Volume 137, pp. 2242-2246.

Brink, E. et al., 2008. Long-term consumption of isoflavone-enriched foods does not affect bone mineral density, bone metabolism, or hormonal status in early postmenopausal women: a randomized, double-blind, placebo controlled study. *The American Journal of Clinical Nutrition,* March, 87(3), pp. 761-70.

Bruhn, H. D., Junker, R., Schäfer, H. & Schreiber, S., 2011. *LaborMedizin: Indikationen, Methodik und Laborwerte, Pathophysiologie und Klinik.* 3rd ed. Schattauer: Schattauer.

Bucar, F., 2013. Chapter 2: Phytoestrogens in Plants-With Special Reference to Isoflavones. In: P. Victor R, ed. *Isoflavones: Chemistry, Analysis, Function and Effects.* s.l.:Royal Society of Chemistry, p. 14–27.

Ceccarelli, I. et al., 2022. Estrogens and phytoestrogens in body functions. *Neuroscience & Biobehavioral Reviews,* Volume 132, pp. 648-663.

Chan, H. W., Rice, G. E. & Mitchell, M. D., 2013. Biotransformation and Transfer of Genistein: a Comparison with Xenoestrogens and a Focus on the Human Placenta. In: V. R. Preedy, ed. *Isoflavones: Chemistry, Analysis, Function and Effects.* s.l.:RCS Publishing, p. 115–130.

Chen, W. et al., 2016. Dietary supplementation with a high dose of daidzein enhances the antioxidant capacity in swine muscle but experts pro-oxidant function in liver and fat tissues. *Journal of Animal Science and Biotechnology,* Volume 7, p. 43.

Cho, C.-H.et al., 2020. pH-adjusted solvent extraction and reversed-phase HPLC quantification of isoflavones from soybean (Glycine max (L.) Merr.). *Journal of Food Science,* Volume 85, pp. 673-681.

Choi, E. J., Ahn, W. S. & Bae, S. M., 2009. Equol induces apoptosis through cytochrome c-mediated caspases cascade in human breast cancer MDA-MB-453 cells. *Chemico-Biological Interactions,* Volume 177, pp. 7-11.

Choi, E. J., Jung, J. Y. & Kim, G.-H., 2014. Genistein inhibits the proliferation and differentiation of MCF-7 and 3T3-L1 cells via the regulation of ERα expression and induction of apoptosis. *Experimental and Therapeutic Medicine,* August, 8(2), pp. 454-458.

Choi, J. & Kim, G.-H., 2013. Antiproliferative activity of daidzein and genistein may be related to ERα/c-erbB-2 expression in human breast cancer cells. *Mol Med Rep,* Volume 7, p. 781–784.

Choo, S.-W.et al., 2022. Estrogen distinctly regulates transcription and translation of lncRNAs and pseudogenes in breast cancer cells. *Genomics,* Volume 114, p. 110421.

Cooke, P. S. et al., 2017. Estrogens in Male Physiology. *Physiological Reviews,* Volume 97, pp. 995-1043.

Dahlman-Wright, K. et al., 2006. International Union of Pharmacology. LXIV. Estrogen Receptors. *Pharmacological Reviews,* Volume 58, p. 773–781.

Dakora, F. D. & Phillips, D. A., 1996. Diverse functions of isoflavonoids in legumes transcend anti-microbial definitions of phytoalexins. *Physiological and Molecular Plant Pathology,* Volume 49, pp. 1-20.

Day, A. J. et al., 2000. Dietary flavonoid and isoflavone glycosides are hydrolysed by the lactase site of lactase phlorizin hydrolase. *FEBS Letters,* Volume 468, pp. 166-170.

Day, A. J. et al., 1998. Deglycosylation of flavonoid and isoflavonoid glycosides by human small intestine and liver β-glucosidase activity. *FEBS Letters,* Volume 436, pp. 71-75.

de Assis, S. et al., 2011. Protective effects of prepubertal genistein exposure on mammary tumorigenesis are dependent on BRCA1 expression. *Cancer Prevention Research (Philadelphia, Pa.),* September, 4(9), pp. 1436-48.

de Padua Mansur, A. et al., 2012. Long-term prospective study of the influence of estrone levels on events in postmenopausal women with or at high risk for coronary artery disease. *The Scientific World Journal,* Volume 2012, p. 363595.

Dellafiora, L. et al., 2018. An integrated in silico/in vitro approach to assess the xenoestrogenic potential of Alternaria mycotoxins and metabolites. *Food Chemistry*, May, Volume 248, pp. 253-261.

Dhamad, A. E., Zhou, Z., Zhou, J. & Du, Y., 2016. Systematic Proteomic Identification of the Heat Shock Proteins (Hsp) that Interact with Estrogen Receptor Alpha (ERα) and Biochemical Characterization of the ERα-Hsp70 Interaction.. *PloS one*, 11(8), p. e0160312.

Doerge, D. R., Chang, H. C., Churchwell, M. I. & Holder, C. L., 2000. Analysis of soy isoflavone conjugation in vitro and in human blood using liquid chromatography-mass spectrometry. *Drug Metabolism and Disposition: The Biological Fate of Chemicals*, March, 28(3), pp. 298-307.

Dong, M., 2019. HPLC Columns and Trends. In: *HPLC and UHPLC for Practicing Scientists.* s.l.:John Wiley & Sons, Ltd, p. 45–79.

Dong, M., 2019. HPLC/UHPLC Instrumentation and Trends. In: *HPLC and UHPLC for Practicing Scientists.* s.l.:John Wiley & Sons, Ltd, pp. 81-115.

Dong, M., 2019. Introduction. In: *HPLC and UHPLC for Practicing Scientists.* 2nd ed. s.l.:John Wiley & Sons, Ltd, p. 1–13.

Du, X.-L.et al., 2004. Differential effects of tyrosine kinase inhibitors on volume-sensitive chloride current in human atrial myocytes: evidence for dual regulation by Src and EGFR kinases. *The Journal of General Physiology*, April, 123(4), pp. 427-39.

EFSA, 2009. Scientific Opinion on the substantiation of health claims related to soy isoflavones and maintenance of bone mineral density (ID 1655) pursuant to Article 13(1) of Regulation (EC) No 1924/2006. *EFSA Journal*, Volume 13.

EFSA, 2011. Scientific Opinion on the substantiation of health claims related to soy isoflavones and protection of DNA, proteins and lipids from oxidative damage (ID 1286, 4245), maintenance of normal blood LDL cholesterol concentrations (ID 1135, 1704a, 3093a), reduction of vasomotor symptoms associated with menopause (ID 1654, 1704b, 2140, 3093b, 3154, 3590), maintenance of normal skin tonicity (ID 1704a), contribution to normal hair growth (ID 1704a, 4254), “cardiovascular health” (ID 3587), treatment of prostate cancer (ID 3588) and “upper respiratory tract” (ID 3589) pursuant to Article 13(1) of Regulation (EC) No 1924/2006. *EFSA Journal*, Volume 9, p. 2264.

EFSA, 2012. Scientific Opinion on the substantiation of health claims related to soy isoflavones and maintenance of bone mineral density (ID 1655) and reduction of vasomotor symptoms associated with menopause (ID 1654, 1704, 2140, 3093, 3154, 3590) (further assessment) pursuant to Article 13(1) of Regulation (EC) No 1924/2006. *EFSA Journal,* Volume 10, p. 2847.

EFSA, 2015. Risk assessment for peri- and post-menopausal women taking food supplements containing isolated isoflavones. *EFSA Journal,* Volume 13.

Enmark, E. et al., 1997. Human Estrogen Receptor β-Gene Structure, Chromosomal Localization, and Expression Pattern. *The Journal of Clinical Endocrinology & Metabolism,* December, Volume 82, pp. 4258-4265.

Ferreira, C. D. et al., 2019. Changes in Phenolic Acid and Isoflavone Contents during Soybean Drying and Storage. *J. Agric. Food Chem.,* January, Volume 67, p. 1146–1155.

Florian, M. & Magder, S., 2008. Estrogen decreases TNF-α and oxidized LDL induced apoptosis in endothelial cells. *Steroids,* Volume 73, pp. 47-58.

Fu, J. et al., 2010. Expression of estrogenicity genes in a lineage cell culture model of human breast cancer progression. *Breast Cancer Research and Treatment,* Volume 120, p. 35–45.

Galanty, A. et al., 2022. In the Search for Novel, Isoflavone-Rich Functional Foods - Comparative Studies of Four Clover Species Sprouts and Their Chemopreventive Potential for Breast and Prostate Cancer. *Pharmaceuticals,* Volume 15.

Ghafoor, K., Al-Juhaimi, F. Y. & Park, J., 2013. Chapter 4: The Chemistry/Biochemistry of the Bioconversion of Isoflavones in Food Preparation. In: P. Victor R, ed. *Isoflavones: Chemistry, Analysis, Function and Effects.* s.l.:Royal Society of Chemistry, p. 49–60.

Gredel, S., Grad, C., Rechkemmer, G. & Watzl, B., 2008. Phytoestrogens and phytoestrogen metabolites differentially modulate immune parameters in human leukocytes. *Food and Chemical Toxicology,* Volume 46, pp. 3691-3696.

Grgic, D. et al., 2022. Estrogenic in vitro evaluation of zearalenone and its phase I and II metabolites in combination with soy isoflavones. *Archives of Toxicology,* Volume 96, p. 3385–3402.

Grgic, D. et al., 2021. Isoflavones in Animals: Metabolism and Effects in Livestock and Occurrence in Feed. *Toxins,* Volume 13.

Gross, J. H., 2017. Electrospray Ionization. In: *Mass Spectrometry.* 3rd ed. s.l.:Springer Cham, p. 721–778.

Gross, J. H., 2017. Hyphenated Methods. In: *Mass Spectrometry.* 3rd ed. s.l.:Springer Cham, p. 831–888.

Gross, J. H., 2017. Introduction. In: *Mass Spectrometry.* 3rd ed. s.l.:Springer Cham, p. 1–28.

Gstraunthaler, G. & Lindl, T., 2013. *Zell- und Gewebekultur.* 7 ed. Berlin(Germany): Springer Spektrum.

Gu, L. et al., 2006. Metabolic Phenotype of Isoflavones Differ among Female Rats, Pigs, Monkeys, and Women. *The Journal of Nutrition,* May, Volume 136, pp. 1215-1221.

Hammond, G. L., 2016. Plasma steroid-binding proteins: primary gatekeepers of steroid hormone action. *The Journal of Endocrinology,* July, 230(1), pp. R13-25.

Han, B.-J.et al., 2015. Effects of daidzein in regards to cytotoxicity in vitro, apoptosis, reactive oxygen species level, cell cycle arrest and the expression of caspase and Bcl-2 family proteins. *Oncology Reports,* September, 34(3), pp. 1115-20.

Hevir-Kene, N. & Rižner, T. L., 2015. The endometrial cancer cell lines Ishikawa and HEC-1A, and the control cell line HIEEC, differ in expression of estrogen biosynthetic and metabolic genes, and in androstenedione and estrone-sulfate metabolism. *Chemico-Biological Interactions,* Volume 234, pp. 309-319.

Hiller-Sturmhöfel, S. & Bartke, A., 1998. The endocrine system: an overview. *Alcohol Health and Research World,* 22(3), pp. 153-64.

Höjer, A. et al., 2012. Effects of feeding dairy cows different legume-grass silages on milk phytoestrogen concentration. *Journal of Dairy Science,* Volume 95, pp. 4526-4540.

Holinka, C. F., Hata, H., Kuramoto, H. & Gurpide, E., 1986. Effects of steroid hormones and antisteroids on alkaline phosphatase activity in human endometrial cancer cells (Ishikawa line). *Cancer Research,* June, 46(6), pp. 2771-4.

Hsieh, C. Y., Santell, R. C., Haslam, S. Z. & Helferich, W. G., 1998. Estrogenic effects of genistein on the growth of estrogen receptor-positive human breast cancer (MCF-7) cells in vitro and in vivo. *Cancer Research,* September, 58(17), pp. 3833-8.

Hur, H.-G. & Rafii, F., 2000. Biotransformation of the isoflavonoids biochanin A, formononetin, and glycitein by Eubacterium limosum. *FEMS Microbiology Letters,* Volume 192, pp. 21-25.

Hüser, S. et al., 2018. Effects of isoflavones on breast tissue and the thyroid hormone system in humans: a comprehensive safety evaluation. *Archives of Toxicology,* September, 92(9), pp. 2703-2748.

Hwang, C. S. et al., 2006. Isoflavone metabolites and their in vitro dual functions: They can act as an estrogenic agonist or antagonist depending on the estrogen concentration. *The Journal of Steroid Biochemistry and Molecular Biology,* Volume 101, pp. 246-253.

Inbaraj, B. S. & Chen, B. H., 2013. Isoflavone Ingestion by Multiethnic Populations: Implications for Health. In: P. Victor R, ed. *Isoflavones: Chemistry, Analysis, Function and Effects.* s.l.:RSC Publishing, p. 349–364.

Islam, M. A. et al., 2015. Deconjugation of soy isoflavone glucuronides needed for estrogenic activity. *Toxicology in Vitro,* Volume 29, pp. 706-715.

Jensen, E. V. et al., 1969. Estrogen-binding substances of target tissues. *Steroids,* Volume 13, pp. 417-427.

Kao, T. H., Lu, Y. F., Hsieh, H. C. & Chen, B. H., 2004. Stability of isoflavone glucosides during processing of soymilk and tofu. *Food Research International,* Volume 37, pp. 891-900.

Kinjo, J. et al., 2004. Interactions of Phytoestrogens with Estrogen Receptors α and β (III). Estrogenic Activities of Soy Isoflavone Aglycones and Their Metabolites Isolated from Human Urine. *Biological and Pharmaceutical Bulletin,* Volume 27, pp. 185-188.

Klein-Hitpaß, L., Schorpp, M., Wagner, U. & Ryffel, G. U., 1986. An estrogen-responsive element derived from the 5′ flanking region of the Xenopus vitellogenin A2 gene functions in transfected human cells. *Cell,* Volume 46, pp. 1053-1061.

Klinge, C. M., 2000. Estrogen receptor interaction with co-activators and co-repressors. *Steroids,* Volume 65, pp. 227-251.

Klinge, C. M., 2001. Estrogen receptor interaction with estrogen response elements. *Nucleic Acids Research,* July, 29(14), pp. 2905-19.

Koide, A. et al., 2007. Identification of regions within the F domain of the human estrogen receptor alpha that are important for modulating transactivation and protein-protein interactions. *Molecular Endocrinology (Baltimore, Md.),* April, 21(4), pp. 829-42.

Kreijkamp-Kaspers, S. et al., 2004. Effect of Soy Protein Containing Isoflavones on Cognitive Function, Bone Mineral Density, and Plasma Lipids in Postmenopausal WomenA Randomized Controlled Trial. *JAMA,* July, Volume 292, pp. 65-74.

Krenn, L., Unterrieder, I. & Ruprechter, R., 2002. Quantification of isoflavones in red clover by high-performance liquid chromatography. *Journal of Chromatography B,* Volume 777, pp. 123-128.

Krum, S. A. et al., 2008. Unique ERα Cistromes Control Cell Type-Specific Gene Regulation. *Molecular Endocrinology,* November, Volume 22, pp. 2393-2406.

Kuiper, G. G. et al., 1997. Comparison of the ligand binding specificity and transcript tissue distribution of estrogen receptors alpha and beta. *Endocrinology,* March, 138(3), pp. 863-70.

Kuiper, G. G. et al., 1996. Cloning of a novel receptor expressed in rat prostate and ovary. *Proceedings of the National Academy of Sciences,* Volume 93, pp. 5925-5930.

Kulling, S. E., Honig, D. M. & Metzler, M., 2001. Oxidative Metabolism of the Soy Isoflavones Daidzein and Genistein in Humans in Vitro and in Vivo. *Journal of Agricultural and Food Chemistry,* Volume 49, pp. 3024-3033.

Kulling, S. E., Honig, D. M., Simat, T. J. & Metzler, M., 2000. Oxidative in Vitro Metabolism of the Soy Phytoestrogens Daidzein and Genistein. *Journal of Agricultural and Food Chemistry,* Volume 48, pp. 4963-4972.

Kumar, R. et al., 2011. The dynamic structure of the estrogen receptor. *Journal of Amino Acids,* Volume 2011, p. 812540.

Leeners, B., Geary, N., Tobler, P. N. & Asarian, L., 2017. Ovarian hormones and obesity. *Human Reproduction Update,* March, Volume 23, pp. 300-321.

Lehmann, L. et al., 2005. Estrogenic and genotoxic potential of equol and two hydroxylated metabolites of Daidzein in cultured human Ishikawa cells. *Toxicology Letters,* Volume 158, pp. 72-86.

Lehmann, L., Wagner, J. & Metzler, M., 2006. Estrogenic and clastogenic potential of the mycotoxin alternariol in cultured mammalian cells. *Food and Chemical Toxicology,* Volume 44, pp. 398-408.

Li, J., Li, Z. & Mo, B.-q., 2006. Effects of ERK5 MAPK signaling transduction pathway on the inhibition of genistein to breast cancer cells. *Journal of Hygiene Research,* March, 35(2), pp. 184-6.

Lin, Y.-J.et al., 2009. Puerariae radix isoflavones and their metabolites inhibit growth and induce apoptosis in breast cancer cells. *Biochemical and Biophysical Research Communications,* Volume 378, pp. 683-688.

Littlefield, B. A. et al., 1990. A Simple and Sensitive Microtiter Plate Estrogen Bioassay Based on Stimulation of Alkaline Phosphatase in Ishikawa Cells: Estrogenic Action of Δ5 Adrenal Steroids. *Endocrinology,* December, Volume 127, pp. 2757-2762.

Li, Y. P. et al., 2020. Effects of soybean isoflavones on the growth performance, intestinal morphology and antioxidative properties in pigs. *Animal,* Volume 14, pp. 2262-2270.

Lo, Y.-L., 2013. A Potential Daidzein Derivative Enhances Cytotoxicity of Epirubicin on Human Colon Adenocarcinoma Caco-2 Cells. *International Journal of Molecular Sciences,* Volume 14, p. 158–176.

Lundh, T., 1995. Metabolism of Estrogenic Isoflavones in Domestic Animals. *Proceedings of the Society for Experimental Biology and Medicine,* Volume 208, pp. 33-39.

Lundh, T. J. O., 1990. Conjugation of the plant estrogens formononetin and daidzein and their metabolite equol by gastrointestinal epithelium from cattle and sheep. *J. Agric. Food Chem.,* April, Volume 38, p. 1012–1016.

Lundh, T. J. O., Pettersson, H. I. & Martinsson, K. A., 1990. Comparative levels of free and conjugated plant estrogens in blood plasma of sheep and cattle fed estrogenic silage. *Journal of Agricultural and Food Chemistry,* Volume 38, pp. 1530-1534.

MacNair, J. E., Lewis, K. C. & Jorgenson, J. W., 1997. Ultrahigh-pressure reversed-phase liquid chromatography in packed capillary columns. *Analytical Chemistry,* March, 69(6), pp. 983-9.

Magee, P. J. et al., 2006. Equol: A Comparison of the Effects of the Racemic Compound With That of the Purified S-Enantiomer on the Growth, Invasion, and DNA Integrity of Breast and Prostate Cells In Vitro. *Nutrition and Cancer,* Volume 54, pp. 232-242.

Manas, E. S., Xu, Z. B., Unwalla, R. J. & Somers, W. S., 2004. Understanding the Selectivity of Genistein for Human Estrogen Receptor-β Using X-Ray Crystallography and Computational Methods. *Structure,* Volume 12, pp. 2197-2207.

Mann, S. et al., 2001. Estrogen receptor beta expression in invasive breast cancer. *Human Pathology,* Volume 32, pp. 113-118.

Manolagas, S. C., O'Brien, C. A. & Almeida, M., 2013. The role of estrogen and androgen receptors in bone health and disease. *Nature Reviews: Endocrinology,* December, 9(12), pp. 699-712.

Mansoury, M. et al., 2021. The edge effect: A global problem. The trouble with culturing cells in 96-well plates. *Biochemistry and Biophysics Reports,* Volume 26, p. 100987.

Marrian, G. F. & Haslewood, G. A., 1932. Equol, a new inactive phenol isolated from the ketohydroxyoestrin fraction of mares' urine. *The Biochemical Journal,* 26(4), pp. 1227-32.

Martínez-Ávila, M., Gutiérrez-Uribe, J. A. & Antunes-Ricardo, M., 2022. Evaluation of Nutraceutical Value. In: L. Nollet & R. Winkler, eds. *Mass Spectrometry in Food Analysis.* 1st ed. Boca Raton: CRC Press, p. 181–208.

Millán, J. L., 2006. Alkaline Phosphatases : Structure, substrate specificity and functional relatedness to other members of a large superfamily of enzymes. *Purinergic Signalling*, June, 2(2), pp. 335-41.

Mitropoulou, T. N. et al., 2002. In vitro effects of genistein on the synthesis and distribution of glycosaminoglycans/proteoglycans by estrogen receptor-positive and -negative human breast cancer epithelial cells. *Anticancer Research*, September, 22(5), pp. 2841-6.

Montano, M. M. et al., 1999. An estrogen receptor-selective coregulator that potentiates the effectiveness of antiestrogens and represses the activity of estrogens. *Proceedings of the National Academy of Sciences of the United States of America*, June, 96(12), pp. 6947-52.

Montano, M. M., Müller, V., Trobaugh, A. & Katzenellenbogen, B. S., 1995. The carboxy-terminal F domain of the human estrogen receptor: role in the transcriptional activity of the receptor and the effectiveness of antiestrogens as estrogen antagonists. *Molecular Endocrinology*, July, Volume 9, pp. 814-825.

Morito, K. et al., 2001. Interaction of Phytoestrogens with Estrogen Receptors α and β. *Biological and Pharmaceutical Bulletin*, Volume 24, pp. 351-356.

Mueller, S. & Korach, K., 2005. Mechanisms of Estrogen Receptor-Mediated Agonistic and Antagonistic Effects. In: M. Metzler, ed. *Endocrine Disruptors – Part I.* s.l.:Handbook of Environmental Chemistry, p. 545–545.

Muthyala, R. S. et al., 2004. Equol, a natural estrogenic metabolite from soy isoflavones: convenient preparation and resolution of R- and S-equols and their differing binding and biological activity through estrogen receptors alpha and beta. *Bioorganic & Medicinal Chemistry*, Volume 12, pp. 1559-1567.

Nakano, H. et al., 2004. Regioselective Monosulfation and Disulfation of the Phytoestrogens Daidzein and Genistein by Human Liver Sulfotransferases. *Drug Metabolism and Pharmacokinetics*, Volume 19, pp. 216-226.

Nishida, M., 2002. The Ishikawa cells from birth to the present. *Human Cell*, Volume 15, p. 104–117.

Nishida, M. et al., 1985. Establishment of a new human endometrial adenocarcinoma cell line, Ishikawa cells, containing estrogen and progesterone receptors. *Nihon Sanka Fujinka Gakkai Zasshi*, July, 37(7), pp. 1103-11.

Nishiyama, T. et al., 2002. Sulfation of Environmental Estrogens by Cytosolic Human Sulfotransferases. *Drug Metabolism and Pharmacokinetics*, Volume 17, pp. 221-228.

Nollet, L. & Winkler, R., 2022. *Mass Spectrometry in Food Analysis.* 1st ed. Boca Raton: CRC Press.

Noteboom, W. D. & Gorski, J., 1965. Stereospecific binding of estrogens in the rat uterus. *Archives of Biochemistry and Biophysics,* Volume 111, pp. 559-568.

Obara, A. et al., 2019. Identification of equol-7-glucuronide-4'-sulfate, monoglucuronides and monosulfates in human plasma of 2 equol producers after administration of kinako by LC-ESI-MS. *Pharmacology Research & Perspectives,* June, 7(3), p. e00478.

O'Malley, B. W. & McGuire, W. L., 1968. Studies on the mechanism of estrogen-mediated tissue differentiation: regulation of nuclear transcription and induction of new RNA species. *Proceedings of the National Academy of Sciences,* Volume 60, pp. 1527-1534.

Ono, M. et al., 2017. Equol Enhances Apoptosis-inducing Activity of Genistein by Increasing Bax/Bcl-xL Expression Ratio in MCF-7 Human Breast Cancer Cells. *Nutrition and Cancer,* Volume 69, pp. 1300-1307.

Park, S. K. & Ko, K. P., 2013. Isoflavones against Gastric Cancer: Function and Effects. In: V. R. Preedy, ed. *Isoflavones: Chemistry, Analysis, Function and Effects.* s.l.:RSC Publishing, p. 438–450.

Penagos-Tabares, F. et al., 2021. Mycotoxins, Phytoestrogens and Other Secondary Metabolites in Austrian Pastures: Occurrences, Contamination Levels and Implications of Geo-Climatic Factors. *Toxins,* Volume 13.

Peterson, G. & Barnes, S., 1991. Genistein inhibition of the growth of human breast cancer cells: independence from estrogen receptors and the multi-drug resistance gene. *Biochemical and Biophysical Research Communications,* August, 179(1), pp. 661-7.

Pike, A. C. et al., 1999. Structure of the ligand-binding domain of oestrogen receptor beta in the presence of a partial agonist and a full antagonist. *The EMBO journal,* September, 18(17), pp. 4608-18.

Privatti, R. T. et al., 2022. Profile and content of isoflavones on flaked and extruded soybeans and okara submitted to different drying methods. *Food Chemistry,* Volume 380, p. 132168.

Promega Corporation, 2016. *Promega.* [Online] Available at: https://at.promega.com/-/media/files/resources/protocols/technical-bulletins/101/celltiter-blue-cell-viability-assay-protocol.pdf?rev=ec67acc051cf4fc9be3346876420d72d&sc_lang=en [Accessed 21 08 2022].

Pugazhendhi, D. et al., 2008. Effect of sulphation on the oestrogen agonist activity of the phytoestrogens genistein and daidzein in MCF-7 human breast cancer cells. *The Journal of Endocrinology,* June, 197(3), pp. 503-15.

Rampersad, S. N., 2012. Multiple Applications of Alamar Blue as an Indicator of Metabolic Function and Cellular Health in Cell Viability Bioassays. *Sensors,* Volume 12, p. 12347–12360.

Roger, P. et al., 2001. Decreased expression of estrogen receptor beta protein in proliferative preinvasive mammary tumors. *Cancer Research,* March, 61(6), pp. 2537-41.

Rogers, K., 2011. Introduction. In: *The Digestive System.* 1st ed. s.l.:Britannica Educational Publishing, p. 10–19.

Rogers, K., 2012. Function and regulation of the human endocrine system. In: *The Endocrine System.* 1 ed. New York: Britannica Educational Publishing, p. 6–31.

Rogers, K., 2012. Major endocrine hormones and evaluation of endocrine function. In: *The Endocrine System.* 1 ed. New York: Britannica Educational Publishing, p. 32–62.

Ronis, M. J. et al., 2006. Sulfation of the Isoflavones Genistein and Daidzein in Human and Rat Liver and Gastrointestinal Tract. *Journal of Medicinal Food,* Volume 9, pp. 348-355.

Rüfer, C. E., Glatt, H. & Kulling, S. E., 2006. Structural elucidation of hydroxylated metabolites of the isoflavan equol by gas chromatography-mass spectrometry and high-performance liquid chromatography-mass spectrometry. *Drug Metab Dispos,* January, Volume 34, p. 51.

Rüfer, C. E. & Kulling, S. E., 2006. Antioxidant Activity of Isoflavones and Their Major Metabolites Using Different in Vitro Assays. *J. Agric. Food Chem.*, April, Volume 54, p. 2926–2931.

Russo, P., Del Bufalo, A. & Cesario, A., 2012. *Flavonoids Acting on DNA Topoisomerases: Recent Advances and Future Perspectives in Cancer Therapy.* s.l.:s.n.

Sakodynskii, K., 1972. The life and scientific workds of Michael Tswett. *Journal of Chromatography A,* Volume 73, pp. 303-360.

Schüler-Toprak, S. et al., 2018. Estrogen receptor β is associated with expression of cancer associated genes and survival in ovarian cancer. *BMC Cancer,* Volume 18, p. 981.

Setchell, K. D., 2001. Soy isoflavones–benefits and risks from nature's selective estrogen receptor modulators (SERMs). *Journal of the American College of Nutrition,* October, 20(5 Suppl), pp. 354S-362S; discussion 381S-383S.

Setchell, K. D. R. et al., 2005. S-equol, a potent ligand for estrogen receptor beta, is the exclusive enantiomeric form of the soy isoflavone metabolite produced by human intestinal bacterial flora. *The American Journal of Clinical Nutrition,* May, 81(5), pp. 1072-9.

Setchell, K. D. R. & Cole, S. J., 2006. Method of Defining Equol-Producer Status and Its Frequency among Vegetarians. *The Journal of Nutrition,* August, Volume 136, pp. 2188-2193.

Sfakianos, J., Coward, L., Kirk, M. & Barnes, S., 1997. Intestinal Uptake and Biliary Excretion of the Isoflavone Genistein in Rats. *The Journal of Nutrition,* July, Volume 127, pp. 1260-1268.

Shandilya, D. K., 2022. Targeted and Untargeted Analysis. In: L. Nollet & R. Winkler, eds. *Mass spectrometry in food analysis.* 1st ed. Boca Raton: CRC Press, p. 19–27.

Shinkaruk, S. et al., 2010. Comparative Effects of R- and S-equol and Implication of Transactivation Functions (AF-1 and AF-2) in Estrogen Receptor-Induced Transcriptional Activity. *Nutrients,* Volume 2, p. 340–354.

Shyamala, G. & Gorski, J., 1969. Estrogen Receptors in the Rat Uterus: Studies on the Interaction of Cytosol and Nuclear Binding Sites. *Journal of Biological Chemistry,* Volume 244, pp. 1097-1103.

Skehan, P. et al., 1990. New Colorimetric Cytotoxicity Assay for Anticancer-Drug Screening. *JNCI: Journal of the National Cancer Institute,* July, Volume 82, pp. 1107-1112.

Soukup, S. T., Al-Maharik, N., Botting, N. & Kulling, S. E., 2014. Quantification of soy isoflavones and their conjugative metabolites in plasma and urine: an automated and validated UHPLC-MS/MS method for use in large-scale studies. *Analytical and Bioanalytical Chemistry,* Volume 406, p. 6007–6020.

Soukup, S. T. et al., 2016. Phase II metabolism of the soy isoflavones genistein and daidzein in humans, rats and mice: a cross-species and sex comparison. *Archives of Toxicology,* Volume 90, p. 1335–1347.

Soukup, S. T. et al., 2021. Metabolism of Daidzein and Genistein by Gut Bacteria of the Class Coriobacteriia. *Foods,* Volume 10.

Speijers, M. H. M., Fraser, M. D., Theobald, V. J. & Haresign, W., 2005. Effects of ensiled forage legumes on performance of store finishing lambs. *Animal Feed Science and Technology,* Volume 120, pp. 203-216.

Squadrito, F. & Bitto, A., 2013. Chapter 10: Genistein Chemistry and Biochemistry. In: P. Victor R, ed. *Isoflavones: Chemistry, Analysis, Function and Effects.* s.l.:Royal Society of Chemistry, p. 148–156.

Sun, Y. et al., 2022. Genistein Up-Regulates the Expression of EGF and E-Cadherin in the Treatment of Senile Vaginitis. *Molecules,* Volume 27.

Thomson, S. J. J., 1911. XXVI. Rays of positive electricity. *The London, Edinburgh, and Dublin Philosophical Magazine and Journal of Science,* Volume 21, pp. 225-249.

Totta, P. et al., 2005. Daidzein-Sulfate Metabolites Affect Transcriptional and Antiproliferative Activities of Estrogen Receptor-β in Cultured Human Cancer Cells. *The Journal of Nutrition,* November, Volume 135, pp. 2687-2693.

Tswett, M. S., 1906. Physikalisch-chemische Studien über das Chlorophyll. Die Adsorptionen. *Berichte der Deutschen Botanischen Gesellschaft,* Volume 24, pp. 316-323.

UK Health Security Agency, n.d. *Culture Collections.* [Online] Available at: https://www.culturecollections.org.uk/products/celllines/generalcell/detail.jsp?refId=99040201&collection=ecacc_gc
[Accessed 11 08 2022].

Varlakhanova, N. et al., 2010. Estrogen receptors recruit SMRT and N-CoR corepressors through newly recognized contacts between the corepressor N terminus and the receptor DNA binding domain. *Molecular and Cellular Biology,* March, 30(6), pp. 1434-45.

Vejdovszky, K., Schmidt, V., Warth, B. & Marko, D., 2016. Combinatory estrogenic effects between the isoflavone genistein and the mycotoxins zearalenone and alternariol in vitro. *Molecular Nutrition & Food Research,* October.Volume 61.

Verma, K. K., Saha, S. & Kroon, P. A., 2020. A Simple and Rapid LC-MS/MS Method for Quantification of Total Daidzein, Genistein, and Equol in Human Urine. *Journal of Analytical Methods in Chemistry,* Volume 2020, p. 2359397.

Wakatsuki, A., Ikenoue, N., Okatani, Y. & Fukaya, T., 2001. Estrogen-induced small low density lipoprotein particles may be atherogenic in postmenopausal women. *Journal of the American College of Cardiology,* Volume 37, pp. 425-430.

Xiong, P. et al., 2015. Design, Synthesis, and Evaluation of Genistein Analogues as Anti-Cancer Agents. *Anti-cancer Agents in Medicinal Chemistry*, 15(9), pp. 1197-203.

Yi, P. et al., 2015. Structure of a Biologically Active Estrogen Receptor-Coactivator Complex on DNA. *Molecular Cell,* March, Volume 57, p. 1047–1058.

Yoriki, K. et al., 2022. Genistein induces long-term expression of progesterone receptor regardless of estrogen receptor status and improves the prognosis of endometrial cancer patients. *Scientific Reports,* Volume 12, p. 10303.

Zhang, Y., Hendrich, S. & Murphy, P. A., 2003. Glucuronides Are the Main Isoflavone Metabolites in Women. *The Journal of Nutrition,* February, Volume 133, pp. 399-404.

Zhang, Y. et al., 1999. Daidzein and Genistein Glucuronides In Vitro Are Weakly Estrogenic and Activate Human Natural Killer Cells at Nutritionally Relevant Concentrations. *The Journal of Nutrition,* February, Volume 129, pp. 399-405.

Zimmerman, M. A., Budish, R. A., Kashyap, S. & Lindsey, S. H., 2016. GPER-novel membrane oestrogen receptor. *Clinical Science (London, England : 1979),* June, 130(12), pp. 1005-16.

List of Figures

List of Tables

Appendix

ALP

Table 18: Estrogenicity data of individual plates for GEN, its metabolites and E2.

Mean values (MV) and standard deviations (SD) are displayed in [%] of ALP activity. Dark colored activities signify detected outliers according to Nalimov and were excluded from the calculation. P0XX denotes the number of each biological replicate. Experiments 3, 5, 12, 22, 25, 28, 29, 44, 53 were found to have many outliers and were therefore excluded. The ALP activity of E2 of experiments 19, 21, 24, 27, 30 was too low and because of this they were not considered in the results.

	P001	P002	P004	P014	P048	P050	P054	MV	SD
0.001 µM GEN	0%	-2%	0%	4%	-3%	-3%	5%	0%	3%
0.01 µM GEN	12%	10%	15%	22%	-2%	-2%	5%	9%	9%
0.1 µM GEN	89%	53%	69%	83%	4%	53%	38%	64%	19%
1 µM GEN	52%	47%	41%	102%	60%	72%	59%	55%	11%
10 µM GEN	83%	33%	22%	40%	83%	77%	74%	59%	26%
1 nM E2	312%	503%	454%	441%	650%	628%	412%		

	P023	P032	P034	P035	P037	P045	P047	P049	MV	SD
0.001 µM G7S	10%	6%	-6%	2%	0%	-8%	-6%	-3%	-1%	6%
0.01 µM G7S	-2%	1%	-4%	-1%	2%	-11%	-2%	-1%	-1%	2%
0.1 µM G7S	4%	1%	-8%	-1%	-2%	-5%	-7%	-8%	-3%	4%
1 µM G7S	3%	6%	-2%	-1%	-1%	-6%	-7%	-7%	-2%	5%
10 µM G7S	22%	14%	48%	31%	3%	56%	40%	6%	28%	19%
1 nM E2	627%	709%	478%	570%	685%	444%	482%	524%		

	P036	P038	P041	P042	MV	SD
0.001 µM G4',7dS	-5%	-2%	-3%	1%	-2%	3%
0.01 µM G4',7dS	-4%	6%	-2%	-5%	-4%	2%
0.1 µM G4',7dS	-6%	0%	-8%	-1%	-3%	4%
1 µM G4',7dS	-6%	8%	-14%	-4%	-4%	9%
10 µM G4',7dS	-6%	8%	-13%	-1%	-3%	9%
1 nM E2	462%	551%	345%	443%		

	P016	P018	P020	P031	P035	P036	MV	SD
0.001 µM G4',7dG	-14%	-1%	-5%	-5%	-	-	-6%	5%
0.01 µM G4',7dG	-16%	-8%	-17%	-3%	-	-	-11%	7%
0.1 µM G4',7dG	-15%	-4%	-18%	-3%	-	-	-10%	8%
1 µM G4',7dG	-19%	-5%	-17%	-1%	-	-	-11%	9%
10 µM G4',7dG	22%	6%	26%	20%	-	-	23%	3%
1 nM E2	311%	478%	274%	538%	570%	685%		

Table 18: continued

	P016	P018	P020	P031	P035	P036	MV	SD
0.001 µM G4'G	-15%	-4%	-13%	-10%	-	-	-11%	5%
0.01 µM G4'G	-17%	-3%	-15%	3%	-	-	-8%	10%
0.1 µM G4'G	-18%	-2%	-21%	-11%	-	-	-13%	8%
1 µM G4'G	-12%	2%	-8%	1%	-	-	4%	6%
10 µM G4'G	55%	15%	9%	7%	-	-	10%	4%
1 nM E2	311%	478%	274%	538%	570%	685%		

	P016	P018	P020	P031	P035	P036	MV	SD
0.001 µM G7G	-10%	0%	12%	-1%	-2%	6%	1%	8%
0.01 µM G7G	-6%	2%	-14%	5%	-1%	-2%	0%	4%
0.1 µM G7G	-16%	-2%	-17%	-3%	-2%	-1%	-7%	7%
1 µM G7G	-14%	4%	-5%	3%	-2%	0%	0%	4%
10 µM G7G	56%	74%	86%	56%	38%	50%	55%	13%
1 nM E2	311%	478%	274%	538%	570%	685%		

	P045	P047	P049	MV	SD
0.001 µM G4'G7S	-3%	0%	-8%	-4%	4%
0.01 µM G4'G7S	-4%	0%	-10%	-5%	5%
0.1 µM G4'G7S	-11%	-17%	-10%	-13%	4%
1 µM G4'G7S	-10%	-11%	-5%	-9%	3%
10 µM G4'G7S	-13%	-7%	-8%	-10%	3%
1 nM E2	444%	482%	524%		

	P039	P040	P043	P046	MV	SD
0.001 µM G7G4'S	-1%	-14%	-5%	0%	-2%	2%
0.01 µM G7G4'S	-2%	3%	-7%	-2%	-2%	4%
0.1 µM G7G4'S	-1%	-3%	-5%	-4%	-3%	2%
1 µM G7G4'S	-8%	-4%	-11%	-5%	-7%	3%
10 µM G7G4'S	-10%	-8%	-13%	-5%	-9%	3%
1 nM E2	453%	374%	444%	562%		

Table 19: Estrogenicity data of individual plates for DAI, its metabolites and E2.

Mean values (MV) and standard deviations (SD) are displayed in [%] of ALP activity. Dark colored activities signify detected outliers according to Nalimov and were excluded from the calculation. P0XX denotes the number of each biological replicate. Experiments 3, 5, 12, 13, 29, 44, 53 were found to have many outliers and were therefore excluded. The ALP activity of E2 of experiments 7, 8, 27 was too low and because of this they were not considered in the results.

	P001	P002	P004	P014	P048	P050	P054	MV	SD
0.001 µM DAI	3%	2%	1%	5%	-2%	0%	-4%	1%	3%
0.01 µM DAI	-1%	1%	1%	5%	-2%	-2%	-3%	-1%	2%
0.1 µM DAI	11%	3%	11%	23%	-3%	0%	8%	5%	6%
1 µM DAI	100%	50%	88%	84%	47%	29%	56%	65%	26%
10 µM DAI	81%	40%	66%	97%	47%	84%	48%	66%	22%
1 nM E2	312%	503%	454%	441%	650%	628%	412%		

	P039	P040	P043	P046	MV	SD
0.001 µM D4'G7S	-5%	0%	-1%	-2%	-1%	1%
0.01 µM D4'G7S	-2%	1%	-8%	-2%	-3%	4%
0.1 µM D4'G7S	-11%	0%	-13%	-6%	-8%	6%
1 µM D4'G7S	-2%	-10%	-13%	-5%	-8%	5%
10 µM D4'G7S	5%	6%	-8%	5%	5%	1%
1 nM E2	453%	374%	444%	562%		

	P039	P040	P043	P046	MV	SD
0.001 µM D7G4'S	2%	5%	-4%	-2%	0%	4%
0.01 µM D7G4'S	-7%	-1%	-5%	-3%	-4%	2%
0.1 µM D7G4'S	-9%	2%	-9%	-6%	-8%	2%
1 µM D7G4'S	-3%	-1%	-13%	-3%	-2%	1%
10 µM D7G4'S	-10%	2%	-10%	-7%	-9%	2%
1 nM E2	453%	374%	444%	562%		

	P036	P038	P041	P042	P045	P047	MV	SD
0.001 µM D4'S	-9%	8%	1%	0%	-5%	-5%	-2%	6%
0.01 µM D4'S	-6%	0%	-7%	-2%	-9%	-6%	-5%	3%
0.1 µM D4'S	-8%	4%	-10%	0%	-10%	-4%	-5%	6%
1 µM D4'S	0%	7%	-12%	1%	0%	8%	3%	4%
10 µM D4'S	57%	66%	-9%	83%	83%	85%	75%	12%
1 nM E2	462%	551%	345%	443%	444%	482%		

Table 19: continued

	P036	P038	P041	P042	P045	P047	MV	SD
0.001 µM D4',7dG	-6%	1%	-4%	-1%	-	-	-2%	3%
0.01 µM D4',7dG	-5%	-2%	-8%	-3%	-	-	-4%	3%
0.1 µM D4',7dG	-4%	-1%	-9%	-3%	-	-	-3%	1%
1 µM D4',7dG	-10%	-3%	-16%	-9%	-	-	-9%	5%
10 µM D4',7dG	-11%	-3%	-6%	-7%	-	-	-7%	4%
1 nM E2	462%	551%	345%	443%	444%	482%		

	P006	P009	P010	P011	P015	P017	P033	MV	SD
0.001 µM D4',7dS	-	0%	-5%	-5%	-1%	0%	-6%	-3%	3%
0.01 µM D4',7dS	-	-1%	-3%	-6%	-2%	-1%	-5%	-3%	2%
0.1 µM D4',7dS	-	-3%	-2%	-8%	-5%	-3%	-1%	-3%	2%
1 µM D4',7dS	-	-4%	-3%	-6%	-3%	-17%	-1%	-3%	2%
10 µM D4',7dS	-	-1%	5%	2%	2%	8%	-3%	2%	4%
1 nM E2	433%	721%	447%	390%	476%	469%	574%		

	P006	P009	P010	P011	P015	P017	P033	MV	SD
0.001 µM D4'G	0%	0%	-2%	-2%	0%	0%	1%	-1%	1%
0.01 µM D4'G	-2%	-1%	-2%	-7%	-3%	4%	1%	-1%	3%
0.1 µM D4'G	-1%	-2%	16%	-7%	-4%	-3%	-5%	-4%	2%
1 µM D4'G	-2%	-4%	-4%	-8%	-4%	-1%	-5%	-3%	1%
10 µM D4'G	3%	2%	3%	0%	15%	0%	-6%	0%	3%
1 nM E2	433%	721%	447%	390%	476%	469%	574%		

	P006	P009	P010	P011	P015	P017	P033	MV	SD
0.001 µM D7G	1%	-3%	0%	-4%	-3%	2%	-5%	-2%	3%
0.01 µM D7G	1%	-2%	-4%	-4%	-3%	4%	-3%	-2%	2%
0.1 µM D7G	-2%	-1%	0%	-5%	-3%	2%	0%	-1%	2%
1 µM D7G	0%	-2%	-2%	-10%	2%	-1%	-5%	-1%	2%
10 µM D7G	5%	1%	6%	-3%	10%	4%	-2%	3%	5%
1 nM E2	433%	721%	447%	390%	476%	469%	574%		

Table 20: Estrogenicity data of individual plates for EQ, its metabolites and E2.

Mean values (MV) and standard deviations (SD) are displayed in [%] of ALP activity. Dark colored activities signify detected outliers according to Nalimov and were excluded from the calculation. P0XX denotes the number of each biological replicate. Experiments 3, 5, 12, 25, 28, 29, 53 were found to have many outliers and were therefore excluded. The ALP activity of E2 of experiments 24, 27, 30 was too low and because of this they were not considered in the results.

	P001	P002	P004	P014	P048	P050	P054	MV	SD
0.001 µM EQ	-1%	1%	1%	4%	0%	-1%	-4%	0%	3%
0.01 µM EQ	-2%	2%	-1%	4%	0%	-1%	0%	0%	1%
0.1 µM EQ	58%	30%	53%	90%	47%	27%	3%	44%	27%
1 µM EQ	82%	66%	68%	86%	65%	88%	52%	72%	13%
10 µM EQ	69%	31%	44%	87%	87%	95%	24%	63%	29%
1 nM E2	312%	503%	454%	441%	650%	628%	412%		

	P023	P032	P034	P035	P037	P049	MV	SD
0.001 µM E4'S	-1%	-2%	-3%	1%	0%	1%	-1%	2%
0.01 µM E4'S	0%	1%	-4%	8%	-1%	-2%	-1%	2%
0.1 µM E4'S	-1%	3%	-5%	3%	1%	-6%	-1%	4%
1 µM E4'S	2%	5%	5%	3%	13%	-3%	2%	3%
10 µM E4'S	24%	59%	60%	59%	49%	42%	54%	8%
1 nM E2	627%	709%	478%	570%	685%	524%		

	P023	P032	P034	P035	P037	P049	MV	SD
0.001 µM E7G	1%	0%	-8%	-	-	-	-2%	5%
0.01 µM E7G	-1%	5%	-5%	-	-	-	0%	5%
0.1 µM E7G	-2%	1%	-13%	-	-	-	-5%	7%
1 µM E7G	-3%	-1%	-12%	-	-	-	-5%	6%
10 µM E7G	10%	-1%	-7%	-	-	-	1%	8%
1 nM E2	627%	709%	478%	570%	685%	524%		

CTB

Table 21: Cytotoxicity data of individual plates for GEN and its metabolites.

Mean values (MV) and standard deviations (SD) are given in [%] of metabolic activity referred to DMSO (1%) as solvent control represented as 100%. Dark colored activities signify detected outliers according to Nalimov and were excluded from the calculation. P0XX denotes the number of each biological replicate. Experiments 12, 20, 21, 31, 34, 35, 37, 44, 45, 46, 48, 49, 50 were found to have many outliers and were therefore excluded. Experiments 29 and 30 were contaminated.

	P001	P002	P003	P004	P005	P014	P027	MV	SD
0.001 µM GEN	110%	96%	100%	94%	103%	95%	104%	100%	6%
0.01 µM GEN	111%	100%	104%	94%	106%	94%	102%	102%	6%
0.1 µM GEN	115%	105%	99%	107%	113%	92%	106%	105%	8%
1 µM GEN	110%	113%	106%	107%	115%	101%	100%	108%	6%
10 µM GEN	113%	115%	108%	97%	103%	98%	110%	106%	7%

	P023	P024	P025	P026	P028	P032	P039	MV	SD
0.001 µM G7S	83%	92%	99%	103%	96%	100%	84%	94%	8%
0.01 µM G7S	97%	91%	99%	-	91%	94%	57%	94%	4%
0.1 µM G7S	99%	92%	101%	109%	92%	96%	89%	95%	5%
1 µM G7S	113%	87%	102%	108%	97%	93%	102%	100%	9%
10 µM G7S	113%	104%	108%	106%	94%	105%	103%	106%	3%

	P036	P038	P042	P047	MV	SD
0.001 µM G4',7dS	84%	110%	102%	86%	96%	12%
0.01 µM G4',7dS	92%	114%	114%	101%	105%	11%
0.1 µM G4',7dS	89%	106%	111%	99%	101%	10%
1 µM G4',7dS	95%	127%	102%	102%	106%	4%
10 µM G4',7dS	98%	121%	114%	92%	106%	13%

	P016	P018	P019	P022	MV	SD
0.001 µM G4',7dG	96%	92%	98%	101%	97%	4%
0.01 µM G4',7dG	95%	98%	99%	103%	99%	3%
0.1 µM G4',7dG	86%	95%	84%	103%	92%	9%
1 µM G4',7dG	90%	96%	98%	103%	97%	5%
10 µM G4',7dG	104%	97%	100%	103%	101%	3%

	P016	P018	P019	P022	MV	SD
0.001 µM G4'G	96%	101%	102%	103%	102%	1%
0.01 µM G4'G	94%	96%	107%	103%	100%	6%
0.1 µM G4'G	97%	91%	97%	97%	96%	0%
1 µM G4'G	101%	98%	94%	100%	98%	3%
10 µM G4'G	104%	103%	104%	103%	103%	1%

Table 21: continued

	P016	P018	P019	P022	MV	SD
0.001 µM G7G	90%	93%	96%	93%	93%	3%
0.01 µM G7G	106%	94%	99%	105%	101%	5%
0.1 µM G7G	95%	100%	99%	105%	100%	4%
1 µM G7G	100%	99%	101%	104%	101%	2%
10 µM G7G	104%	110%	111%	114%	110%	4%

	P047	P051	P052	MV	SD
0.001 µM G4'G7S	86%	105%	106%	99%	11%
0.01 µM G4'G7S	101%	103%	100%	101%	1%
0.1 µM G4'G7S	99%	109%	97%	101%	7%
1 µM G4'G7S	102%	108%	105%	105%	3%
10 µM G4'G7S	92%	113%	110%	105%	11%

	P043	P051	P052	P053	P054	MV	SD
0.001 µM G7G4'S	98%	97%	96%	82%	104%	99%	4%
0.01 µM G7G4'S	87%	101%	99%	95%	105%	97%	7%
0.1 µM G7G4'S	81%	101%	105%	92%	103%	96%	10%
1 µM G7G4'S	95%	98%	105%	98%	109%	101%	6%
10 µM G7G4'S	103%	112%	102%	92%	104%	103%	7%

Table 22: Cytotoxicity data of individual plates for DAI and its metabolites.

Mean values (MV) and standard deviations (SD) are given in [%] of metabolic activity referred to DMSO (1%) as solvent control represented as 100%. Dark colored activities signify detected outliers according to Nalimov and were excluded from the calculation. P0XX denotes the number of each biological replicate. Experiments 8, 12, 39, 40, 41, 44, 45, 46, 48, 50 were found to have many outliers and were therefore excluded. Experiment 29 was contaminated.

	P001	P002	P003	P004	P005	P014	P027	MV	SD
0.001 µM DAI	102%	105%	92%	89%	110%	91%	106%	99%	8%
0.01 µM DAI	105%	94%	98%	94%	114%	96%	101%	98%	4%
0.1 µM DAI	106%	99%	98%	94%	117%	103%	105%	101%	5%
1 µM DAI	111%	100%	100%	104%	119%	103%	104%	104%	4%
10 µM DAI	113%	104%	102%	101%	119%	105%	105%	105%	4%

	P043	P051	P052	P053	P054	MV	SD
0.001 µM D4'G7S	95%	102%	112%	93%	106%	102%	8%
0.01 µM D4'G7S	89%	106%	108%	93%	101%	100%	8%
0.1 µM D4'G7S	87%	100%	105%	90%	109%	98%	10%
1 µM D4'G7S	86%	101%	100%	89%	95%	94%	7%
10 µM D4'G7S	109%	100%	110%	100%	113%	107%	6%

Table 22: continued

	P043	P051	P052	P053	P054	MV	SD
0.001 µM D7G4'S	102%	96%	99%	92%	84%	95%	7%
0.01 µM D7G4'S	67%	96%	102%	68%	51%	77%	22%
0.1 µM D7G4'S	90%	96%	102%	65%	91%	95%	6%
1 µM D7G4'S	93%	99%	102%	95%	94%	97%	4%
10 µM D7G4'S	78%	100%	101%	95%	103%	100%	3%

	P036	P038	P042	P047	P051	P052	MV	SD
0.001 µM D4'S	88%	97%	113%	75%	101%	106%	97%	13%
0.01 µM D4'S	81%	114%	94%	89%	99%	100%	96%	11%
0.1 µM D4'S	85%	92%	102%	101%	98%	105%	97%	7%
1 µM D4'S	81%	105%	90%	80%	103%	108%	94%	13%
10 µM D4'S	97%	117%	124%	102%	116%	87%	107%	14%

	P036	P038	P042	P047	P051	P052	MV	SD
0.001 µM D4',7dG	84%	108%	107%	80%	105%	108%	99%	13%
0.01 µM D4',7dG	87%	116%	108%	91%	102%	98%	100%	11%
0.1 µM D4',7dG	93%	86%	102%	95%	102%	101%	99%	4%
1 µM D4',7dG	89%	111%	108%	100%	104%	103%	105%	4%
10 µM D4',7dG	86%	115%	102%	85%	107%	110%	101%	13%

	P006	P009	P010	P011	P013	P015	P017	P033	MV	SD
0.001 µM D4',7dS	-	102%	100%	91%	91%	100%	98%	85%	95%	6%
0.01 µM D4',7dS	-	106%	98%	99%	93%	104%	103%	93%	99%	5%
0.1 µM D4',7dS	-	108%	103%	104%	99%	108%	100%	95%	102%	4%
1 µM D4',7dS	-	107%	99%	99%	95%	100%	109%	91%	100%	6%
10 µM D4',7dS	-	105%	86%	100%	102%	106%	108%	96%	103%	5%

	P006	P009	P010	P011	P013	P015	P017	P033	MV	SD
0.001 µM D4'G	95%	108%	95%	90%	90%	102%	105%	107%	99%	8%
0.01 µM D4'G	97%	94%	94%	97%	96%	99%	111%	95%	96%	2%
0.1 µM D4'G	97%	93%	100%	91%	96%	101%	97%	90%	96%	4%
1 µM D4'G	95%	102%	105%	96%	93%	102%	114%	87%	97%	6%
10 µM D4'G	103%	95%	107%	99%	94%	105%	114%	74%	103%	7%

	P006	P009	P010	P011	P013	P015	P017	P033	MV	SD
0.001 µM D7G	104%	100%	106%	91%	101%	104%	100%	91%	99%	6%
0.01 µM D7G	103%	106%	103%	89%	97%	100%	102%	94%	101%	4%
0.1 µM D7G	103%	102%	103%	99%	94%	101%	97%	100%	101%	2%
1 µM D7G	103%	101%	99%	96%	92%	111%	107%	77%	101%	6%
10 µM D7G	109%	89%	100%	102%	100%	104%	111%	95%	101%	7%

Table 23: Cytotoxicity data of individual plates for EQ and its metabolites.

Mean values (MV) and standard deviations (SD) are given in [%] of metabolic activity referred to DMSO (1%) as solvent control represented as 100%. Dark colored activities signify detected outliers according to Nalimov and were excluded from the calculation. P0XX denotes the number of each biological replicate. Experiments 12, 34, 35, 37, 48, 49, 50 were found to have many outliers and were therefore excluded. Experiments 29 and 30 were contaminated.

	P001	P002	P003	P004	P005	P014	P027	MV	SD
0.001 µM EQ	107%	96%	101%	94%	102%	96%	103%	100%	5%
0.01 µM EQ	106%	98%	100%	95%	101%	99%	104%	101%	4%
0.1 µM EQ	112%	99%	104%	99%	114%	105%	104%	105%	6%
1 µM EQ	118%	108%	107%	108%	112%	103%	110%	109%	5%
10 µM EQ	118%	107%	111%	110%	113%	92%	114%	112%	4%

	P023	P024	P025	P026	P028	P032	P039	MV	SD
0.001 µM E4'S	99%	85%	101%	103%	86%	99%	103%	97%	8%
0.01 µM E4'S	105%	91%	100%	107%	86%	91%	102%	97%	8%
0.1 µM E4'S	104%	94%	105%	104%	87%	97%	100%	101%	4%
1 µM E4'S	106%	99%	98%	101%	79%	101%	99%	101%	3%
10 µM E4'S	118%	108%	108%	105%	103%	104%	93%	106%	8%

	P023	P024	P025	P026	P028	P032	P039	MV	SD
0.001 µM E7G	101%	81%	92%	99%	99%	100%	86%	94%	8%
0.01 µM E7G	104%	81%	100%	103%	96%	110%	99%	102%	5%
0.1 µM E7G	104%	-	103%	103%	96%	91%	96%	99%	5%
1 µM E7G	103%	94%	98%	99%	100%	99%	95%	98%	3%
10 µM E7G	99%	80%	96%	103%	83%	101%	104%	95%	10%

SRB

Table 24: Cytotoxicity data of individual plates for GEN and its metabolites.

Mean values (MV) and standard deviations (SD) are given in [%] of protein content referred to DMSO (1%) as solvent control represented as 100%. Dark colored activities signify detected outliers according to Nalimov and were excluded from the calculation. P0XX denotes the number of each biological replicate. Experiments 1, 5, 12, 16, 20, 21, 25, 28, 35, 36, 39, 40, 41, 46, 48, 49 were found to have many outliers and were therefore excluded. Experiments 29 and 30 were contaminated.

	P002	P003	P004	P014	P027	P050	MV	SD
0.001 µM GEN	97%	105%	100%	102%	98%	54%	100%	3%
0.01 µM GEN	105%	107%	94%	107%	103%	110%	106%	2%
0.1 µM GEN	124%	121%	117%	117%	106%	115%	119%	3%
1 µM GEN	130%	129%	110%	114%	98%	115%	116%	12%
10 µM GEN	109%	126%	101%	105%	106%	95%	103%	5%

	P023	P024	P026	P032	P034	P037	MV	SD
0.001 µM G7S	89%	91%	96%	97%	93%	100%	94%	4%
0.01 µM G7S	96%	94%	96%	99%	93%	115%	96%	2%
0.1 µM G7S	94%	93%	102%	101%	93%	102%	97%	5%
1 µM G7S	101%	95%	98%	98%	116%	103%	99%	3%
10 µM G7S	106%	115%	99%	96%	113%	117%	108%	9%

	P038	P042	P044	MV	SD
0.001 µM G4',7dS	91%	91%	84%	91%	0%
0.01 µM G4',7dS	77%	88%	82%	82%	5%
0.1 µM G4',7dS	79%	94%	71%	81%	12%
1 µM G4',7dS	78%	88%	79%	82%	6%
10 µM G4',7dS	104%	102%	97%	101%	4%

	P018	P019	P022	P031	MV	SD
0.001 µM G4',7dG	94%	99%	98%	114%	97%	3%
0.01 µM G4',7dG	111%	100%	97%	109%	104%	7%
0.1 µM G4',7dG	89%	77%	98%	97%	90%	10%
1 µM G4',7dG	94%	100%	96%	107%	99%	5%
10 µM G4',7dG	161%	108%	97%	112%	106%	8%

	P018	P019	P022	P031	MV	SD
0.001 µM G4'G	166%	105%	98%	91%	98%	7%
0.01 µM G4'G	165%	107%	94%	89%	97%	9%
0.1 µM G4'G	171%	99%	93%	94%	95%	3%
1 µM G4'G	102%	93%	97%	99%	98%	4%
10 µM G4'G	116%	112%	99%	116%	115%	2%

Table 24: continued

	P018	P019	P022	P031	MV	SD
0.001 µM G7G	100%	104%	89%	103%	102%	2%
0.01 µM G7G	89%	102%	93%	100%	96%	6%
0.1 µM G7G	164%	99%	92%	92%	94%	4%
1 µM G7G	86%	108%	95%	95%	96%	9%
10 µM G7G	104%	110%	101%	108%	106%	4%

	P047	P051	P052	MV	SD
0.001 µM G4'G7S	89%	103%	79%	91%	12%
0.01 µM G4'G7S	103%	90%	95%	96%	7%
0.1 µM G4'G7S	103%	99%	105%	102%	3%
1 µM G4'G7S	91%	105%	97%	98%	7%
10 µM G4'G7S	95%	103%	81%	93%	11%

	P043	P051	P052	P053	P054	MV	SD
0.001 µM G7G4'S	96%	89%	109%	70%	72%	87%	17%
0.01 µM G7G4'S	96%	100%	105%	103%	80%	101%	4%
0.1 µM G7G4'S	92%	94%	95%	90%	79%	93%	2%
1 µM G7G4'S	98%	91%	122%	95%	92%	94%	3%
10 µM G7G4'S	106%	100%	121%	94%	97%	99%	5%

Table 25: Cytotoxicity data of individual plates for DAI and its metabolites.

Mean values (MV) and standard deviations (SD) are given in [%] of protein content referred to DMSO (1%) as solvent control represented as 100%. Dark colored activities signify detected outliers according to Nalimov and were excluded from the calculation. P0XX denotes the number of each biological replicate. Experiments 1, 5, 9, 10, 11, 12, 15, 17, 36, 39, 40, 41, 46, 48 were found to have many outliers and were therefore excluded. Experiment 29 was contaminated.

	P002	P003	P004	P014	P027	P050	MV	SD
0.001 µM DAI	91%	79%	92%	82%	98%	86%	88%	7%
0.01 µM DAI	81%	92%	107%	80%	96%	91%	91%	10%
0.1 µM DAI	95%	93%	108%	89%	100%	80%	94%	10%
1 µM DAI	92%	88%	119%	92%	100%	101%	95%	6%
10 µM DAI	89%	115%	122%	90%	109%	107%	105%	13%

	P043	P051	P052	P053	P054	MV	SD
0.001 µM D4'G7S	108%	115%	118%	93%	95%	106%	11%
0.01 µM D4'G7S	107%	112%	114%	84%	104%	109%	4%
0.1 µM D4'G7S	105%	104%	104%	91%	116%	104%	9%
1 µM D4'G7S	106%	108%	123%	77%	92%	101%	17%
10 µM D4'G7S	114%	97%	111%	91%	93%	101%	11%

Table 25: continued

	P043	P051	P052	P053	P054	MV	SD
0.001 µM D7G4'S	101%	113%	88%	93%	97%	99%	9%
0.01 µM D7G4'S	100%	110%	111%	99%	95%	103%	7%
0.1 µM D7G4'S	102%	100%	109%	101%	96%	102%	5%
1 µM D7G4'S	101%	88%	89%	101%	98%	95%	6%
10 µM D7G4'S	97%	97%	110%	82%	94%	96%	10%

	P038	P042	P044	P045	P047	P051	MV	SD
0.001 µM D4'S	74%	102%	95%	106%	92%	103%	100%	6%
0.01 µM D4'S	97%	106%	96%	101%	100%	108%	101%	5%
0.1 µM D4'S	112%	98%	105%	103%	105%	106%	105%	5%
1 µM D4'S	98%	105%	102%	102%	106%	104%	103%	3%
10 µM D4'S	93%	114%	103%	109%	110%	102%	105%	7%

	P038	P042	P044	P051	MV	SD
0.001 µM D4',7dG	94%	95%	89%	111%	93%	3%
0.01 µM D4',7dG	89%	101%	83%	103%	94%	10%
0.1 µM D4',7dG	93%	94%	97%	103%	97%	5%
1 µM D4',7dG	90%	102%	108%	101%	100%	7%
10 µM D4',7dG	94%	91%	99%	105%	97%	6%

	P007	P008	P013	P033	MV	SD
0.001 µM D4',7dS	111%	99%	94%	88%	98%	10%
0.01 µM D4',7dS	104%	100%	97%	91%	98%	5%
0.1 µM D4',7dS	128%	86%	99%	99%	95%	7%
1 µM D4',7dS	118%	96%	97%	95%	96%	1%
10 µM D4',7dS	141%	100%	97%	96%	98%	2%

	P006	P007	P008	P013	P033	MV	SD
0.001 µM D4'G	115%	117%	95%	83%	99%	102%	14%
0.01 µM D4'G	111%	111%	95%	89%	98%	101%	10%
0.1 µM D4'G	109%	101%	83%	93%	89%	95%	10%
1 µM D4'G	105%	80%	79%	92%	76%	86%	12%
10 µM D4'G	101%	102%	89%	90%	93%	95%	6%

	P006	P007	P008	P013	P033	MV	SD
0.001 µM D7G	127%	115%	100%	87%	94%	105%	16%
0.01 µM D7G	115%	133%	93%	90%	75%	93%	16%
0.1 µM D7G	103%	99%	93%	88%	84%	93%	8%
1 µM D7G	111%	109%	98%	84%	93%	99%	12%
10 µM D7G	122%	127%	102%	92%	94%	108%	16%

Table 26: Cytotoxicity data of individual plates for EQ and its metabolites.

Mean values (MV) and standard deviations (SD) are given in [%] of protein content referred to DMSO (1%) as solvent control represented as 100%. Dark colored activities signify detected outliers according to Nalimov and were excluded from the calculation. P0XX denotes the number of each biological replicate. Experiments 1, 5, 12, 25, 28, 35, 48, 49 were found to have many outliers and were therefore excluded. Experiments 29 and 30 were contaminated.

	P002	P003	P004	P014	P027	P050	MV	SD
0.001 µM EQ	84%	101%	98%	95%	94%	91%	94%	6%
0.01 µM EQ	85%	69%	96%	89%	97%	92%	92%	5%
0.1 µM EQ	87%	105%	111%	107%	97%	93%	100%	9%
1 µM EQ	110%	117%	125%	105%	104%	105%	111%	10%
10 µM EQ	96%	126%	132%	102%	105%	112%	112%	14%

	P023	P024	P026	P032	P034	P037	MV	SD
0.001 µM E4'S	97%	94%	99%	87%	104%	102%	99%	4%
0.01 µM E4'S	95%	94%	90%	88%	105%	97%	93%	4%
0.1 µM E4'S	96%	96%	98%	86%	95%	108%	97%	7%
1 µM E4'S	98%	102%	97%	103%	106%	117%	101%	3%
10 µM E4'S	104%	115%	95%	109%	115%	130%	111%	12%

	P023	P024	P026	P032	P034	MV	SD
0.001 µM E7G	96%	97%	96%	81%	96%	97%	1%
0.01 µM E7G	96%	91%	77%	86%	95%	92%	4%
0.1 µM E7G	95%	102%	94%	78%	91%	95%	5%
1 µM E7G	94%	108%	96%	81%	93%	94%	10%
10 µM E7G	94%	93%	97%	88%	104%	95%	6%

UHPLC-MS/MS

Table 27: Transition list for UHPLC-MS/MS.

The table includes precursor name, mass, retention time and fragment mass. For all substances, precursor and fragment charge was -1.

Molecule List Name	Precursor Name	Precursor Mass	Fragment Mass	Precursor Retention Time
Daidzein	DAI	252.851	132.0	10.1
Daidzein	DAI	252.851	208.0	10.1
Daidzein	DAI	252.851	223.8	10.1
Daidzein-Met	DAI-4',7-diglucuronide	604.809	112.9	3.8
Daidzein-Met	DAI-4',7-diglucuronide	604.809	253.0	3.8
Daidzein-Met	DAI-4',7-diglucuronide	604.809	429.0	3.8
Daidzein-Met	DAI-4',7-disulfate	412.774	224.9	6.9
Daidzein-Met	DAI-4',7-disulfate	412.774	253.1	6.9
Daidzein-Met	DAI-4',7-disulfate	412.774	332.8	6.9
Daidzein-Met	DAI-7-sulfate	332.823	116.9	8.3
Daidzein-Met	DAI-7-sulfate	332.823	134.8	8.3
Daidzein-Met	DAI-7-sulfate	332.823	253.0	8.3
Daidzein-Met	DAI-4'-sulfate	332.823	116.9	8.4
Daidzein-Met	DAI-4'-sulfate	332.823	134.8	8.4
Daidzein-Met	DAI-4'-sulfate	332.823	253.0	8.4
Daidzein-Met	DAI-sulfate_SUM	332.823	116.9	8.4
Daidzein-Met	DAI-sulfate_SUM	332.823	134.8	8.4
Daidzein-Met	DAI-sulfate_SUM	332.823	253.0	8.4
Daidzein-Met	DAI-4'-glucuronide-7-sulfate	508.781	429.0	5.7
Daidzein-Met	DAI-4'-glucuronide-7-sulfate	508.781	174.7	5.7
Daidzein-Met	DAI-4'-glucuronide-7-sulfate	508.781	253.0	5.7
Daidzein-Met	DAI-7-glucuronide-4'-sulfate	508.781	332.9	5.2
Daidzein-Met	DAI-7-glucuronide-4'-sulfate	508.781	174.7	5.2
Daidzein-Met	DAI-7-glucuronide-4'-sulfate	508.781	253.0	5.2
Daidzein-Met	DAI-4'-glucuronide	428.893	112.9	7.1
Daidzein-Met	DAI-4'-glucuronide	428.893	174.9	7.1
Daidzein-Met	DAI-4'-glucuronide	428.893	253.0	7.1
Daidzein-Met	DAI-7-glucuronide	428.893	112.9	6.4
Daidzein-Met	DAI-7-glucuronide	428.893	174.9	6.4
Daidzein-Met	DAI-7-glucuronide	428.893	253.0	6.4

Table 27: continued

Molecule List Name	Precursor Name	Precursor Mass	Fragment Mass	Precursor Retention Time
Equol	EQ	240.879	118.9	10.8
Equol	EQ	240.879	121.1	10.8
Equol	EQ	240.879	134.9	10.8
Equol-Met	EQ-4’-sulfate	320.841	119.0	8.9
Equol-Met	EQ-4’-sulfate	320.841	121.1	8.9
Equol-Met	EQ-4’-sulfate	320.841	241.0	8.9
Equol-Met	EQ-7-sulfate	320.841	119.0	8.9
Equol-Met	EQ-7-sulfate	320.841	121.1	8.9
Equol-Met	EQ-7-sulfate	320.841	241.0	8.9
Equol-Met	EQ-sulfate_SUM	320.841	119.0	8.9
Equol-Met	EQ-sulfate_SUM	320.841	121.1	8.9
Equol-Met	EQ-sulfate_SUM	320.841	241.0	8.9
Equol-Met	EQ-7-glucuronide	416.914	113.0	7.7
Equol-Met	EQ-7-glucuronide	416.914	120.9	7.7
Equol-Met	EQ-7-glucuronide	416.914	174.9	7.7
Equol-Met	EQ-4’-glucuronide	416.914	113.0	8.0
Equol-Met	EQ-4’-glucuronide	416.914	120.9	8.0
Equol-Met	EQ-4’-glucuronide	416.914	174.9	8.0
Genistein	GEN	268.866	131.8	11.0
Genistein	GEN	268.866	133.1	11.0
Genistein	GEN	268.866	159.0	11.0
Genistein-Met	GEN-4’,7-diglucuronide	620.807	112.9	4.5
Genistein-Met	GEN-4’,7-diglucuronide	620.807	268.9	4.5
Genistein-Met	GEN-4’,7-diglucuronide	620.807	444.8	4.5
Genistein-Met	GEN-4’,7-disulfate	428.811	268.9	7.5
Genistein-Met	GEN-4’,7-disulfate	428.811	348.9	7.5
Genistein-Met	GEN-4’-glucuronide-7-sulfate	524.800	445.0	6.3
Genistein-Met	GEN-4’-glucuronide-7-sulfate	524.800	112.9	6.3
Genistein-Met	GEN-4’-glucuronide-7-sulfate	524.800	269.1	6.3
Genistein-Met	GEN-7-glucuronide-4’-sulfate	524.800	348.7	5.8
Genistein-Met	GEN-7-glucuronide-4’-sulfate	524.800	112.9	5.8
Genistein-Met	GEN-7-glucuronide-4’-sulfate	524.800	269.1	5.8
Genistein-Met	GEN-7-sulfate	348.800	131.9	9.1
Genistein-Met	GEN-7-sulfate	348.800	132.9	9.1
Genistein-Met	GEN-7-sulfate	348.800	269.0	9.1
Genistein-Met	GEN-4’-sulfate	348.800	131.9	9.1
Genistein-Met	GEN-4’-sulfate	348.800	132.9	9.1
Genistein-Met	GEN-4’-sulfate	348.800	269.0	9.1

Table 27: continued

Molecule List Name	Precursor Name	Precursor Mass	Fragment Mass	Precursor Retention Time
Genistein-Met	GEN-sulfate_SUM	348.800	131.9	9.1
Genistein-Met	GEN-sulfate_SUM	348.800	132.9	9.1
Genistein-Met	GEN-sulfate_SUM	348.800	269.0	9.1
Genistein-Met	GEN-7-glucuronide	444.881	113.0	7.2
Genistein-Met	GEN-7-glucuronide	444.881	175.0	7.2
Genistein-Met	GEN-7-glucuronide	444.881	268.9	7.2
Genistein-Met	GEN-4'-glucuronide	444.881	113.0	7.8
Genistein-Met	GEN-4'-glucuronide	444.881	175.0	7.8
Genistein-Met	GEN-4'-glucuronide	444.881	268.9	7.8

Spike preparations and calculations of mass concentrations

Altogether, four spiking solutions were prepared for the UHPLC-MS/MS experiments, one for the IFs (IF), one for the metabolites of GEN (G_MET), one for the metabolites of DAI (D_MET) and one for the EQ (E_MET) metabolites. In order to prepare them, the theoretical amount of each substance in 80 µL (equal to the amount taken from the wells incubated with the substances in 4.2.5.3. Workflow) was calculated using the following equation,

$$\beta = \frac{C_1 \cdot M \cdot 80}{1000}$$

with M the molar mass, C_1 the original concentration of the substance and β the mass concentration of the substance in 80 µL. In order to derive the volume V of the stocks needed for the spiking solution, β was divided by the mass concentration of the stock solutions β_{Stock}. This volume was then multiplied by 10 since each substance was to be tested three times for a statistical analysis, thus deriving the V_{TARGET}. Depending on the spiking solution, these volumes of the test substances were summed and subtracted from 100 µL, which was the end volume. For the remainder of the volume, ACN was used as a solvent. Given that certain values were not possible to exactly prepare using the micropipettes of the lab, approximate volumes were used to simplify. The correction factor F was finally calculated as follows and all data is summarized in Table 28.

$$F = \frac{Target}{Real}$$

Table 28: Volume and concentration data for the preparation of the four spiking solutions.

Spike	M	C_1	C_2	β	$β_{Stock}$	V	V_{TARGET}	V_{REAL}	F
IF	g/mol	µmol/L	µg/L	ng/80 µL	mg/L	µL	for 100 µL	for 100 µL	-
GEN	270.2	1	270.2	21.62	10	2.2	21.6	20.0	1.08
DAI	254.2	1	254.2	20.34	10	2.0	20.3	20.0	1.02
EQ	242.3	1	242.3	19.38	10	1.9	19.4	20.0	0.97
					Sum	6.1	61.3	60.0	1.02
					Solvent	**ACN**	38.7	40	
G_MET									
G4'G	446.4	1	446.4	35.71	100	0.4	3.6	5.0	0.71
G7G	446.4	1	446.4	35.71	100	0.4	3.6	5.0	0.71
G4',7dG	622.5	1	622.5	49.8	100	0.5	5.0	5.0	1.00
G7S	350.3	1	350.3	28.02	100	0.3	2.8	5.0	0.56
G4',7dS	430.4	1	430.4	34.43	100	0.3	3.4	5.0	0.69
G7G4'S	526.4	1	526.4	42.11	100	0.4	4.2	5.0	0.84
G4'G7s	526.4	1	526.4	42.11	100	0.4	4.2	5.0	0.84
					Sum	2.7	26.8	35.0	0.77
					Solvent	**ACN**	73.2	65.0	
D_MET									
D4'G	430.4	1	430.4	34.43	100	0.3	3.4	5.0	0.69
D7G	430.4	1	430.4	34.43	100	0.3	3.4	5.0	0.69
D4',7dG	606.5	1	606.5	48.52	100	0.5	4.9	5.0	0.97
D4'S	334.3	1	334.3	26.74	100	0.3	2.7	5.0	0.53
D4',7dS	414.4	1	414.4	33.15	100	0.3	3.3	5.0	0.66
D7G4'S	510.4	1	510.4	40.83	100	0.4	4.1	5.0	0.82
D4'G7S	510.4	1	510.4	40.83	100	0.4	4.1	5.0	0.82
					Sum	2.6	25.9	35.0	0.74
					Solvent	**ACN**	74.1	65.0	
E_MET									
E7G	418.4	1	418.4	33.47	10	3.3	33.5	35.0	0.96
E4'S	322.3	1	322.3	25.78	10	2.6	25.8	25.0	1.03
					Sum	5.9	59.3	60.0	0.99
					Solvent	**ACN**	40.7	40.0	

Next, the theoretical concentration of each substance in the spiked samples used for recovery rates, matrix effects and eluent, which amounted to 10 µL, was calculated. First, the mass concentration β_{REAL} was derived as follows,

$$\beta_{REAL} = \frac{V_{TARGET} \cdot \beta_{STOCK}}{V}$$

with V_{REAL} the volume of each substance in the 100 µL spike, β_{STOCK} the mass concentration of the substance stock and V the end volume of the spike (=100 µL). This was then multiplied by 10 to derive the mass concentration in the volume with which each sample was spiked. Lastly, this concentration was divided by 160, which was the end volume of each spiked sample, and then recalculated to µg/L as the theoretical value, which will be later used to calculate the recovery rates.

Table 29: Theoretical mass concentration of each spiked substance.

Spike	β_{REAL}	β (in 10 µL spike)	β (in 160 µL)	β_{THEOR}
IF	mg/L=µg/mL=ng/µL	ng/10µL	ng/µL=µg/mL=mg/L	µg/L=ppb
GEN	2	20	0.125	125
DAI	2	20	0.125	125
EQ	2	20	0.125	125
G_MET				
G4'G	5	50	0.313	313
G7G	5	50	0.313	313
G4',7dG	5	50	0.313	313
G7S	5	50	0.313	313
G4',7dS	5	50	0.313	313
G7G4'S	5	50	0.313	313
G4'G7s	5	50	0.313	313
D_MET				
D4'G	5	50	0.313	313
D7G	5	50	0.313	313
D4',7dG	5	50	0.313	313
D4'S	5	50	0.313	313
D4',7dS	5	50	0.313	313
D7G4'S	5	50	0.313	313
D4'G7S	5	50	0.313	313
E_MET				
E7G	4	35	0.219	219
E4'S	3	25	0.156	156

Recovery rates and matrix effects

The concentrations of each sample were calculated with the Skyline software according to 4.2.5.3. Workflow and are listed in Table 30.

Table 30: Concentrations of DMSO for the recovery rates (REC), matrix effects (ME) and the eluent MeOH:H_2O.

Spike	DMSO (REC)			DMSO (ME)			MeOH:H2O		
IF	ppb = µg/L = ng/mL = pg/µL								
GEN	100	118	122	113	107	112	84	80	79
DAI	93	103	113	105	108	106	77	80	77
EQ	91	106	104	115	110	107	80	77	72
G_MET									
G4'G	299	285	223	290	273	260	173	148	147
G7G	321	272	265	287	285	302	168	134	147
G4',7dG	335	189	219	217	242	179	100	91	120
G7S	183	286	270	307	275	274	207	184	181
G4',7dS	256	285	270	333	298	276	187	179	196
G7G4'S	365	292	280	323	324	275	194	151	173
G4'G7s	343	294	271	307	294	280	179	162	167
D_MET									
D4'G	330	241	231	271	307	266	68	70	110
D7G	391	266	256	273	285	287	74	62	109
D4',7dG	<LOQ	<LOQ	<LOQ	<LOQ	<LOQ	<LOQ	<LOQ	<LOQ	<LOQ
D4'S	313	355	321	314	360	313	122	103	159
D4',7dS	318	225	257	230	228	216	101	90	146
D7G4'S	348	227	197	267	253	250	75	69	130
D4'G7S	355	243	216	273	258	260	78	75	138
E_MET									
E7G	198	202	198	184	185	191	72	67	84
E4'S	121	177	160	154	153	163	74	73	88

Unfortunately, the concentrations for the eluent MeOH:H_2O were lower compared to those of DMSO (1%) and were not useful in further calculations. Due to this, the recovery rates were considered in order to correct the results from 5.3. HPLC-MS/MS when necessary. For this, the concentration reads from the Skyline data were multiplied by 100 and divided with the theoretical concentration β_{THEOR} of each spiking solution listed in Table 29. Then, the mean values and standard deviations were derived and are listed in Table 31. For the recovery rates ranging between 80 and 120%, no corrections were taken into consideration.

Table 31: Mean values and standard deviations of recovery rates (REC) and matric effects (ME).

Spike	DMSO (REC)		DMSO (ME)	
IF	MV±SD [%]			
GEN	90	9	88	3
DAI	82	8	85	1
EQ	81	6	88	3
G_MET				
G4'G	86	13	88	5
G7G	91	10	93	3
G4',7dG	79	25	68	10
G7S	79	18	91	6
G4',7dS	86	5	97	9
G7G4'S	100	15	98	9
G4'G7s	97	12	94	4
D_MET				
D4'G	86	17	90	7
D7G	97	24	90	2
D4',7dG	**<LOQ**	**<LOQ**	**<LOQ**	**<LOQ**
D4'S	106	7	105	9
D4',7dS	85	15	72	3
D7G4'S	82	25	82	3
D4'G7S	87	24	84	3
E_MET				
E7G	91	1	85	2
E4'S	98	18	100	4